Aus der Klinik für Neurologie
Geschäftsführender Direktor: Prof. Dr. med. Lars Timmermann

des Fachbereichs Medizin
der Philipps-Universität Marburg

Investigating the role of glial cells in neurodegenerative disorders by depleting astrocytes and oligodendrocytes in a model of amyloid-beta induced cytotoxicity in organotypic hippocampal slice cultures

Inaugural-Dissertation

zur Erlangung des Doktorgrades

der Naturwissenschaften

dem Fachbereich Medizin

der Philipps-Universität Marburg

vorgelegt von

Natascha Vidovic

aus Düsseldorf

Marburg an der Lahn, 2021

Angenommen vom Fachbereich Medizin der Philipps-Universität Marburg
am: **22.04.2021**

Gedruckt mit Genehmigung des Fachbereichs Medizin

Dekanin: Frau Prof. Dr. D. Hilfiker-Kleiner

Referent: Herr Prof. Dr. R. Dodel

1. Korreferent: Herr Prof. Dr. A. Pagenstecher

Meiner Familie,

meinen Freunden,

mit großem Dank an Lukas,

Allen die mich auf dem Weg begleitet haben!

„Die Wissenschaft ist Teil der Lebenswirklichkeit; es ist das Was, das Wie und das Warum von allem in unserer Erfahrung.“

Rachel Carson

Table of content

List of figures

List of tables

Abbreviations

Abbreviation	Description
Aβ/ abeta	Amyloid beta
AD	Alzheimer's disease
APOE	Apolipoprotein E
APP	Amyloid precursor protein
α-Syn	Alpha Synuclein
ATP	Adenosine triphosphate
AQP4	Aquaporin 4
Aqua bidest.	Double-distilled water
BBB	Blood-brain barrier
BCA	Bicinchoninic acid
BME	Basal medium eagle
BSA	Bovine serum albumin
BV-2	Microglial cell line
CA1-3	Cornu ammonis 1-3
CD	Cluster of differentiation
CLSM	Confocal laser scanning microscopy
CNPase	2',3'-Cyclic-nucleotide 3'-phosphodiesterase
CNS	Central nervous system
CO_2	Carbon dioxide
CTRL	Control condition
DAPI	4',6-diamidino-2-phenylindole
DAR	Dye-antibody-ratio
DAT	Dopamine transporter
dbcAMP	Dibutyryl cyclic adenosine monophosphate
DG	Dentate gyri
DIV	Days in vitro
DMEM	Dulbecco's modified eagle medium
DMSO	Dimethyl sulfoxide

DNA	Desoxyribonucleic acid
DTT	Dithiothreitol
EAAT1 and EAAT2	Excitatory amino acid transporter 1 and 2
EC50	Half maximal effective concentration
EDTA	Ethylendiaminotetraacetic acid
ELISA	Enzyme linked immunosorbent assay
EOAD	Early onset Alzheimer's disease
FCS	Fetal calf serum
Fig.	Figure
GABA	gamma-Aminobutyric acid
GFAP	Glial fibrillary acidic protein
GLAST-1	Glutamate aspartate transporter 1
GLT-1	Glutamate transporter 1
GLYC-2	Glycine transporter 2
GM-CSF	Granulocyte-macrophage colony-stimulating factor
GPCR	G-protein coupled receptor
GPR17	G-protein receptor 17
H	hours
HBSS	Hank's balanced salt solution
HEPES	4-(2-hydroxyethyl)-1-piperazineethanesulfonic acid
HRP	Horse-radish peroxidase
IbA 1	Ionized calcium binding adaptor molecule 1
IFN-γ	Interferon gamma
Igg	Immunoglobulin G
IL-1	Interleukin 1
IL-6	Interleukin 6
IL-10	Interleukin 10
iNOS	Inducible nitric oxide synthase
IVIg	Intravenous immunoglobulins
Lα-AAA	L-alpha aminoadipic acid

LOAD	Late onset Alzheimer's disease
LPS	Lipopolysaccharides
LTP	Long-term potentiation
mAb	Monoclonal antibody
MAP	Microtubule associated protein
MCI	Mild cognitive impairment
mg	Milligram
ml/ µl	Milliliter/ µicro liter
mm/ µm	Millimeter/ µicro meter
mM/ µM	Millimolar/ µicro molar
M	Molar
MS	Multiple sclerosis
MTT	3-(4,5-dimethylthiazol-2-yl)-2,5-diphenyltetrazolium bromide
MW	Molecular weight
NaOH	Sodium hydroxide
NeuN	Neuronal nuclei
NFT	Neurofibrillary tangle
NG2	Neuron-glia antigen 2
NGF	Nerve growth factor
NMDAR	N-methyl-D-aspartate receptor
NMO	Neuromyelitis optica
NO	Nitric oxide
n.s.	Not significant
O4	Oligodendrocyte marker 4
OHSC	Organotypic hippocampal slice cultures
Oli-neu	Oligodendrocyte precursor cell line
OPC	Oligodendrocyte precursor cell
PBS	Phosphate buffered saline
PD	Parkinson's disease
Pen/ Strep	Penicillin and streptavidin
PFA	paraformaldehyde

PI	Propidium iodide
PLP	Proteolipid protein
PMDs	Protein misfolding disorders
RAGE	Receptor for advanced glycosylation end products
RFU	Relative fluorescence unit
ROS	Reactive oxygen species
Rpm	Rounds per minute
RT	Room temperature
SD	Standard deviation
SERT	Serotonin transporter
SLC	Solute carrier
SV-40	Simian-virus 40
Tab.	Table
TGF-β	Tumor growth factor beta
TLR	Toll-like receptor
TMB	3,3’,5,5’-Tetramethylbenzidine
TNF-α	Tumor necrosis factor alpha
TREM 1 and 2	Triggering receptors expressed on myeloid cells 1 and 2
TschG	Tierschutzgesetz

1. Introduction

Neurodegenerative diseases, such as Alzheimer's disease (AD) and Parkinson's disease (PD), belong to a group of so-called protein misfolding disorders and share the characteristic of aggregated proteins; in AD, the prevailing protein is the beta-amyloid peptide (Aβ/Abeta), and in PD, it is alpha-synuclein (α-Syn) (Chiti and Dobson, 2006) as well as the microtubule associated–protein tau, which is common in both disorders (Bancher *et al.*, 1993; Hanger *et al.*, 2009; Lei *et al.*, 2010). The aetiology of AD, the most common cause of dementia, is still under debate (Viana *et al.*, 2012; Wu and Nakanishi, 2015).

Since 1992, when the amyloid-hypothesis was postulated, research focused on the toxicity of $A\beta_{1\text{-}42}$ oligomers and the underlying mechanisms of neurodegeneration observed in the hippocampus (Hardy and Higgins, 1992; Hardy, 2002). Next, to examine various mechanisms of amyloid toxicity, more attention was also drawn to inflammatory processes as causing the onset or at least the progression of the disorder (Griffin *et al.*, 1998; Heppner *et al.*, 2015). As early as 1907, Alois Alzheimer already mentioned inflammatory involvement in his observations taken from *post mortem* AD brains (Takami *et al.*, 1997; Rubio-Perez and Morillas-Ruiz, 2012; Ridolfi *et al.*, 2013). Additionally, evidence pinpoints to a crucial role of inflammatory processes in the progression of the disease (Heppner *et al.*, 2015). Support for this hypothesis comes from autopsies of AD patient *post mortem* brains, in which high amounts of activated glial cells were found around senile plaques (Walsh and Selkoe, 2004a; Lue *et al.*, 2010; Heneka *et al.*, 2015; Shadfar *et al.*, 2015). In PD brains, active microglial cells were also found around the substantia nigra, which is the prominent area affected in Parkinson's disease (McGeer *et al.*, 1988; Liu and Hong, 2003; Tang *et al.*, 2014; Yang *et al.*, 2017). It is therefore of great interest, that the microglial population is higher in the midbrain and in the substantia nigra (Lawson *et al.*, 1990; Kumar *et al.*, 2013) in comparison with the cortex.

It has long been thought that the immune system of the brain is unique and separated from the blood and the remaining organism by the blood brain barrier. Actually, the central nervous system (CNS) has a special set of defence mechanisms against pathogens and invaders that is distinct from the innate or adaptive immune system (Akiyama *et al.*, 2000b). Important players of this defence system are glial cells. Glial cells are non-neuronal cells that are subdivided into

three cell types, including microglia, astrocytes and oligodendrocytes, with different modes of action and function. Astrocytes and microglia actively take part in the defence process, whereas oligodendrocytes seem to have a more supportive function, e.g., by creating the myelin sheath around axons to maintain signal transfer (Berger and Frotscher, 1994). Destruction of these cells leads to the decreased isolation of axons and a loss of transmission (Birgbauer *et al.*, 2004), which is a major hallmark of multiple sclerosis (MS) (Frohman *et al.*, 2006; Oksenberg *et al.*, 2008).

In general, astrocytes and microglia secrete cytokines to support the growth of neurons and maintain their function (Liberto *et al.*, 2004; Rossner *et al.*, 2005). In addition, astrocytes, for example, form the first line of defence by supporting the blood-brain barrier (BBB) (Liberto *et al.*, 2004). In AD *post mortem* brains, astrocytes were found detached from endothelial cells and near senile plaques (Wisniewski and Wegiel, 1991; Orre *et al.*, 2013). Disruption of the BBB can lead to infiltration by peripheral monocytes and disturbances in brain homeostasis (Lee and Landreth, 2010). Cytokines released by activated glial cells can in turn activate other glial cells in a self-perpetuating cycle (Millington *et al.*, 2014). The cellular mechanisms leading to acute/chronic neuroinflammation and neuronal death observed in AD are still unclear (Ransohoff and Perry, 2009).

1.1 Alzheimer's Disease pathology

Alzheimer's disease is the most common form of dementia (60% - 70%) affecting the elderly (Cunningham *et al.*, 2015; Kumar *et al.*, 2015) with a prevalence of 5% in European middle-aged (> 50 years) men and women and an incidence of 1.1% per year. To date the major risk factor is aging. In times of the demographic change numbers of patients diagnosed with AD are rising. According to predictions up to 13 million people (in Germany) will be suffering from AD in the near future (Tomaskova *et al.*, 2016).

AD was first described by Alois Alzheimer in 1907 when he described observations he made of his female patient Auguste Deter, who was brought to him in the beginning of the 20th century with symptoms of discomposure and severe memory deficits (Alzheimer, 1907; Alzheimer *et al.*, 1995). Later on, examining her brain *post mortem*, he found unusual protein aggregates in the cortex that are nowadays known as senile (amyloid) plaques.

Additionally, he described the occurrence of neurofibrillary tangles (NFTs). Due to his findings, this form of dementia was later called Alzheimer's disease (Engelhardt and Gomes, 2015). The processing and production of Aβ and NFTs will be described in detail below. The occurrence of senile plaques and NFTs consisting of hyper phosphorylated tau-proteins, which were already observed by Alzheimer, are still regarded as characteristics of the disease (Viana *et al.*, 2012). Further examinations over the last 100 years showed that misfolded proteins tend to aggregate and form deposits that in the case of AD consist of amyloid beta (Aβ) fibrils. In particular, regions that are responsible for memory and cognition are affected by these two types of lesions (Selkoe, 2004). Enhanced and early neurodegeneration in these areas can explain the disease symptomatic.

Most patients suffer from a sporadic form of AD with no precise triggering factor. Since patients at higher ages (> 65 years) are starting to notice symptoms it is called late-onset AD (LOAD). Next to unknown causes, LOAD is often connected to mutations in the genetic coding for the E4 allele of apolipoprotein E (APOE) (Rogaeva, 2002). APOE is a glycoprotein mainly expressed in the liver and brain by neurons, astrocytes and macrophages (Siest *et al.*, 1995) and serves in transport of cholesterol as well as neuronal growth and repair (Mahley, 1988). Heterozygous carriers of this gene mutation have a 3-fold risk of developing AD whereas carriers homozygous for this genetic variant have a risk that is 15-fold higher compared to controls (Ashford, 2004). The APOE protein was found to be a target of the oral infection causing *porphyromonas gingivalis* (*p. gingivalis*) virulent factor gingipain (protease) (Lönn *et al.*, 2018), which could be a mechanism of creating neurotoxic fragments of APOE.

Familial or inherited AD patients make up about < 5% of all cases (Guerreiro *et al.*, 2012; Karch and Goate, 2015). These cases are commonly called early onset AD (EOAD) because symptoms mostly appear before the age of 65 years (Guerreiro *et al.*, 2012; Müller *et al.*, 2013). EOAD cases often occur within a family cohesion. Up to now, there are three different genes know to be affected by mutations related to EOAD (Rogaeva, 2002). These genes include the genetic information for the amyloid precursor protein (APP) and both presenilins (PS1 and PS2) which are functional subunits of the γ-secretase that is crucial for the cleavage of APP into the 40-42 amino acids long Aβ peptide (Jankowsky *et al.*, 2004). Mutations in the APP gene often result in enhanced expression of APP protein that can abnormally often be cleaved by γ-secretases to yield toxic forms of Aβ. Interestingly, as late as 2002, re-approved examinations of genetic

material from Auguste D. revealed mutations in the presenilin-1 gene, suggesting that she suffered from an autosomal inherited form of EOAD (Müller *et al.*, 2013).

In addition, genetic variations in the triggering receptors expressed on myeloid cells 1 and 2 (TREM1, TREM2) have also been linked to increased risk of AD (Jay *et al.*, 2017). TREM2 is mainly expressed on microglial cells and involved in the regulation of inflammatory reactions in the CNS as well as in recognizing bacterial invaders (N'Diaye *et al.*, 2009; Gao *et al.*, 2013). As well as TREM2, TREM1 is associated with a risk for AD, since *p. gingivalis* can induce the expression of a risk-associated TREM1 allele that leads to a decrease in TREM1 surface receptor expression and a decreased response to bacterial infections (Bostanci *et al.*, 2013).

1.2 Clinics

Clinical manifestations are not profoundly different in patients suffering from EOAD or LOAD (Tellechea *et al.*, 2018). The major difference is the time of onset as described earlier. Nevertheless, patients of both forms begin to have mild cognitive impairment (MCI) mostly before being diagnosed with dementia (Jack *et al.*, 2010). Loss of short-term memory and impairment in forming new memory and learning events often is a profound sign of dementia and the time point when patients will be examined by a neurologist. Unfortunately, this is already late in regard to disease progression, since it is suggested that the preclinical phase begins even decades before the first symptoms are feasible (Price and Morris, 1999).With progression of the disease, symptoms will worsen, and severe AD will manifest. In these phases, patients can develop agnosia, aphasia, apraxia and apathy (Tarawneh and Holtzman, 2012). Besides, because of these physical impairments, patients will get mental problems since they can no longer participate in social life which often results in severe depression and isolation (Bature *et al.*, 2017; Zubenko *et al.*, 2003). In the very late stages, cognitive decline is increasing and usually patients suffer from the inability to form new memories, since the transition from the short- to long-term memory is affected. More dramatically, patients are no longer able to recognize relatives and there is a strong need of nursing (Tarawneh and Holtzman, 2012). AD itself is not lethal, but mostly patients die from secondary diseases or complications, like infections and cardio vascular impairments (Todd *et al.*, 2013).

1.3 Molecular basis

On the brain level, during AD increased brain atrophy is happening, especially in the hippocampal area where memories are made and stored. The neurons of the hippocampal formation are mostly glutamatergic and highly sensitive to stressors and excitotoxicity by neurotransmitters such as glutamate (Vinet *et al.*, 2012). The enhanced loss of neurons in this area is responsible for the symptoms of memory loss. Plaque formation throughout the cortex is observable in patients with AD and Aβ plaques as well as Tau-aggregates can be visualized with positron emission tomography scans (PET-scans) whereas a distinct diagnosis is mostly made *post mortem* (Fleisher *et al.*, 2020).

It is generally accepted that the amyloid beta protein (Aβ) is the major component of senile plaques which are found in *post mortem* patient's brains. Aβ is a 37 to 43 amino acid long peptide (Walter et al., 2001) derived from a gene coding for the β-amyloid precursor protein (APP) located on chromosome 21 (Hardy and Selkoe, 2002) and generated via beta (β)- and gamma (γ)-secretase cleavage. Aβ is found in cerebrospinal fluid (CF), plasma and almost all peripheral and brain cells of healthy people. The physiological function of APP and Aβ is not clear, however, evidence points towards a possible protective role of Aβ in normal neuronal function and synaptic communication (Castellani et al., 2009; Carrillo-Mora et al., 2014).

APP can be cleaved by α-, β-, and γ-secretases. Under physiological conditions, APP is mainly cleaved by α-secretase first and then by a γ-secretase, resulting in soluble APP fragments that are secreted into the extracellular space and will be degraded after completing its function (the non-amyloidogenic pathway). Mutations of the secretases can lead to enhanced production of Aβ by favouring proteolytic processing of APP by β (BACE1) - or γ-secretase (Haass, 2004; Kayed and Lasagna-Reeves, 2013). Therefore, preferred cleavage of APP by β- and γ-secretases leads to the formation of an amyloidogenic Aβ fragment and is connected to extracellular deposition of Aβ (the amyloidogenic pathway). γ-secretase consists of two components known as presenilin-1 (PS 1) and presenilin-2 (PS 2) (Zhang *et al.*, 2014a). Mutations in these domains were found to result in abnormal cleavage of APP leading to Aβ of 42 amino acids at least in cases of familial AD (Walter *et al.*, 2001). Aβ in its monomeric form is thought to be non-toxic, however, aggregated forms of Aβ are supposed to be neurotoxic with several mechanisms of toxicity currently under debate (Walsh and Selkoe, 2004b). The oligomeric form can interact with synapses, thereby altering their function.

Oligomers have been found to reduce synaptic plasticity, to impair calcium homeostasis, lead to increased oxidative stress, hyper phosphorylation of tau, and excitotoxicity (Cornejo and Hetz, 2013). Soluble oligomers can move between the intra- and extracellular space. One possible mechanism of Aβ-derived toxicity is receptor-mediated. One of these receptors is the N-methyl-D-aspartate receptor (NMDA-R) which is involved, among others, in the formation of long-term memory by a term called long-term potentiation (LTP). LTP was shown to be impaired by Aβ oligomers. Additionally, via binding of Aβ to NMDA-R, reactive oxygen species (ROS) formation and mitochondrial dysfunction are supposed to be promoted (Kayed and Lasagna-Reeves, 2013).

Besides NMDA-R, Aβ oligomers can, for instance, interact with the neuronal insulin receptor, resulting in insulin signalling disruption and reduced receptor expression. Additionally, Aβ can disturb synaptic function via the cellular prion protein receptor and induce apoptotic mechanisms by binding to nerve growth factor (NGF) receptors (Kayed and Lasagna-Reeves, 2013).

Another way of Aβ-mediated toxicity is supposed to take place via increased membrane permeability by the formation of cation channels. Additionally, Aβ oligomers are supposed to increase membrane conductance and permeability, without the formation of pores or channels (Kayed and Lasagna-Reeves, 2013) These mechanisms presumably lead to disruptions in ionic homeostasis and subsequently to cell death, since maintenance of an intact plasma membrane is important for cell viability. Disruptions in the lipid bilayer can have severe consequences as, among others, disturbance in calcium homeostasis (Ca^{2+}) that will result in various processes leading to neurodegeneration.

Besides these extracellular actions, Aβ can also mediate neurotoxicity intracellularly. Uptake of Aβ oligomers probably takes place via endocytosis. Once the oligomers are inside the cell they can have an impact on mitochondrial function, proteasomes and autophagy, again resulting in neuronal cell death (Kayed and Lasagna-Reeves, 2013).

1.4 Microglia

Microglial cells contribute to the brain's cellular content at about 10 % (Rubio-Perez and Morillas-Ruiz, 2012; Aguzzi *et al.*, 2013). Depending on the context, microglia can appear in various phenotypes. Under healthy conditions, microglial cells display a "ramified" morphology and function as the brain's controlling unit (Fetler and Amigorena, 2005; Ridolfi *et al.*, 2013). With their long processes they are scanning the surrounding for invaders and pathogens or aggregated misfolded proteins, ceaselessly (Nimmerjahn *et al.*, 2005; Kettenmann *et al.*, 2011; Heneka *et al.*, 2014). Because of this, and their ability to phagocytose cellular debris in the brain like accumulated proteins (Rogers *et al.*, 2002; Boissonneault *et al.*, 2009), they are also referred to as the brain's macrophages and form the "first line of defence" (Fetler and Amigorena, 2005; Johnston *et al.*, 2011; Rubio-Perez and Morillas-Ruiz, 2012). In conditions of inflammation or damage, they change to an active state formerly referred to as M1 or M2 respectively (Aguzzi *et al.*, 2013; Ridolfi *et al.*, 2013), but in 2015 Joachim Schultze from the LIMES institute in Bonn and colleagues proposed a more diverse activation pattern of microglia which can react to various "input signals" since it is not all black and white (Schultze, 2015). These input signals can have a broad spectrum and among others include pathogen-associated molecular patterns (PAMPs), damage-associated molecular patterns, cytokines, growth and stimulating factors (Xue *et al.*, 2014). When activated as a reaction to environmental changes, microglia produce cytokines that are preferentially pro-inflammatory (Liu and Hong, 2003). A typical activating signal for the more pro-inflammatory phenotype is interferon-γ (IFN-γ), which is mainly produced by T-cells in the periphery (Colton, 2009; Ransohoff and Perry, 2009), but also produced by microglial cells and astrocytes after stimulation of PAMPs in the brain (Suzuki *et al.*, 2005). As described earlier, activated microglia are found in the surrounding of amyloid plaques indicating an interaction with amyloid oligomers and fibrils (Ferretti *et al.*, 2012). Supporting evidence for an involvement of amyloid oligomers in the activation of microglial cells are derived from the fact that on microglial cells, receptors were found capable of binding to $A\beta_{1\text{-}42}$ (Murgas *et al.*, 2012). Among others, these receptors are surface proteins like CD14, which has gained importance as the lipopolysaccharide (LPS)-receptor involved in innate immunity (Fassbender *et al.*, 2004; Liu *et al.*, 2005), RAGE (Yan *et al.*, 1996), CD36 and various scavenger receptors (Husemann *et al.*, 2002).

Binding to these receptors activates a signalling cascade resulting in the expression of cytokines of either pro- or anti-inflammatory origin or leads to the internalization of Aβ molecules, which has been investigated for the CD14 receptor by Liu and co-workers (Liu *et al.*, 2005). Additionally, Fassbender and co-workers hypothesized an involvement of CD14 long-time-activation by Aβ fibrils in the chronic neuroinflammatory process in AD (Fassbender *et al.*, 2004). Other pattern recognition receptors belong to the group of Toll-like receptors (TLRs) that are expressed by microglial cells (Papageorgiou *et al.*, 2016). Upon activation, these receptors act via signalling induction through interferon-γ and nuclear factor (NF)-κB (Stewart *et al.*, 2010). TLR4 acts together with CD14 in the recognition of bacterial LPS. Like TLR4, TLR6 is also known for its Abeta binding properties and the provoking of neuroinflammation (Stewart *et al.*, 2010; Lynch, 2014; Papageorgiou *et al.*, 2016). CD36 acts as a co-receptor for TLR4 and TLR6, which is triggered by Aβ (El Khoury *et al.*, 2003), whereas only bacterial peptides are able to act vial CD36-TLR2-TLR6 signalling. In line with these findings, experiments done with CD36, TLR4 and TLR6 deficient mice that were challenged with $A\beta_{1\text{-}42}$ showed no production of ROS and nitric oxide (NO) which is likely to happen to Aβ challenged wild-type mice. These results support the importance of the receptors in Aβ-induced inflammatory activation. Likewise, wild-type microglia expressed elevated levels of interleukin (IL)-1β mRNA in comparison to TLR4 and TLR6 deficient mice after the stimulation with $A\beta_{1\text{-}42}$ (Stewart *et al.*, 2010).

Alternative phenotypes in turn are capable of producing anti-inflammatory cytokines and morphological changes (Gordon and Taylor, 2005; Minogue, 2017). If an inflammation occurs in the CNS, as a consequence of a trauma e.g., microglial cells begin to function in repairing and protecting the surrounding tissue and neurons (Blasko *et al.*, 2004; Ridolfi *et al.*, 2013). In addition, microglia will secrete anti-inflammatory cytokines that will further support the protection of nerve cells (Ridolfi *et al.*, 2013). Furthermore, when microglia face such inflammation sites for the first time, they are said to be “primed” and undergo a change in their morphology towards an amoeboid appearance (Lue *et al.*, 2010; Heneka *et al.*, 2015). Furthermore, these activated microglial cells were found to release excessive amounts of the excitatory neurotransmitter glutamate which itself is neurotoxic (Lopategui Cabezas *et al.*, 2014). This change of morphology includes an up regulation of cell-surface receptors described above that are involved in pathogen recognition (PRRs) and varies from ramified to amoeboid (Suh and Checler, 2002; Glass *et al.*, 2010; Lopategui Cabezas *et al.*, 2014; Minogue,

2017). Though, the transition to different activation phenotypes is not irreversible and may be altered during inflammation progress (Minogue, 2017).

Besides the above described activation states, (Wyss-Coray and Rogers, 2012) there is another phenotype, which is called “acquired deactivation” (Gordon and Taylor, 2005; Colton, 2009). The term was first introduced by Gordon in 2003 and differs from the “classical alternative activation state”, also formerly known as M2, in the way, that next to cytokines (interleukins (IL-10); tumor growth factor-β (TGF-β)) also apoptotic cells themselves can give rise to this second alternative state (Gordon, 2003; Mosser, 2003; Colton, 2009). Microglial cells with this phenotype are said to be “immunosuppressive” and are not capable of producing cytokines of either pro- or anti-inflammatory origin. Their main function is to take up apoptotic cells.

1.5 Astrocytes

The most widespread glial cell type in the CNS is the astrocytic cell, which is named for its star-shaped morphology (Farfara *et al.*, 2008; Hou *et al.*, 2011). According to Mark Ellisman and Philip Haydon and colleagues, an estimation of 100,000 synapses are under the control of one single astrocytic cell (Bushong *et al.*, 2002; Halassa *et al.*, 2007). Disturbances in astrocyte homeostasis may have considerable consequences for neighbouring neurons. In healthy brains, astrocytes form part of the BBB (Liberto *et al.*, 2004; Strooper and Karran, 2016), are responsible for maintaining the extracellular environment and for regulating neurotransmitter levels, especially glutamate homeostasis, and actively take part in the promotion of synapse formation (Maragakis and Rothstein, 2006; Liddelow *et al.*, 2017). In addition to microglial cells, astrocytes were found to also be able to internalize and degrade β-amyloid oligomers to some extent (Lee and Landreth, 2010; Nagele *et al.*, 2003; Nagele *et al.*, 2004). Liddelow and colleagues described two subtypes of astrocytes in analogy to the microglial classification: A1 and A2 (Liddelow *et al.*, 2017; Liddelow and Barres, 2017). The A1 phenotype is capable of inducing classical complement genes and thereby contributing to the destruction of synapses, whereas the A2 phenotype is protective because of the upregulation of neurotrophic factors that contribute to the maintenance and repair of neurons and synapses (Liddelow *et al.*, 2017). A1 astrocytes are induced by inflammatory processes, and A2 astrocytes are induced by ischaemic conditions. The activation of astrocytes, independent of the type of activation

towards the A1 or A2 phenotype, is termed “astrogliosis”. Astrogliosis is defined by an increase in the number, size and enhanced motility (Glass *et al.*, 2010) of astrocytes and is accompanied by increased expression of the intermediate filament glial fibrillary acidic protein (GFAP) and S100B (Simpson *et al.*, 2010), which both were found to be elevated in AD (McGeer and McGeer, 1995; Mrak *et al.*, 1996; Petzold *et al.*, 2003; Kashon *et al.*, 2004). After the transition to the A1 phenotype, astrocytes release pro-inflammatory cytokines (Lopategui Cabezas *et al.*, 2014), including IL-1β and the soluble factor NO (Hou *et al.*, 2011), thereby contributing to the process of inflammation. Studies of cultured astrocytes exposed to fibrillar, oligomeric or nonfibrillar β-amyloid showed that IL-1β, tumor necrosis factor (TNF)-α, inducible nitric oxide synthase (iNOS) and NO levels significantly increased. The changes in cytokine levels depended on the form of β-amyloid applied. While oligomeric forms were found to increase TNF-α, IL-1β, iNOS and NO more rapidly but transiently, fibrillar β-amyloid had more prolonged effects (White *et al.*, 2005). Nevertheless, astrocytes also may have a neuroprotective function. It is well known that an excess of glutamate, which is an excitatory neurotransmitter, can be toxic to neuronal cells (Li *et al.*, 1997). Glutamate, among other neurotransmitters, is taken up by astrocytes to maintain a balance in the extracellular space and synaptic cleft between neurons (Rose *et al.*, 2018). This uptake is transporter-mediated, and their levels seem to be upregulated in aged astrocytes in vitro (Pertusa *et al.*, 2007), whereas neuronal uptake declines with ageing (Segovia *et al.*, 2001). Two kinds of transporters are important in this context: excitatory amino acid transporter 1 and 2 (EAAT1 and EAAT 2). EAAT2 levels were found to be reduced with increased Alzheimer’s pathology (Simpson *et al.*, 2010; Li *et al.*, 1997), suggesting a loss of neuroprotection by astrocytes in the aged brain. In contrast, EAAT1 levels were not decreased but rather maintained at a constant level (Beckstrøm *et al.*, 1999). According to these studies, there is a balance of EAAT1 and 2 in AD patients, and it is not clear whether the loss of EAAT2 is a consequence or a cause.

1.6 Oligodendrocytes

Oligodendrocytes, better known as the "myelin sheath-producing" cells of the CNS, have long been underestimated regarding their role in neurodegenerative diseases. Loss of function in these cells has a tremendous effect on the brain's homeostasis and survival of neurons and synaptic connections (Roth *et al.*, 2005). As described earlier in this thesis, oligodendrocytes and the myelin sheath are the targets of immune attacks in another disorder of the CNS, namely, Multiple Sclerosis (Compston and Coles, 2008). Therefore, the possible consequences are well understood when these cells are decreased or destroyed by pathogenic invaders or inflammatory processes. What remains a matter of debate is whether the cause of myelin breakdown is the first event, or a result of another pathogenic process present in the CNS.

Damage to oligodendrocytes mainly occurs through oxidative stress (Wyss-Coray and Rogers, 2012; Goldstein *et al.*, 2016) because a lack of glutathione and high iron content makes them more vulnerable (Juurlink, 1997). One can imagine that in an environment with activated microglial and astrocytic cells, the concentration of reactive oxygen species in the form of NO is very high, which is a strong damaging agent to oligodendrocytes. In addition, microglial cells secrete the neurotransmitter glutamate, which is cytotoxic to oligodendrocytes (Czeh *et al.*, 2011) (Czeh *et al.*, 2011; Ridolfi *et al.*, 2013). Further, oligodendrocytes express neurotrophic molecules such as S100B to support neuronal cells. S100B is also expressed to a lesser extent by other CNS cells but is often associated with astrocytes, which can lead to misinterpretation of cytokine measurements (Steiner *et al.*, 2007; Simpson *et al.*, 2010).

1.7 Presence of $A\beta_{1\text{-}42}$ induces a signalling cascade leading to the expression of inflammatory mediators

The cytokine profiles of microglia and astrocytes are highly similar with only little differences. Both cell types are capable of secreting cytokines, chemokines and other soluble molecules that regulate inflammatory processes in the CNS (McGeer and McGeer, 1995; Akiyama *et al.*, 2000a). Figure 1 summarizes cytokines that are expressed by microglial and astrocytic cells of either pro- (red) or anti- (blue)-inflammatory origin. Additionally, molecules expressed by astrocytes that have neurotrophic functions are shown in the orange-circle (Blasko *et al.*, 2004). Typical pro-inflammatory cytokines produced in response to Aβ oligomers are inter-

leukins IL-1α and β, IL-6 and TNF-α as has been described by (Bamberger and Landreth, 2001; Rogers *et al.*, 2002) and (Akiyama *et al.*, 2000b).

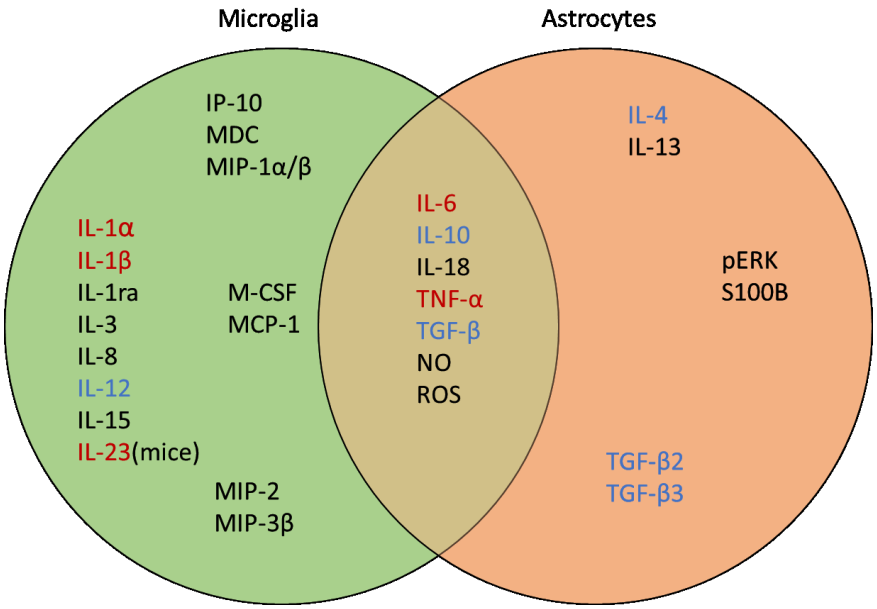

Figure 1.1: Schematic overview of cytokine and chemokine-expression by microglial and astrocytic cells. *Blue-colored factors are of major anti-inflammatory origin while red-colored factors enhance an inflammatory reaction (McGeer and McGeer, 1995; Akiyama et al., 2000b). Orange-colored factors represent neurotrophic molecules (Blasko et al., 2004). Overlapping cytokines are shown in the overlying circle. BDNF=brain-derived neurotrophic factor; IL=interleukins; IP-10=interferon γ induced protein; M-CSF=macrophage colony-stimulating factor; MCP=CC-chemokine ligand; MIP=macrophage inflammatory protein; NGF=nerve growth factor; NO=nitric oxide; NT-3=neurotrophin 3; NT-4/5=neurotrophin 4 and 5; pERK=protein kinase RNA-like Endoplasmic reticulum kinase; ROS=reactive oxygen species; TGF=transforming growth factors; TNF=tumor necrosis factor.*

IL-6 is produced very early in the development of the nervous system and is not only thought to have detrimental effects on neuronal survival but it also has immunosuppressive and other beneficial functions (Castell *et al.*, 1989; Akiyama *et al.*, 2000b). But because of its ability to induce the expression of acute phase proteins and its thereby assistance in disease progression, it is commonly viewed to be destructive (Castell *et al.*, 1989; Akiyama *et al.*, 2000b). Another prominent marker of inflammation is TNF-α which is increased in the serum

of AD (Fillit *et al.*, 1991) and PD (Hsu *et al.*, 1996) patients and glial cultures in response to Aβ oligomers (Breder *et al.*, 1993; Rubio-Perez and Morillas-Ruiz, 2012).

Next to cytokines and chemokines, there are molecules like NO and free radicals that serve as markers of inflammatory processes in the CNS. NO is produces by the inducible form of nitric oxide synthase (iNOS) (Xie *et al.*, 1992) in response to inflammatory stimulus like IL-1β expression by both astrocytes and microglial cells (Akiyama *et al.*, 2000b; Murgas *et al.*, 2012). NO and ROS are produced during phagocytosis of cellular debris by microglia. The oxygen radicals contribute to lipid peroxidation thereby damaging cells and DNA, they are capable of altering proteins in a toxic way and take part in neurotoxicity and can induce apopto-sis/programmed cell death (Vodovotz *et al.*, 1996; Siddiqui *et al.*, 2016). To produce NO the amino acid L-arginine is essential. The ligand is predominately produced by the enzymes argininosuccinate synthetase and argininosuccinate lyase (ASS) that are found to be active in glial cells (Jackson *et al.*, 1996; Heneka *et al.*, 2001). ASS expression was found to be increased in the periphery of senile plaques containing Aβ. Interestingly, the number of ASS-positive neurons and expression levels of neuronal ASS was found to be elevated in AD compared to control brains. Whereas the number of ASS-positive astrocytes remained stable in AD and controls, but the expression levels of astrocyte-derived ASS increased. Furthermore, the neuronal- and astrocytic-derived iNOS levels and iNOS-positive cells were significantly higher in AD than in controls (Heneka *et al.*, 2001). Together these results could explain the sustained oxidative damage in the course of the pathology since Aβ was also found to be a potent inducer of NO itself (Akama *et al.*, 1998).

On the opposite, glial cells are also known to secrete anti-inflammatory cytokines. These include IL-4, IL-10, IL-12 and the TGF-β-family whereas IL-10 and TGF-β are produced by microglial and astrocytic cells as well (figure 1). A more detailed overview of the occurrence and expression levels of cytokines during the course of mild cognitive impairment and AD is given in a previous publication (Brosseron *et al.*, 2014). In short, there are many studies about cytokines in the context of AD and most results are contradictory, since longitudinal data is missing and probably the outcome depends on the methods that were used (ELISA, Western Blot) or the way patients were diagnosed and divided into study-groups.

1.8 Microglia and astrocytes take part in the early development of AD

Astrocytes and microglia make up most of the non-neuronal cells in the CNS. Both cell types also secrete the majority of cytokines during inflammatory processes and especially during the progress of AD. Cytokines and chemokines are actually reliable parameters to measure inflammation in the CNS (Piazza and Lynch, 2009) because typical markers of inflammation like swelling and reddening are missing. Nevertheless, cytokine measurements also bear difficulties that have been discussed already in detail by Ransohoff (Ransohoff and Perry, 2009). The difficulties regarding general cytokine measurements are that there is still a lack of assays detecting very low levels of soluble cytokines in the CNS since they have a short half-life (Ransohoff and Perry, 2009) and it is not easy to differentiate between cytokines expressed by different cell types. There are opposing opinions about the contribution of the different cell types in the beginning and progression of the disease.

One major obstacle in defining the role of distinct cell types during the disease progression is that there is no gradual progression and no clear cut between the different stages of the inflammatory process ongoing in AD brains. To distinguish between an acute phase and a chronic phase is still difficult as is to differentiate which cells are specifically active in which part of the reaction and in which brain region, as the deposition and ongoing neurodegenerating processes are not synchronous between brain areas. Another factor is that in very early stages of the disease there are up to no human studies regarding this point because further examinations are mostly made after clinical symptoms have become manifest. Most patients will be diagnosed with AD years after the molecular processes have begun. Especially regarding the non-inherited (sporadic) forms of AD, it is still impossible to exactly mark the beginning as the causing factors are unknown.

Astrocytes and microglial cells exhibit a highly similar cytokine profile which makes it even more difficult to separate which part the single cell types play in which stage of inflammation. Therefore, acute and chronic processes in AD are explained by means of recent studies and by establishing model systems that display the interaction of glial cells. According to Albert Cheung Hoi Yu and colleagues, during the beginning of AD “intense astrogliosis” takes place - meaning that there is an increased activation of astrocytes rather than microglial cells (Li *et al.*, 2011).

Astrocyte activation increases with aging (Sheng *et al.*, 1996) and in 2010 Wharton and his colleagues examined the correlation between the extent of astrogliosis and cognitive impairment in an elderly cohort unaware of pathology status (Simpson *et al.*, 2010). According to their results, there is a significant increase in gliosis in correlation with Braak stages and activated astrocytes were found to co-localize with amyloid plaques which is in line with findings from Jarek Wegiel and his research group (Nagele *et al.*, 2004). But the results also show that enhanced astrogliosis in the elderly is not primarily linked to AD but can be a natural consequence of the aging process (Simpson *et al.*, 2010).

In contrast to astrogliosis, Gloria Klapstein's working group and researchers around Claudio Cuello propagated that microglial participation is the predominant event in the beginning of AD (Broussard *et al.*, 2012; Hanzel *et al.*, 2014). Supporting evidences come from experiments done with 3-month-old McGill-Thy1-APP mice. During their investigation, the authors discovered that microglial activation based on soma size extension and thickening of processes, occurred earlier than plaque deposition in the hippocampus (Ferretti *et al.*, 2012). Additionally, higher iNOS and CD40 (which is a typical marker of microglial activation) expression was detected prior to plaque deposition. Interestingly, they could not detect any phagocytic activities of microglial cells in this early stage of protein accumulation.

Furthermore, microglial cells are able to produce short-length Aβ species themselves during the process of clearing unfolded Aβ molecules which can give rise to even more $A\beta_{1\text{-}42}$ aggregation (Mazzitelli *et al.*, 2016). A similar situation was described by Carmen Venegas and colleagues, who presented microglia-derived apoptosis-associated speck-like protein containing a CARD (ASC specks) as important triggers of Aβ aggregation and seeding (Venegas *et al.*, 2017). Injections of ASC specks into APP/PS1 mice resulted in increased Aβ load compared to control mice, likewise injections of APP/PS brain homogenates into APP/PS1 mice lead to an increase in Aβ positive deposits, whereas the injection of the homogenates into APP/PS1; ASC-/- did not result in any deposition. These results suggest, that there is a strong correlation of ASC specks and Aβ deposition *in vivo* (Venegas *et al.*, 2017). Microglia facing $A\beta_{1\text{-}42}$ results in the release of ASC specks; this might be a mechanism of perpetuation and enhanced Aβ deposition.

Astrocytes and microglia are in a close relation on the spatial and molecular level (Jinno *et al.*, 2007) since co-culturing of microglia with astrocytes showed that factors secreted by astrocytes can modulate microglial activation and result in decreased production of ROS and iNOS (Min *et al.*, 2006). This attenuating effect may derive from the fact that astrocytes are gamma-Aminobutyric acid (GABA)-ergic cells, whereas microglia express GABA-receptors (Lee *et al.*, 2011). On the other hand, there are lots of studies that give evidence for an activating role of astrocytes as mentioned before (Pascual *et al.*, 2012).

1.9 Organotypic hippocampal slice cultures as a model to study glial cell interactions

Organotypic slice cultures (OHSCs) in general serve as an excellent model system to study cell to cell interactions and communications. The term was first introduced by Crain because of the cytoarchitecture that is reminiscent to *in situ* preparations (Crain, 1966). Advantages of this kind of cell preparations are the enormous cultivation times which can last from several weeks to months (Stoppini *et al.*, 1991; Nägerl *et al.*, 2004; Galimberti *et al.*, 2006); in addition, the need for animal experiments is dramatically reduced and they display all cell types of a specific tissue in a steady-state situation (Vinet *et al.*, 2012).

Slice cultures of the hippocampal region, referred to as organotypic hippocampal slice cultures have been frequently utilized during the last three decades to investigate the toxicity and impact of compounds and treatments on neuronal cells (Gähwiler, 1981). Tough, the technique and idea has already begun to be used about 80 years ago. There are two major ways of preparing slice cultures. The first described method is the roller tube cultivation and was introduced by Mary Jane Hogue as early as 1947 (Hogue, 1947). Hogue used human foetal brains which were cut into tiny pieces of about 2 mm and put on the inside walls of test tubes. The brain pieces were attached to the wall with a clot of chicken plasma and globulin. The tubes were filled with medium and put into a roller tube apparatus (Gey and Gey, 1936) and cultivated for 3-4 months. The advantage of the roller tube technique is that the slices are moistened with every turn and not constantly soaked by the medium. One disadvantage of this technique - depending on the experimental set up - is the quick flattening and spreading of the cell layers due to the constant movement of medium around the slices. An advanced approach was described by Gähwiler in the early 1980s (Gähwiler, 1981).

In his lab, slices were cut with a tissue chopper into 300-400 µm thin slices and embedded on coverslips. The coverslip technique was first described in 1951 by Costero and Pomerat (Costero and Pomerat, 1951). Using coverslips, it is easier to observe the cells during cultivation processes and perform staining at the end of the experiment. A great advantage of the coverslip method is that the slices thin down to a monolayer of cells and so individual cells can be visualized using phase contrast microscopy.

The second, yet more often used method for OHSCs is the so-called interface method which was described by Stoppini and colleagues (Stoppini *et al.*, 1991). Here, slices were cultured on membrane surfaces allowing to be exposed to medium and air at the same time (Cho *et al.*, 2007). The membranes are placed into 6-well plates that are filled with a special amount of medium that varies from 1 to 1.2 ml (Simoni and Yu, 2006; Vinet *et al.*, 2012), allowing the slices to not dry out and to not drown in medium. Slices prepared with this kind of technique usually thin down to 5-8 cell layers after several days whereas the cytoarchitecture is preserved. Because of the missing clot for attachment onto tube walls or coverslips, it is easier to perform electrophysiological experiments.

Furthermore, other differences during the preparation process are the type of animals and ages that were used as well as the way the hippocampi were sliced. Most protocols make use of a vibratome (Simoni and Yu, 2006), whereas others use tissue section machines or choppers (Gähwiler, 1981). Whereas, there are different ways of preparing slice cultures, there are only a few attempts to deplete distinct cell types from these cultures. We and others (Masuch *et al.*, 2016; Richter *et al.*, 2020) could show that microglial cells can be depleted from OHSCs using a pharmaceutical compound called clodronate. The depletion of microglia dramatically affected the survival of hippocampal neurons in Aβ-induced neurotoxicity (Richter *et al.*, 2020).

1.10 Aims of the thesis

To examine the individual roles of glial cells in Aβ-induced neurotoxicity and inflammatory processes, slice cultures from murine hippocampi were cultured with different conditions. First, microglia were depleted using clodronate, afterwards astrocytes and or oligodendrocytes were eliminated with antibody-toxin-conjugates. After the treatment of slices with Aβ, cytokine levels and cell viability were determined. In the present study, two ways of depleting astrocytes from slice cultures and the corresponding difficulties were examined. Furthermore, immunotoxin conjugates were also tested on their ability on depleting oligodendrocytes. Afore, the search for specific literature by performing MeSH (Medical Subject Heading) term search in Pubmed was done. In the first place, searching for "organotypic hippocampal slice cultures" and "preparation" yielded 42 results. Thereafter, the terms "astrocytes" and "organotypic hippocampal slice cultures" were used and 85 results were yielded when additionally, the "other animals" filter was applied - 80 results remained. From these 80 results, by adding "depletion" to the MeSH terms, two results remained that were not relevant for the experimental set up. When replacing the term "depletion" with "ablation", again one led relevant result occurred. Obviously, there is a lack of methods to examine the role of individual cell types in *ex vivo* models that display *in vivo* characteristics.

Therefore, two different approaches were designed for the specific ablation of astrocytes and oligodendrocytes. The first approach is an adaptation of the work from Higgins and co-workers (Higgins *et al.*, 2015). Herein, the authors successfully targeted two antigens: Neuron-glia antigen 2 (NG2) and ganglioside mainly expressed on developing migratory glia ($GD3^A$) of glioblastoma cells with a toxin-coupled murine antibody (Mab-ZAP). Excitatory amino acid transporter 1, also referred to as glutamate aspartate transporter 1 in rodents was found to be a suitable candidate for internalization since it was found to be predominantly expressed in glial cells and especially astrocytes (Kondo *et al.*, 1995; Parkin *et al.*, 2018; Parkin *et al.*, 2018). GLAST-1 belongs to a family of different glutamate transporters, that are crucial for the re-uptake of glutamate from the synaptic cleft after transmission of neurotransmitters from pre-synapses to post-synapses (Schousboe *et al.*, 1977; Fullana *et al.*, 2020). As conjugated toxin, the ribosome-inactivating plant-derived saporin was chosen. Next to GLAST-1, a second glutamate transporter (GLT-1) as well as a pore-forming protein Aquaporin 4 (AQP4) were investigated on their ability to be used in ablation studies.

In accordance with the immunoablation of astrocytes, antibody complexes consisting of a primary and a suitable secondary toxin-coupled antibody was used for the ablation of oligodendrocytes as well. Here, two different complexes were designed and tested. Two targets on the cell membrane were chosen: the G protein coupled receptor 17 (GPCR GPR17) belongs to the G protein coupled receptor 1 family and is localized in the cell membrane of cerebellar oligodendrocyte precursor cells (OPCs) (Viganò *et al.*, 2016) and Claudin-11 which is an oligodendrocyte-specific target expressed on the cell membrane and tight junctions of myelin sheaths (Morita *et al.*, 1999).

For the second approach for the depletion of astrocytes, the known gliotoxin L-alpha aminoadipic acid (Lα-AAA) was used in cell culture experiments. A-aminoadipic acids (αAA) are glutamate-homologues and therefore have the potential to be used as astrocyte-specific gliotoxins (Olney *et al.*, 1971). Two derivates L- and D- isomers have been investigated of which the L-isoform exerted greater effects (Olney *et al.*, 1980; Garthwaite and Regan, 1980) and was used here in *in vitro* and *ex vivo* experiments. Due to the similarity to the neurotransmitter glutamate, the effect of the intermediate was found to be the inhibition of the glutamate synthesis (Tsai *et al.*, 1996; Gochenauer and Robinson, 2001) and uptake (Khurgel *et al.*, 1996). In the late 70s and early 80s, a couple of research was done with this compound (Garthwaite and Regan, 1980; Huck *et al.*, 1984) *in vitro* and *in vivo* by injecting solutions containing the gliotoxin. Several studies were published concerning the astrocyte-specific-toxic action leaving neurons rather unaffected (Olney *et al.*, 1980). Interestingly, since the late 90s, the use of Lα-AAA vanished. Here, this method was taken up again and adopted for the slice cultures.

2. Material and methods

2.1 Material

2.1.1 Cell Culture media components

Table 2.1 Cell culture components and manufacturers.

Component	Manufacturer
Aqua ad injectabilia	Berlin-Chemie AG Menarini, Berlin, Germany
Gibco™ B-27 Supplement	Thermo Fisher Scientific Inc., Waltham, USA
BME (0.35 g/L sodium bicarbonate, HBSS, w/o L-Glutamine)	PAN Biotech, Aidenbach, Germany
D-(+)-Glucose solution (45 %)	Sigma-Aldrich, Taufkirchen, Germany
DMEM (phenol red, 4.5 g/L glucose, sodium pyruvate, 3.7 g/L NaHCO3, w/o L-Glutamine)	PAN Biotech, Aidenbach, Germany
DMEM (phenol red, 4.5 g/L Glucose, 3.7 g/L NaHCO3, w/o: L-Glutamine, Sodium pyruvate)	PAN Biotech, Aidenbach, Germany
Fetal calf serum	PAN Biotech, Aidenbach, Germany
Gibco™ GlutaMAX (100x)	Thermo Fisher Scientific Inc., Waltham, USA
GM-CSF	Roche, Basel, Switzerland
Gibco™ HBSS with phenol red	Thermo Fisher Scientific Inc., Waltham, USA
HEPES (1 M)	PAN Biotech, Aidenbach, Germany
Horse serum, heat inactivated, New Zealand origin	Thermo Fisher Scientific Inc., Waltham, USA
Insulin	Thermo Fisher Scientific Inc., Waltham, USA
L-glutamine 200 mM	PAA, Pasching, Austria
L-3,3',5-Triiodothyronine, sodium salt	Merck, Darmstadt, Germany
L-Tyroxine sodium salt pentahydrate	Merck, Darmstadt, Germany

Gibco™ MEM (10x) (phenol red, w/o L-Glutamine, HEPES, sodium bicarbonate)	Thermo Fisher Scientific Inc., Waltham, USA
MEM Eagle (EBSS, 2.2 g/L NaHCO3, w/o L-Glutamine)	PAN Biotech, Aidenbach, Germany
Penicillin and streptomycin	PAA Laboratories, Pasching, Austria
Progesterone	Sigma-Aldrich, Taufkirchen, Germany
Putrescine	Sigma-Aldrich, Taufkirchen, Germany
Sodium bicarbonate solution (7.5 %)	Thermo Fisher Scientific Inc., Waltham, USA
Sodium pyruvate	Sigma-Aldrich, Taufkirchen, Germany
Sodium selenite	Sigma-Aldrich, Taufkirchen, Germany
Stable Glutamine 200 mM (100x)	PAN Biotech, Aidenbach, Germany
Transferrin	Merck, Darmstadt, Germany

2.1.2 Chemicals

Table 2.2 Chemicals and manufacturers.

Chemical	**Manufacturer**
Aqua	Carl Roth, Karlsruhe, Germany
Bovine Fraction V	Serva Electrophoresis GmbH, Heidelberg, Germany
Clodronate, Disodium Salt	Merck, Darmstadt, Germany
N6,2'-O-Dibutyryladenosine 3',5'-cyclic monophosphate sodium salt (dbcAMP)	Sigma-Aldrich, Taufkirchen, Germany
Dimethylsulfoxide for synthesis	AppliChem, Darmstadt, Germany
Ethanol	Carl Roth, Karlsruhe, Germany
Hexafluoroisopropanol	Sigma-Aldrich, Taufkichen, Germany
Hydrochloric acid (37 %)	Carl Roth, Karlsruhe, Germany
L-α-amino adipic acid	Santa Cruz Biotechnology Inc., Heidelberg, Germany
Methanol	Carl Roth, Karlsruhe, Germany
Sodium azide	Sigma-Aldrich, Taufkirchen, Germany

Paraformaldehyde solution in PBS (4%)	Santa Cruz Biotechnology Inc., Heidelberg, Germany
Phosphate-buffered saline (w/o Ca, Mg)	PAN Biotech, Aidenbach, Germany
Poly-L/D-Lysine	Sigma-Aldrich, Taufkirchen, Germany
Sodium bicarbonate solution (7.5 %)	Thermo Fisher Scientific Inc., Waltham, USA
Sodium hydroxide	Sigma-Aldrich, Taufkirchen, Germany
Sulforic acid	Carl Roth, Karlsruhe, Germany
Thiazolyl blue Tetrazolium Bromide (MTT)	Sigma-Aldrich, Taufkirchen, Germany
Triton-X 100	Carl Roth, Karlsruhe, Germany
Trypsin/ EDTA (0.25 % trypsin, 0.53 mM EDTA, HBSS, phenol red, w/o Ca, Mg)	PAN Biotech, Aidenbach, Germany
Tween-20	AppliChem, Darmstadt, Germany

2.1.3 Peptides

Table 2.3 Peptide and manufacturer.

Peptide	Manufacturer
Beta-Amyloid 1-42	Bachem, Bubendorf, Switzerland

2.1.4 Antibodies

2.1.4.1 Primary antibodies

Table 2.4 Primary antibodies, protein specificity, manufacturer and clone number.

Protein specificity	Manufacturer	Clone number
Aquaporin 4 Rabbit, polyclonal	Abcam, Cambridge, UK	
Claudin-11 Rabbit, polyclonal	Thermo Fisher Scientific Inc., Waltham, USA	
CNPase Goat, polyclonal	Santa Cruz Biotechnology Inc., Heidelberg, Germany	K-14
EAAT1/ GLAST-1 Rabbit, monoclonal	Abcam, Cambridge, UK	EPR12686

EAAT1/ GLAST-1 Mouse, monoclonal	Santa Cruz Biotechnology Inc., Heidelberg, Germany	A-3
EAAT2/ GLT-1 Mouse, monoclonal	Santa Cruz Biotechnology Inc., Heidelberg, Germany	E-1
GFAP Goat, polyclonal	Thermo Fisher Scientific Inc., Waltham, USA	
GPCR/ GPR17 Goat, polyclonal	Abcam, Cambridge, UK	
IbA 1 Rabbit, polyclonal	Fujifilm WAKO Chemicals, Neuss, Germany	
NeuN Mouse, monoclonal	Merck, Darmstadt, Germany	A60
NG2 Rat, monoclonal	R&D Systems, Minneapolis, USA	546930
Oligodendrocyte Marker 4 Mouse, monoclonal	R&D Systems, Minneapolis, USA	O4
PLP Chicken, polyclonal	Merck, Darmstadt, Germany	

2.1.4.2 Secondary antibodies

Table 2.5 Secondary antibodies, protein specificity, manufacturer and clone number.

Protein specificity	**Manufacturer**
Chicken IgG (H+L) Alexa Fluor 555	Thermo Fisher Scientific Inc., Waltham, USA
Chicken IgG (H+L) Alexa Fluor 594	Jackson Immuno Research, Cambridgeshire, UK
Goat IgG (H+L) Alexa Fluor 555	Thermo Fisher Scientific Inc., Waltham, USA
Goat-ZAP (Saporin conjugated secondary antibody)	ATS Bio, Joure, The Netherlands
Mouse IgG (H+L) Alexa Fluor 488	Thermo Fisher Scientific Inc., Waltham, USA
Rabbit IgG (H+L) Alexa Fluor 647	Thermo Fisher Scientific Inc., Waltham, USA

Rabbit-ZAP (Saporin conjugated secondary antibody)	ATS Bio, Joure, The Netherlands
Rat IgG (H+L) Alexa Fluor 594	Abcam, Cambridge, UK

2.1.5 Dyes

Table 2.6 Dyes for immunohistochemistry and manufacturer.

Dye	Manufacturer
DAPI	Sigma-Aldrich, Taufkirchen, Germany
Propidium Iodide	Sigma-Aldrich, Taufkirchen, Germany

2.1.6 Kits

Table 2.7 Kits for cell viability assessment and internalization analysis and manufacturer.

Kit	Manufacturer
Celltiter-Glo 2.0	Promega, Madison, USA
pHAb amine and thiol reactive dyes	Promega, Madison, USA

2.1.7 Expendables

Table 2.8 Expendable material and manufacturer.

Material	Manufacturer
Cell scraper	Sarstedt, Nümbrecht, Germany
8-well chamber slides	Falcon,
Culture flasks (25 cm^2, 75 cm^2)	Sarstedt, Nümbrecht, Germany
Falcons (15, 50 ml)	Sarstedt, Nümbrecht, Germany
Glass bottles (50, 100, 250, 500, 1.000, 2.000 ml)	Schott, Mainz, Germany
IVIg 5 %	Octapharma, Langenfeld, Germany
Low binding tubes (0.5, 1.5 2 ml)	Eppendorf, Hamburg, Germany
Millicell membrane inserts (0.4 µm pore size)	Merck, Darmstadt, Germany

Microtiterplates (6, 24, 48, 96-well)	Sarstedt, Nümbrecht, Germany
pH stripes pH fix	Carl Roth, Karlsruhe, Germany
Pipet tips	Thermo Fisher Scientific Inc., Waltham, USA
Sterile filters (0.2 µm) puradisc	Oehmen, Essen, Germany
Sterile-filter rapid flow bottle top filter	Thermo Fisher Scientific Inc., Waltham, USA
Sterile pipettes (2, 5, 10, 25 ml)	Sarstedt, Nümbrecht, Germany
Syringes (50 ml)	B. Braun, Melsungen, Germany

2.1.8 Devices

Table 2.9 Devices and manufacturer.

Device	**Manufacturer**
Accujet Pro	Brand, Wertheim, Germany
Biofuge Stratos	Heraeus, Hanau, Germany
Freezer (-20, -80°C)	Sanyo, Osaka, Japan
Incubator (C150) + CO_2	Binder, Tuttlingen, Germany
Incubator (Function line B6) without CO_2	Heraeus, Hanau, Germany
Laminar air flow, sterile HERA safe KS 12	Thermo Fisher Scientific Inc, Waltham, USA
Leica SP8 gSTED super-resolution Confocal and FLIM laser scanning microscope	Leica, Wetzlar, Germany
Magnetic stirrer MR-Hei Standard	Heidolph, Schwabach, Germany
Neubauer Hemocytometer	Brand, Wertheim, Germany
Orbital shaker Unimax 1010	Heidolph, Schwabach, Germany
pH Meter InLab Routine Pro	Mettler Toledo, Columbus, USA
Pipettes Reference and Research Plus (2.5, 5, 10, 20, 200, 1.000 µl)	Eppendorf, Hamburg, Germany
Plate reader Tecan Infinite M200	Tecan, Männedorf, Switzerland
Refrigerators	Bosch, Gerlingen, Germany and Liebherr, Bulle, Switzerland
Spectrophotometer Nanodrop ND-1000	Thermo Fisher Scientific Inc., Waltham, USA

Stereomicroscope TS1000	Nikon, Minato, Japan
MyFuge mini centrifuges	Benchmark Scientific, Sayreville, USA
Tissue chopper	Mc Ilwain, Mickle laboratory engineering, Surrrey, UK
Ultrapure water Easypure II	Werner, Reinstwassersysteme
Waterbath	Labortechnik Medingen
Zeiss Axio Observer.Z1 and Apotome	Carl Zeiss, Jena, Germany

2.1.9 Software

Table 2.10 Software and developer company.

Software	**Developer**
Excel 365	Microsoft
GIMP 2.10.18	Free software
ImageJ	Fuji
Magellan TM 6.4	Tecan
ND-1000	Thermo Fisher
Word 365	Microsoft
ZEN 3.0 Blue and black edition	Carl Zeiss

2.1.10 Animals

Animals were purchased and delivered pregnant at day E14 from Charles River, Germany. For isolation of primary cells derived from embryonic mice (E13.5), pregnant mice were delivered at day E13 and sacrificed by cervical dislocation at the day of arrival.

2.2 Methods

2.2.1 Cultivation of *BV-2* and Oli-*neu* cells

Murine *BV-2* derived from an immortalized cell line that was kindly provided by Dr. med. Jens Neumann (Jens Neumann, Magdeburg). Cells were cultivated in cell culture medium at 37°C and in a humidified atmosphere of 5% CO_2 (tab. 1). Complete medium was changed three times a week and successive subcultures were made by washing in PBS following trypzination (0.53 mM EDTA/ 0.25 % trypsin). Cells were cultured in 75 cm^2 flasks.

Table 2.11: Composition of microglial cell culture medium for a total of 500 ml.

Component	Amount
Dulbecco's modified Eagle's medium (DMEM)	500 ml
Fetal calf serum (heat-inactivated)	50 ml (10 %)
200 mM L-glutamine	5 ml (1 %)
100 U/ml penicillin and 100 µg/ml streptomycin	5 ml (1 %)

Oligodendrocyte precursor cells referred to as the Oli-*neu* cell line were kindly provided by Dr. Andreas Junker from the Department of Neuropathology of the University Hospital Essen and Dr. Doron Merkler from the Department of Pathology and Immunology in Geneva. This murine cell line was first developed and described by Jung and coworkers (Jung *et al.*, 1995) by transfecting GPE-*neu*-86 cells (Boulter and Wagner, 1987) with *t-neu* tyrosine kinase (Söhl *et al.*, 2013). Cells were kept in PDL-coated T75 cm^2 flasks with sterile-filtered SATO medium (tab. 2) for three days and were harvested by scraping cells from the bottom of the flasks with a cell scraper. Cells were cultured until passage 35.

Table 2.12: Composition of Oli-neu culture medium for a total of 500 ml.

Component	Amount/ Concentration
DMEM high Glucose	500 ml
Sodium Pyruvate	110 µg/ml
Transferrin	5 µg/ml
Insulin	10 µg/ml
Putrescin	100 µM
Progesterone	200 nM
L-3,3',5-Triiodothyronine, Sodium Salt	50 pM
Na-Selenite	220 nM
L-Tyroxine	520 nM
Stable Glutamine 200 mM (100X)	5 ml (1 %)
Horse Serum	25 ml (5 %)

Optional, *Oli-neu* cells were treated with 1 mM dibutyryl cAMP (dbcAMP) for differentiation for 5 days (Söhl *et al.*, 2013).

2.2.2 Isolation of primary astrocytes and oligodendrocytes from postnatal mice

Isolation of pure glia cell cultures was done as previously described with minor modifications (McCarthy and Vellis, 1980). Postnatal mice of the strain C57BL/6J and at age p2-4 were sacrificed by decapitation. After the dissection of the brain, hemispheres were cut with a scalpel to achieve smaller pieces that can be resuspended in 1 ml preparation medium A (tab. 2.13). The same procedure was done for the hippocampi. Afterwards, suspensions of 2 brains or 4 hippocampi were collected in 15 ml-tubes filled with even amounts of preparation medium A (in case of brains: 10 ml/ tube and in case of hippocampi: 5 ml/ tube). Tubes were incubated for 5 minutes at room temperature and later supernatants were transferred into fresh tubes. Centrifugation of tubes occurred at 300 g for 5 minutes. Then supernatants were discarded, and pellets were resuspended in 10 ml glia cell culture medium (tab. 2.11) and seeded into cell culture flasks. Cells were maintained in humidified atmosphere at 5% CO_2 and 37°C.

The day after preparation, half of the medium was replaced and whole medium change occurred every 2-4 days. The day before the first separation a whole medium change was done. On DIV 10 flasks were washed 3 times with warm culture medium or PBS. Cells were incubated with fresh medium for 2 hours at 37°C and 5 % CO_2. Afterwards, flasks were sealed with specific lids and put on orbital shakers for 15-17 hours at 37°C and 250 rpm without CO_2.

The next day (DIV11), flasks were taken off the shakers and supernatants were collected. Supernatants should contain oligodendrocytes and astrocytes remain attached to the bottom of the flasks. Before centrifugation of supernatants, suspension was filtered through a 70 µm and a 30 µm cell strainer (Miltenyi biotech, Bergisch Gladbach, Germany) and centrifuged at 300 g for 5 minutes.

Meanwhile, astrocytes were detached from the flask's bottoms by trypzination, pooled and centrifuged as well. Both pellets were resuspended in 10 ml medium (for astrocytes: tab. 2.14 and oligodendrocytes: tab. 2.12) and cells were transferred into T75 cm^2 flasks. On the following days, astrocytes proliferated and were transferred into new flasks, if needed. Oligodendrocytes began to develop multiple branches from day 7 after separation. Total media changes occurred every 2-3 days. Astrocytes were also deep-frozen from time to time.

Table 2.13: Composition of preparation medium A.

Component	Amount
Hank's Balanced Salt Solution (HBSS) 1x	100 ml
45% D-(+)-glucose solution	1.3 ml
1 M HEPES	1.5 ml

2.2.3 Isolation of primary glial cells from embryonic mice

Isolation of astrocytes was additionally done by the preparation of primary cells from embryonic mice (E13.5). The day before preparation, 6-well plates were coated with PDL. The next day, plates were washed three times with PBS. Pregnant (E13) C57BL/6J mice were supplied by the company Charles River Labs. On the day of supply, mice were sacrificed by cervical dislocation and embryos were carefully dissected from the womb and embryonic sacs

were opened using very fine forceps. Mesencephali were dissected from the brain, collected in preparation medium A and incubated for 5 minutes at RT. The supernatant was transferred into fresh tubes and centrifuged for 5 minutes at 300g. Again, supernatant was discarded, and the pellet was resuspended in glial culture medium (tab. 2. 11). Per well, 1 ml of the cell suspension was plated, and 1 ml of fresh medium was added to the wells. Cells were cultivated at 37°C and 5 % CO_2. The next day (DIV1) half of the medium was replaced by fresh medium. On DIV7, 5 ng/ml granulocyte-macrophage colony-stimulating factor (GM-CSF) was added to the medium of cells to induce growth of macrophages. Half of the medium was replaced every 2-3 days by GM-CSF-conditioned medium until DIV14. Medium was replaced and plates were washed once in PBS. Thereafter, DMEM (without FCS) supplemented with trypsin (0.25 %) was mixed and added to the cells. Plates were incubated at 37°C for 15-20 minutes until most of the astrocytic layer was detached from the bottom of the plates. The suspension was collected in fresh tubes, glial culture medium (1/3 of total cell suspension volume) was added and centrifuged for 5 minutes at 300g. The pellet was resuspended in astrocyte medium (tab. 2.14) and transferred onto pre-coated culture flaks for further cultivation.

Table 2.14 Composition of primary astrocyte medium.

Component	Amount
BME	500 ml
FBS	75 ml (15 %)
45% D-(+)-glucose solution	3 ml (0.6 %)
200 nM L-glutamine	0.5 ml (0.1 %)

2.2.4 Freezing and thawing of cells

Freezing medium (tab. 2.15) was pre-cooled on ice. For the freezing of cells from time to time, culture flasks were washed with warm PBS first and cells were dissolved from the flasks by the addition of trypsin. Afterwards, the cell suspension was centrifuged at 300 g for 5 minutes and the cell pellet was resuspended in freezing medium. For the pellet from T75 cm^2 flasks, 6 ml of freezing medium was used and for cell pellets derived from T25 cm^2 flasks 3 ml of freezing medium was used. The newly formed cell suspension was distributed over 1 ml cryo tubes and

deep-freezing was done with a cryo trap that was filled with 250 ml of isopropanol and pre-cooled at -80°C. Cells were stored at -80°C.

Table 2.15: Composition of freezing medium for cells.

Component	Amount
Dulbecco's modified Eagle's medium	60 %
Fetal bovine serum	20 %
Dimethylsulfoxide	20 %

Frozen cell cultures were stored in the water bath until half-thawed. Falcon flasks were filled with pre-cooled cell culture medium up to 13 ml. One or two of the cell suspension-containing cryo-tubes were added to the cold culture medium and slightly inverted. Further, cell suspensions were centrifuged at 4°C, 12,000 rpm for 2-3 minutes and the newly formed cell pellet was resuspended in warm medium and transferred into cell culture flasks for further cultivation.

2.2.5 Organotypic hippocampal slice cultures (OHSC)

For preparation of OHSC, postnatal mice of the strain C57BL/6J were used. Pregnant mice were supplied one week before delivery by the company Charles River Labs. Mice were housed on a 12 h light-dark schedule (lights on 07:00–19:00). They were kept under standard conditions, had free access to tap water and were fed *ad libitum.*

All animal experiments were reported to the "*Tierschutzbeauftragten der Universität Marburg and Duisburg-Essen*" according to § 4 (3) *TSchG "Tötung von Wirbeltieren zu wissenschaftlichen Zwecken".*

Newborn mice at the age of 2-4 days were sacrificed by decapitation and brains were dissected. Therefore, the skin surrounding the scull was cut open with a fine scissor. Then, the sculp itself was opened using very fine forceps. At least, the brain was uncovered, taken out of the scull using a special metallic "spoon" and transferred into a tube filled with cold preparation

medium (tab. 2. 13). During the whole preparation, brains and slices were kept on ice and in preparation medium. Using a stereomicroscope, hippocampi were dissected. First, a single brain was transferred onto a petri dish filled with medium A. Then, the hemispheres were separated using a scalpel. During this step it is important to remove as much midbrain as possible so that the dissection of the hippocampus is easier.

The next step was to dissect the hippocampus out of the hemispheres with a very fine forceps. The dissection has to be done very carefully, since it is of main importance that the hippocampus is freed in its entire composition. Only slices that have all regions of interest can be used for experiments. It is also of great importance, to remove the meninges as well as the remaining of the cortex as much as possible. Hippocampi containing the CA1-3 region and the dentate gyrus were transferred onto a new petri dish filled with medium A and stored on ice. This procedure is done for all brains one by one. Afterwards, the hippocampi were cut into 375 µm thick slices using a tissue chopper (McIlwain via Fisher Scientific, Waltham, USA) (fig. 2.1).

Per well, 6 slices were applied and cultured on special membrane inserts (Millicell cell culture inserts 0.4 µM pore size, Millipore, Darmstadt, Germany) in 6-well plates for 6 days in a humidified atmosphere containing 5% CO_2 and 35°C before treatment was performed as was described by (Stoppini *et al.*, 1991). Slice cultures were maintained in 1.2 ml culture medium (tab. 2.16), so that the surface of the slices cannot dry out and the medium was replaced every 2-3 days.

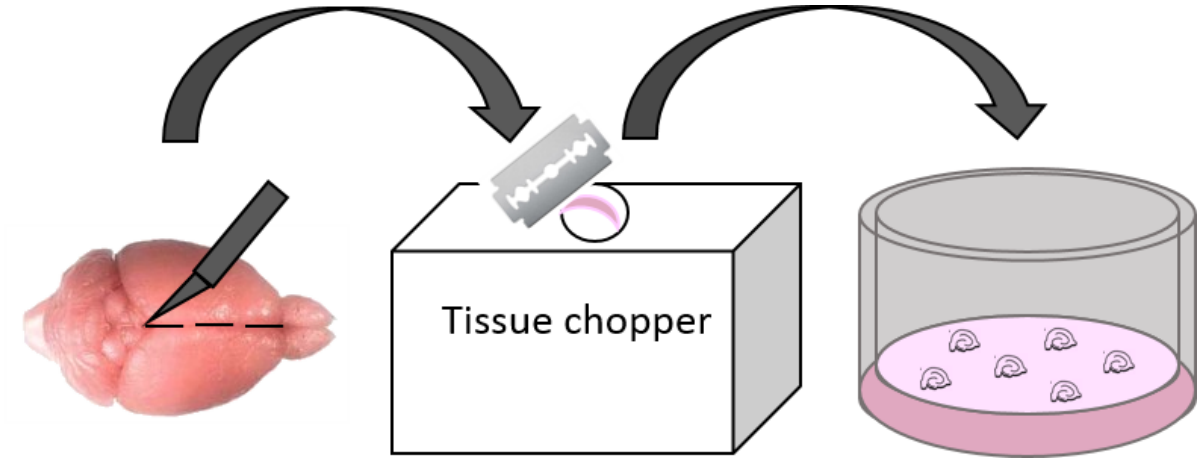

Figure 2.1: Preparation and cultivation of organotypic hippocampal slice cultures. *Brains were cut in hemispheres using a scalpel. Hippocampi were cut using tissue chopper and cultured on membrane inserts. Per membrane insert 6 slices are applied and the well is filled with exactly 1.2 ml of OHSC medium that forms a thin layer on top of the slices by capillary forces.*

Table 2.16: Composition of OHSC medium for a total of 100 ml, pH 7.2.

Component	Amount
Aqua ad inijectabilia	41.6 ml
Minimum Essential Medium (MEM) 10x	5 ml
Basal Medium Eagle + Earle' s (BME) 1x	25 ml
Hyclone Donor Equine Serum	25 ml
GlutaMax 100x	1 ml
45% D-(+)-glucose solution	1.44 ml
Sodium bicarbonate solution 7.5 %	For adjustment of pH

2.2.6 Depletion of microglia from OHSC

For the specific depletion of microglia from slice cultures, clodronate disodium salt (Merck Millipore, Darmstadt, Germany) that was prior dissolved in *aqua ad injectabilia* and aliquoted at 1 mg/ ml was dissolved in culture medium at a concentration of 100 µg/ ml and added to the slices at the day of preparation for 24 hours. The following day, slices were washed with

warm PBS and slices were transferred onto a new culture plate with fresh culture medium for further cultivation.

2.2.7 Internalization assay

Binding ability and internalization of GLAST-1, EAAT2 and AQP4 was investigated using the pHAb amine and thiol reactive-dyes kit according to the manufacturer's protocol (Promega). pHAb reactive dyes are pH sensitive and when internalized into the cytoplasm and the lysosome, due to the acidic pH, fluorescence increases and can be taken as a measure of internalization.

Antibodies were desalted by buffer exchange using Zeba™ columns (Pierce) and amine conjugation buffer (10 mM sodium bicarbonate buffer, pH 8.5). The dye was shortly centrifuged and reconstituted to 10 mg/ml in a DMSO and aqua bidest. mix at a ratio of 1:1 and thoroughly mixed by vortexing.

For the conjugation of the dye and antibody, per 100 µg of antibody 1.2 µl of dye-solution were added and incubated at room temperature and constant shaking for 1 hour in dark conditions. To remove unconjugated dyes, the solution was purified using Zeba™ columns and the antibody to dye ratio was calculated as follows.

Antibody concentration (mg/ml): $\frac{A_{280}-(A_{532} \times 0.256)}{1.4}$

Dye-to-antibody ratio (DAR): $\frac{(A_{532} \times 150{,}000)}{(Ab\ concentration\ (mg/ml) \times 75{,}000)}$

- 150,000: Molecular weight of antibody
- 75,000: Extinction coefficient of pHAb reactive dye
- 0.256: Correction factor for pHAb reactive dye

Astrocytes were seeded at densities of 10,000 – 30,0000 cells/ well in 24-well-plates and treated with various concentrations of the antibody-dye conjugate (0.5, 1; 2.5; 5 µg/ml) that was diluted in culture medium. Plates were measured at starting point (0 hours) and after 4, 20 and 24 hours using a plate reader (Infinite M1000, Tecan) at λ: E_x: 532 nm and E_m: 560 nm. Plates were once measured in culture medium and once the media was replaced by PBS.

2.2.8 Immunoablation of astrocytes by toxin-coupled antibodies *in vitro* and *ex vivo*

For the ablation of astrocytes derived from mixed glial cultures and embryonic cells, astrocytes were plated on 96 well-plates at a density of 6,000-10,000 cells per well (100 µl) in glial culture medium and incubated for 1-3 days before treatment started. Various concentrations (0.25-1 µg/ml) of EAAT1/GLAST-1 (Abcam, Cambridge, UK; clone EPR12686) and anti-rabbit-saporin (Rab-ZAP; Advanced Targeting Systems, San Diego, USA) antibodies were generated by dissolving both in culture medium. After 30 minutes of incubation at room temperature, antibody-solutions were added to the cells and incubated for additional 3 days. As controls, only primary or secondary antibodies at corresponding concentrations and 1 M sodium hydroxide (NaOH) were added to the cells. On the third day of incubation, treatment was repeated for another 3 days.

Additionally, as a primary target anti-Aquaporin 4 (AQP4; Abcam, Cambridge, UK) antibody was used. On the last day of incubation, cell viability was assessed using MTT-assay.

For the immunoablation of astrocytes from slice cultures, higher concentrations were used (1-5 µg/ml) of both antibodies. The treatment of slices began on the 6th day of incubation and was repeated every second day for a total of 7 days. On the last day of incubation, slices were fixated with 4% PFA and either stored in PBS or immunofluorescent staining was performed.

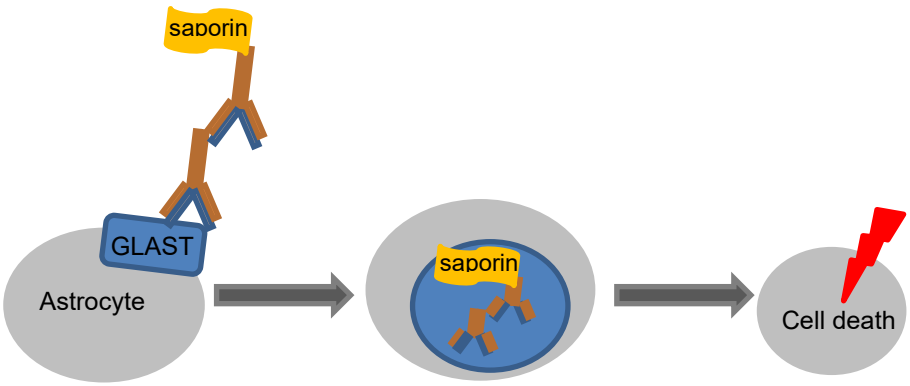

Fig. 2.2 Schematic drawing of the immunoablation using Rab-ZAP technology. *Astrocytic cells expressing GLAST-1-transporters on the cell surface are targeted by primary antibodies. Suitable secondary antibodies coupled with saporin-molecules bind to primary antibodies; the complex is internalized into the cytosol. Once inside the cell, the saporin-molecule is released from the antibody and can lead to apoptosis of the cell.*

2.2.9 Depletion of astrocytes *in vitro*

Astrocytes were plated on 96 well-plates at a density of 6,000 – 10,000 cells per well (100 µl) and incubated for 1-3 days before treatment. The gliotoxin L-α-amino adipic acid (Lα-AAA; Abcam, Cambridge, UK) was dissolved in aqua bidest. to yield a concentration of 2 mg/ml. The pH was adjusted with 1 M NaOH to a final between 6 and 7.5 with a concentration of 11.55 mM. For the treatment of cells, Lα-AAA was dissolved in culture medium to various concentrations (0.125 - 10 mM). As controls, cells were treated with 100 mM NaOH and the vehicle (bidest. + NaOH). The treatment was either repeated over various timepoints or performed once and then cells were incubated for several days. After the incubation, the cell viability was assessed using CytoGlo-assay (Promega, Madison, USA).

2.2.10 Depletion of astrocytes *ex vivo*

For the depletion of astrocytes from slice cultures, different concentrations and durations of treatment were used. Additionally, slices were either treated on the first, second or sixth day of incubation after preparation. Lα-AAA was prepared in several ways to achieve higher molecular solutions. First, the compound was dissolved in pure aqua bidest. (250 mg in 20 ml ~ 77.5 mM), this solution was cloudy, and the powder precipitated, even after ultrasonic bath incubation. Because the solving process just described yielded a precipitated solution and according to the manufacturer, the powder is less soluble in water, but could be dissolved in 1N HCL, the powder was dissolved in 1N HCL (24.5 mg in 1 ml ~ 152.02 mM). After the addition to culture medium for dilutions, the medium shifted towards acidic (pH 1.4). Since an acidic pH is toxic to cells, the pH was adjusted to 7.2 by the addition of sodium bicarbonate.

Another solution was made by directly solving the powder in OHSC culture medium (10 mM), again the pH was adjusted to 7.2 by sodium bicarbonate. Both approaches yielded a cloudy solution that was unable to be sterile filtered and was therefore rejected.

In another attempt, 250 mg Lα-AAA was dissolved in 20 ml aqua bidest. and 5 ml 1N HCL (~ 62.05 mM). A 30 mM dilution was made in culture medium and pH was adjusted to 7.2 by the addition of 7.5 ml sodium bicarbonate (17.14 mM). From this stock solution several dilutions were made in culture medium (2; 5; 10 and 12.5 mM). Thereby at 10 and 12.5 mM the added solution exceeded the volume of medium. The slices treated with these solutions,

either directly detached from the membrane inserts after fixation or during staining processes and could not be analysed using confocal laser scanning microscopy. Lα-AAA (10 mg) was also tried to be dissolved in little amounts of 1N HCL (90 µl) and aqua bidest. (910 µl), to diminish the amount of HCL in the stock solution. Nevertheless, pH dropped to 1, due to the amino acid itself. 2, 5- and 10-mM dilutions were prepared in culture medium, without the adjustment of pH. As a result, most of the slices were detached from the membrane inserts during the staining process and could not be further examined. Final experiments were made with the same solution that was used in *in vitro* experiments.

2.2.11 Immunoablation of oligodendrocytes *in vitro*

For the immunoablation of oligodendrocytes, *Oli-neu* cells were seeded at a density of 2,000 – 10,000 cells per well and incubated for 24-72 hours prior to treatment. Like the immuno-ablation of astrocytes, an antibody complex consisting of a primary and a suitable secondary toxin-coupled antibody was used. Two complexes were designed and tested. G protein coupled receptor 17 (GPR17) belongs to the G protein coupled receptor 1 family and is localized in the cell membrane of cerebellar oligodendrocyte precursor cells (OPCs) (Viganò *et al.*, 2016). Anti-GPCR GPR17 (Abcam, Cambridge, UK) is a goat polyclonal antibody, therefore the anti-goat-saporin antibody (Gab-ZAP; Advanced Targeting Systems, San Diego, USA) was chosen as suitable secondary candidate. The second complex consisted of an anti-Claudin-11 (Thermo Fisher Scientific Inc., Waltham, USA) antibody in combination with an anti-rabbit-saporin secondary antibody (Rab-ZAP). Claudin-11 is an oligodendrocyte-specific target that is expressed on the cell membrane and tight junctions of myelin sheaths (Morita *et al.*, 1999).

2.2.12 Cell viability assessment (MTT assay and Celltiter Glo)

To determine cell viability, colorimetric MTT assay was performed. The principle of this assay is that mitochondrial enzymes of viable cells can convert the yellow compound methyl-thiazolyl diphenyl tetrazolium bromide (MTT; Sigma-Aldrich, Taufkirchen, Germany) into a blue-violet formazan as was previously described (Mosmann, 1983) (fig. 2.3). This conversion can be measured by absorption that correlates with cell viability.

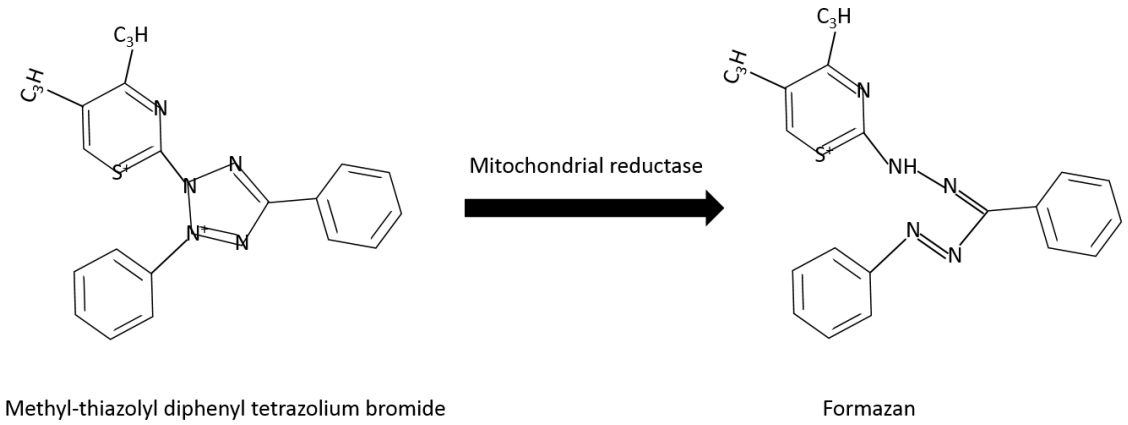

Figure 2.3: Principle of the MTT assay. *Conversion of tetrazolium bromide into formazan by mitochondrial reductase activity of viable cells leads to a shift in absorption levels that can be measured using plate reader techniques.*

To do so, MTT-working solution was diluted to a final concentration of 0.5 mg/ml in culture medium and was added to the cells and incubated for 1 hour in humidified atmosphere at 37°C. In a next step, the whole medium was removed, and cells were frozen at -80°C for 1 hour. Afterwards, DMSO was applied to solve the purple dye and cells were incubated for another hour at room temperature with mild shaking. Absorbance was measured at λ = 570 nm using a microplate reader (Infinite M200, Tecan, Männedorf, Switzerland).

Another way to determine cell viability is to measure adenosine triphosphate (ATP) concentration in the supernatant of cells that were treated with Lα-AAA for several days. Therefore, the CellTiter-Glo® 2.0 Cell viability assay (Promega, Madison, Wisconsin, USA) was utilized by adding 100 µl of the ready-to-use solution per well and incubated the plate with mild shaking for 2 minutes in dark conditions. Afterwards, the plate was additionally incubated in the dark without shaking. Luminescence was measured using a microplate reader (Infinite M200, Tecan, Männedorf, Switzerland).

2.2.13 Preparation of amyloid beta species

Recombinant amyloid beta ($A\beta_{42}$) (Bachem, Bubendorf, Switzerland) was delivered lyophilized and stored at -20°C. Before usage, the peptide was dissolved in hexafluorisopropanol (HFIP; Sigma-Aldrich, Taufkirchen, Germany) at a concentration of 1 mg/ml. After 30 minutes of incubation at room temperature, peptide solution was aliquoted at 100 µg into low-binding tubes and sonicated for 15 minutes. Using a speed vac, HFIP was evaporated from the tubes and remaining peptide was stored at -80°C.

Before treatment, monomeric $A\beta_{42}$ aliquots were dissolved in 5 % dimethylsulfoxide (DMSO; AppliChem, Darmstadt, Germany), mixed rigorously by vortexing and added up with 95 % PBS to yield a concentration of 1 mg/ ml. To produce oligomeric $A\beta_{42}$, aliquots dissolved in DMSO and PBS were incubated for 24 hours at 37°C and mild shaking at 50 rpm. Monomeric and oligomeric $A\beta_{42}$ could be stored at -80°C for up to 120 hours.

2.2.14 Treatment of slice cultures with amyloid beta

One week after preparation, slices were treated with different concentrations of oligomer-enriched $A\beta_{1\text{-}42}$ solution diluted in PBS (1 µM and 2 µM). Dilutions were added to the slices as small droplets by pipetting a maximum of 2 µl on top of each slice. Treatment of slices following a complete media change every two days for a total of seven days incubation.

2.2.15 Immunofluorescence staining of cells

Cells were plated on chamber slides and incubated for two to three days. When cells have grown and differentiated, medium was removed, and chambers were washed with 1x PBS. Afterwards, chambers were filled with 4% PFA for fixation at 4°C for 30 minutes to one hour.

After washing chambers in 1x PBS for 3 times, cells were blocked in 1% BSA-PBS for one hour at room temperature. Primary antibodies (tab. 2.17) were diluted 1:1000 in PBS + 0.1% Triton-X and incubated for one hour at room temperature. Following three washing steps, secondary antibodies (tab. 2.17) were diluted 1:1000 in PBS + 0.1 % Triton-X for 30 minutes at room temperature.

Table 2.17: List of primary and secondary antibodies and species.

Primary antibody	**Species**
Anti-GFAP	goat
Anti-GPR17	goat
Anti-Iba1	rabbit
Anti-NeuN	mouse
Anti-O4	mouse
Anti-PLP	chicken
Secondary antibody	**Species**
Anti-chicken-AlexaFluor594	donkey
Anti-goat-AlexaFluor555	donkey
Anti-mouse-AlexaFluor488	donkey
Anti-rabbit-AlexaFluor647	donkey
Anti-rat-AlexaFluor594	goat

After the last three washing steps, grids from chamber slides were removed and cells were embedded in “Dako Fluorescent Mounting Medium” (Dako, Agilent Technologies, Glostrup, Denmark) and kept in dark at 4 °C until further use. Confocal laser scanning microscopy (Leica SP8) with a dry plan apochromat CS 20x/ 0.7 objective was used for the visualization of fluorescence signals.

2.2.16 Immunofluorescence staining of OHSC

Slices were either treated with different concentrations of $A\beta_{1-42}$ (0.25, 0.5, 1, 10 µg/ml) or PBS as control for a duration of 48 hours to 7 days. Additionally, 24 hours before treatment, slices were pre-incubated with 100 µg/ml clodronate to remove microglial cells. After the incubation of 7 days, the medium was removed from the wells and slices were washed once in warm 1x PBS, before they were fixated in 4 % paraformaldehyde (PFA) for at least 30 minutes. Then slices were washed 3 times in cold PBS. Afterwards, slices were cut off the membrane inserts with a scalpel and transferred into a 24-well plate containing 500 µl of 3 % BSA in PBS blocking solution. Blocking lasted 1 hour, then slices were washed again 3 times in 1x PBS for 20 minutes.

Staining of cells was done by using primary antibodies directed against specific marker proteins (tab. 2.18), diluted 1:1000 in immunostaining buffer I (tab. 2.19) and incubation took place over night at 4°C.

Table 2.18: list of primary and secondary antibodies and species.

Primary antibody	**Species**
Anti-CNPase	goat
Anti-GFAP	goat
Anti-IbA1	rabbit
Anti-NeuN	**mouse**
Anti-PLP	chicken
Secondary antibody	**Species**
Anti-mouse-AlexaFluor488	donkey
Anti-goat-AlexaFluor555	donkey
Anti-rabbit-AlexaFluor647	donkey

The following day, the fluorescent-labeled secondary antibodies (tab. 6) were diluted 1:1000 in immunostaining buffer II without Triton-X (tab. 7), applied to the slices and incubated for 2 hours at room temperature. Again, slices were washed 3 times in PBS for 20 minutes,

transferred onto glass microslides and embedded in “Dako Fluorescent Mounting Medium” and kept in dark at 4 °C until further use.

Table 2.19: composition of immunostaining buffer I and immunostaining buffer II.

Component	Amount
Bovine serum albumin (BSA)	3 g
Triton-X (only immunostaining buffer I)	0.4 g
NaN_3	0.1 g
PBS	*ad* 100 ml

Confocal laser scanning microscopy (Leica SP8) with a dry plan apochromat CS 20x/ 0.7 objective and a fluorescence microscope (Zeiss, AxioObserver) with an 5x and 10x dry objective was used for the visualization of fluorescence signals. Immunofluorescence images were analyzed by ImageJ (Fuji) by comparing fluorescence signals from different conditions regarding GFAP- or IbA1-signal.

2.2.17 Statistical Analysis

Data from the internalization assays are given as relative fluorescence units with no normalization in order to compare different antibodies. Data from the viability assays are given as mean values ± standard deviation (SD) from multiple repeats per condition of one or multiple experiments as stated in figure legends. Untreated controls were set as 100 % and treatment conditions were normalized to that unless as stated otherwise. All statistical tests were performed with Microsoft Excel and data was previously checked for normal distribution using the Anderson Daling test. Significance was tested using student’s t-test with parameters: single-sided and paired. *p*-values were indicated with asterisks (not significant (n.s.) > 0.05; ** $p < 0.05$; ***$p < 0.001$).

3. Results

3.1 Microglia

To investigate amyloid-beta mediated cytotoxicity in slice cultures, it is necessary to verify that specific cell types can be depleted from the slices. First, experiments were done with *BV-2* cells a microglia cell line and the bisphosphonate clodronate.

3.1.1 Depletion of BV-2 cells by clodronate *in vitro*

The cytotoxic ability of non-capsulated clodronate on the murine microglia cell line *BV-2* was investigated using cell viability assessment assays. In a first attempt, 6,000 cells per well were seeded and cultivated for 24 hours, before treatment with 100 µg/ml clodronate started. As a positive control 1 M NaOH was added to the cells. Additionally, untreated cells served as a negative control. After additional 24 hours cell viability was assessed using MTT assay (fig. 3.1 A). Interestingly, even the positive control did not sufficiently kill all cells. Moreover, clodronate treatment exceeded untreated controls (102.31 %), whereas there is a high standard deviation (28.22 %).

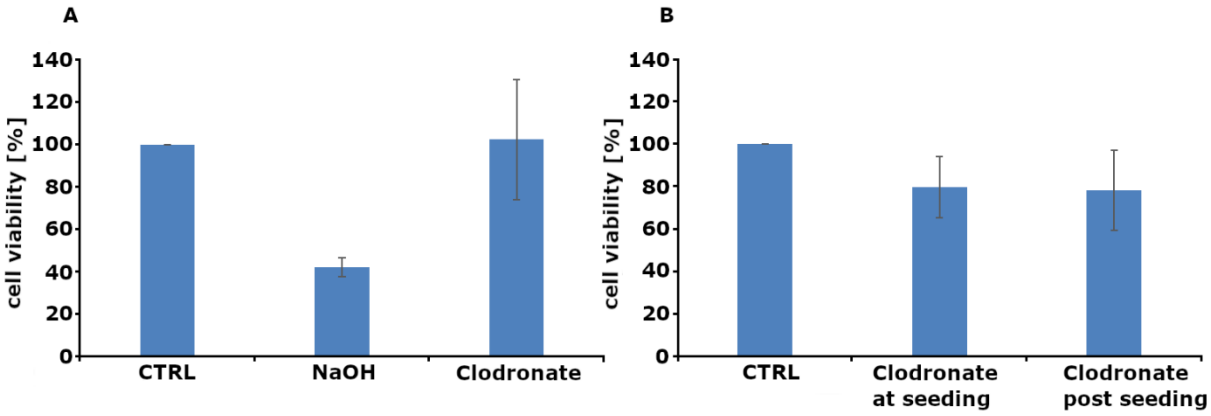

Fig. 3.1 *BV-2* cells are not severely affected by clodronate treatment assessed by MTT. A *BV-2 cells were seeded at a density of 6,000 cells/well of a 96-well plate and incubated for 24 hours prior to treatment. Cells were treated with 1 M NaOH and 100 µg/ml clodronate for additionally 24 hours.* ***B*** *BV-2 cells were seeded at a density of 10,000 cells/ well of a 48-well plate and incubated for 24 hours prior to treatment. Cells were either treated with 100 µg/ml clodronate on the day of seeding (pre-treatment) or 24 hours later, then cells were additionally incubated for 24 hours. MTT assay was performed to measure cell viability. Mean values ± SD of one experiment are shown.*

Since clodronate treatment for 24 hours had little to no effects compared to the control conditions, the same experiment with a pre-treatment condition was performed. On the day of seeding, 100 µg/ml clodronate was added to the cells concurrently. The next day, remaining cells were treated with 100 µg/ml clodronate and all cells were incubated for another 24 hours before cell viability assessment was performed (fig. 3.1 B). Now, both treatment conditions had little effects on the cell viability compared to control conditions. Moreover, both conditions only differ in about 1 % (pre-treatment 79.85 % and treatment 78.25 %), though standard deviations of both conditions are quite high (14.27 % and 18.77 %).

3.1.2 Depletion of microglia from slice cultures

Depletion of microglial cells from organotypic hippocampal slice cultures was successfully done by the pre-treatment of slices with clodronate. Clodronate was added to the culture medium at the day of preparation. The next day, slices were once washed in PBS and cultivated for another 6 days before immunofluorescence staining or treatments with Aβ occurred. This method is widely used and was done according to (Richter *et al.*, 2020) and does not affect neurons or other glial cells (Vinet *et al.*, 2012).

There is no total depletion achievable, since individual IbA1-positive cells still are detectable (fig. 3.2 D-F). But more than 50 % have been depleted compared to untreated slices (fig. 3.2 A-C). Mean intensity and individual intensities of six slices per condition were analysed and summarized in fig. 3.2 G. A significant difference was observed (*p*-value*:* 0.0008). More important, the architecture of the slices and especially the number and viability of neurons (NeuN staining) was not affected by the chemical, making clodronate a useful tool for further studies where depletion of microglia is required. Interestingly, depletion of microglia was more effective in slice cultures compared to *in vitro* experiments, indicating that *BV-2* cells react different from primary cells and seem not to be a good model to study the role of microglia in the context of neuroinflammation and Aβ. Additionally, this reveals that slices are a more suitable way to investigate the influence of individual cells in the complex of more cell types.

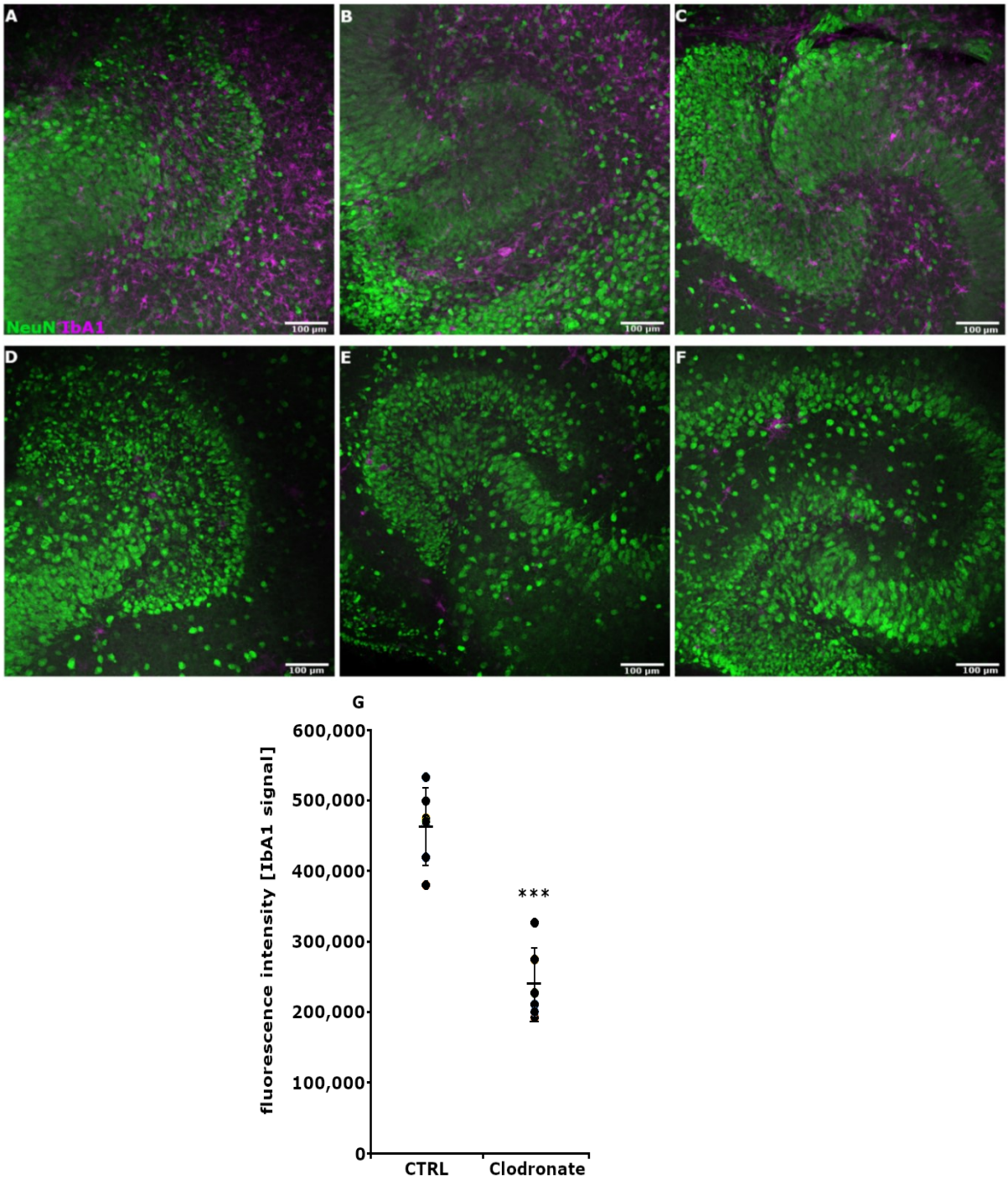

Fig. 3.2 Depletion of microglia from OHSCs is almost completely done with clodronate. *Most microglia were successfully depleted from organotypic hippocampal slice cultures using 100 µg/ml clodronate (D-F) for a duration of 24 hours. Untreated slices (A-C) served as controls. NeuN (green) was used for staining of neurons and IbA1 (purple) was used for the staining of microglia. Images were taken with a Leica SP8 confocal laser scanning microscope at a magnification of 20x/0.70 and a zoom of 0.75.* ***G*** *shows individual IbA1 signal intensity of untreated and clodronate treated slices, 6 slices per condition were analyzed. Black line indicates mean ± SD. *** $p < 0.001$.*

3.1.3 Induction of cytotoxicity by amyloid-beta species in OHSCs

To test whether the application of an oligomer-enriched Aβ-solution has an impact on cellular survival, 2 µM of two amyloid species (monomeric and oligomeric) were applied on top of each slice every second day in combination with a media change. On the 7th day of incubation, slices were stained with PI and fixated with PFA before immunofluorescent staining was performed. Compared to control slices (fig. 3.3 A), there were barely any PI-positive cells in both conditions (fig. 3.3).

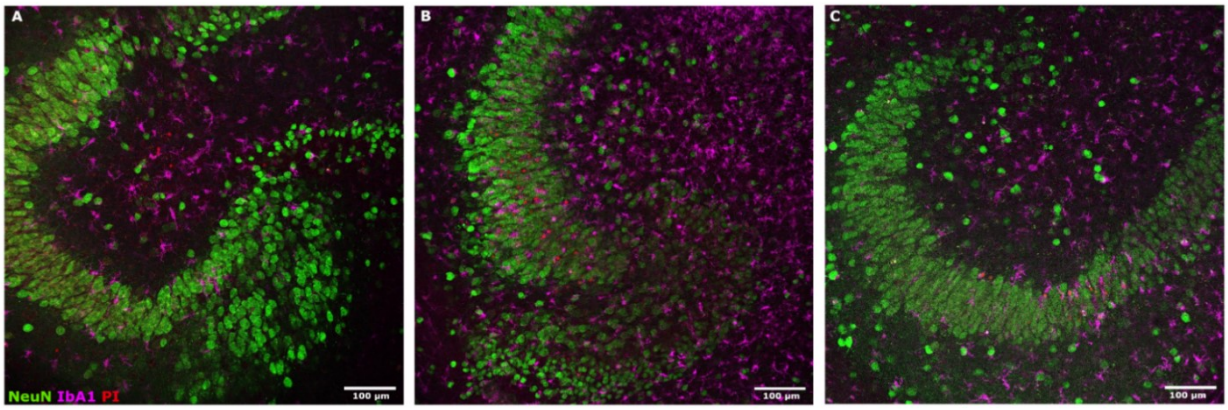

Fig. 3.3 Slices are not affected by treatment of with mono- and oligomeric amyloid beta-species. *Slices were cultured for 6 days with culture medium. On the 7th day, either monomeric (B) or oligomeric (C) amyloid beta solution at a concentration of 2 µM was applied on top of each slice. This procedure was repeated every second day for a duration of 7 days. Immuno-fluorescence staining was performed (neuronal cells NeuN: green; microglia IbA1: purple). Cell death was visualized by PI (red).*

In all three conditions, microglia display a ramified and "resting" shape and the cell architecture of slices and neurons remained intact. Since microglia did not adapt their morphological shape towards amoeboid, they are stated to be not reactive or induced by the application of Aβ. Only a few PI-positive cells were detected when slices were treated with monomeric $A\beta_{42}$ (B). This could have numerous reasons besides the treatment application. To investigate the role of microglia in amyloid-beta induced toxicity, half of the slices were treated with clodronate for 24 hours to specifically deplete microglia. After an incubation of 6 days with constant media changes, slices were treated with various concentrations of an oligomer-enriched $A\beta_{42}$-solution. The concentrations that were used ranged from 0.3 to 1.6 µM.

The treatment was repeated every second day including a media change. After 7 days of incubation, slices were stained with PI and fixated with PFA in order to conserve the cell structure and steady-state protein levels. Immunofluorescence was performed as described in (2.2.16) and images were obtained using a confocal laser scanning microscope. Representative images are shown in fig. 3.4. Additionally, cell death was calculated and plotted regarding the oligomer-concentration (E and F). Interestingly, in slices containing microglia (B) barely any cell death was visualized with PI staining, whereas in slices that were pre-treated with clodronate (D) and treated with the oligomer-enriched solution a considerable increase of cell death verified by PI staining was observed. Moreover, cell death was significantly increased with an increased oligomer-concentration, but solely in slices without microglia (E and F). Data taken from the doctoral thesis of Dr. Maren Richter and the publication from Richter and Vidovic *et al.* (Richter *et al.*, 2020).

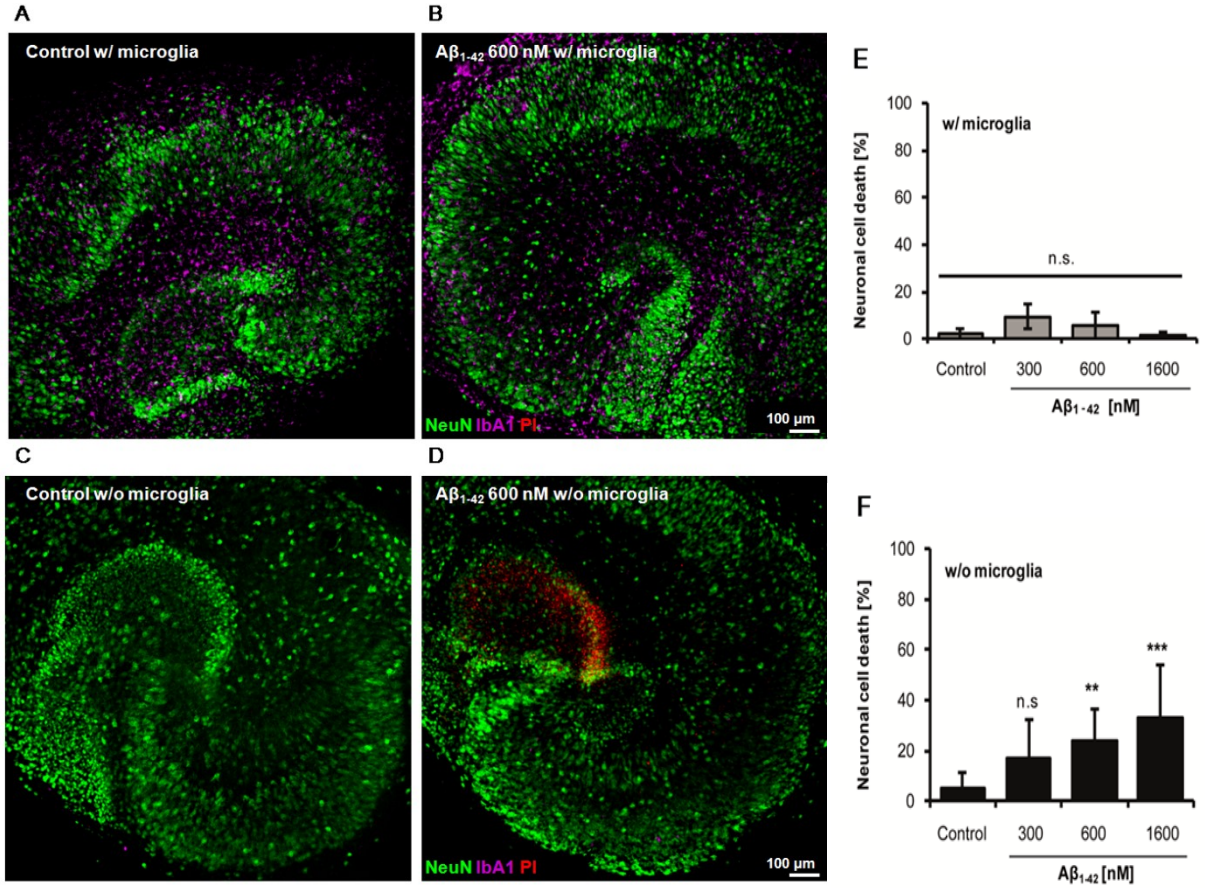

Figure 3.4 Microglia provide protection of neuronal cells against beta-amyloid induced cell death in slice cultures. *Slice cultures were cultured for 6 days either with (C and D) or without (A and B) a pre-treatment of 100 µg/ml clodronate for 24 hours. Slices were treated with different concentrations of an oligomer-enriched beta-amyloid solution (300, 600, 1600 nM) for 7 days. Untreated slices served as control. Immunocytochemistry was performed for neuronal (NeuN) and microglial staining (IbA1). Additionally, cell death was visualized using PI staining. Representative images are shown. Images were taken with an LSM 510 META laser scanning microscope (Carl Zeiss, Jena, Germany) at a magnification of 10x.* ***E*** *Quantification of neuronal cell death after treatment of slices with different concentrations of an oligomerized Aβ42-solution for 7 days. Slices were stained with NeuN and PI and cell death was calculated as PI-signal divided by NeuN-signal.* ***F*** *Quantification of neuronal cell death after treatment of microglia-depleted slices with different concentrations of an oligomer-enriched Aβ42-solution for 7 days. Mean values ±SD of 3 independent experiments are shown. Not significant (n.s.) > 0.05; ** p < 0.001; *** p < 0.001. Data taken from Richer et al. (Richter et al., 2020).*

3.2 Astrocytes

3.2.1 Finding the right antibody for toxin-induced ablation of astrocytes

Since the existence of microglial cells in slice cultures is detrimental to neuronal survival, the role of astrocytic cells still needs to be investigated. Next to microglia, astrocytes are also capable of releasing cytokines of pro- and anti-inflammatory origin as responds to cellular and environmental stress signals. To further investigate their putative role in inflammation and neurodegeneration, a way to distinctive deplete these cells from the slices is needed. For this purpose, a method designed by the manufacturer Advanced Targeting Systems (ATS) using toxin-coupled antibodies was adapted (Kohls and Lappi, 2000). A similar work was published by Pilkington's group from the University of Portsmouth. The authors designed an antibody-complex to deplete NG2 and $GD3^A$ positive cells from glioblastoma cells (Higgins *et al.*, 2015). The principle behind this method is described in section 2.2.8. Briefly, a primary target on the cell surface of the desired cell type is targeted with a suitable antibody. Additionally, a suitable secondary antibody is used. This secondary antibody is bound to a saporin molecule, referred to as the toxin. In theory, both antibodies should form a complex that can bind to the cell surface target and subsequently will be internalized into the cell's cytoplasm. Once inside the cells, brought to the lysosome, the toxin molecule will be released from the antibody and the cell will undergo apoptosis.

The initial idea was to find a surface target, e.g. a receptor or transporter, that is exclusively expressed on astrocytes in the hippocampus of mice. The excitatory amino acid transporter 1 (EAAT1), called glutamate aspartate transporter (GLAST-1) in rodents was found to be a suitable candidate, since it is predominantly expressed by astrocytes (Kirkley *et al.*, 2017; Parkin *et al.*, 2018). In addition, aquaporin 4 (AQP4) was also tested on its binding ability on murine astrocytes *in vitro* since it is a specific water channel expressed by astrocytes (Zhang *et al.*, 2014b). Therefore, internalization assays were performed using the pHAb reactive dye-kit (section 2.2.6). Antibody-conjugates and corresponding Dye-to-Antibody Ratios (DARs) were measured and dilutions of 1:10 and 1:50 of each conjugate were made in medium and added to the cells. At timepoints 0, 2, 4, 21- and 24-hours fluorescence measurements were performed with a plate reader and results are plotted in fig. 3.5 A. According to the DAR, AQP4 conjugation (DAR: 3.3) with pHAb-sensitive dye was higher than conjugation to GLAST-1 (DAR: 2.5). But also, antibody concentration of AQP4 was higher than of GLAST-1 when conjugation

took place, resulting in a two-fold higher dilution-concentrations (fig. 3.5 B). Higher concentrations led to higher intensities as observed at initial measurement (0 hours). AQP4 already had a baseline intensity of 3741 RFU at a dilution of 1:10 (36.5 µg/ml; red dots), whereas the 1:50 dilution reached 1241 RFU (yellow dots). With time, intensities of all conjugates increased until a peak at 2 hours was reached. Thereafter, intensities decreased again in all conditions. Intensities of AQP4 reached a maximum of 8621 RFU whereas GLAST-1 had its peak at 2261 RFU. Overall, the lowest intensities were obtained when GLAST-1 was diluted at 1:50 (3.5 µg/ml; orange dots).

A

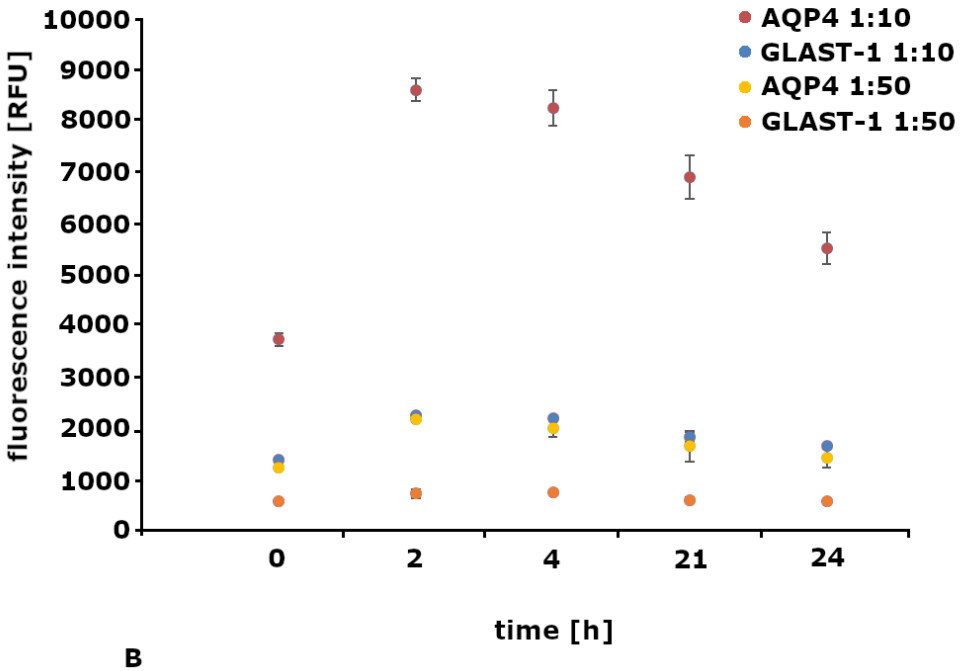

B

	Dye-Antibody-Ratio	Concentration [µg/ml]	
Dilution		1:10	1:50
AQP4	3.3	36.5	7
GLAST-1	2.5	18	3.5

Fig. 3.5 Targeting Aquaporin 4 and GLAST-1 in Astrocytes results in enhanced fluorescence intensity over a time period of 24 hours *in vitro*. *Primary astrocytes were seeded on a 96-well plate and incubated with dilutions (1:10 and 1:50) of AQP4-dye and GLAST-1-dye conjugates. The plate was measured containing medium at 0, 2, 4, 21- and 24-hours. Cells were incubated at 37°C between measurements.* ***A*** *Fluorescence intensity measurement of antibody-dye conjugates at various time points. Mean values ± SD of 6 wells per condition is shown.* ***B*** *Overview of DAR and concentrations of dilutions for each conjugate.*

Consistently, higher concentrations of antibody-dye conjugate led to higher intensities (fig. 3.6) that are comparable to the intensities achieved in fig. 3.5 though the peak is obtained after 20 hours of incubation. After 24 hours, intensity decreased again, but did not attend baseline-levels. Interestingly, when the plate was measured after 41 hours of total incubation, intensity still decreased at all concentrations. Only 1 and 0.5 µg/ml of antibody-dye conjugate resulted in intensities lower than baseline.

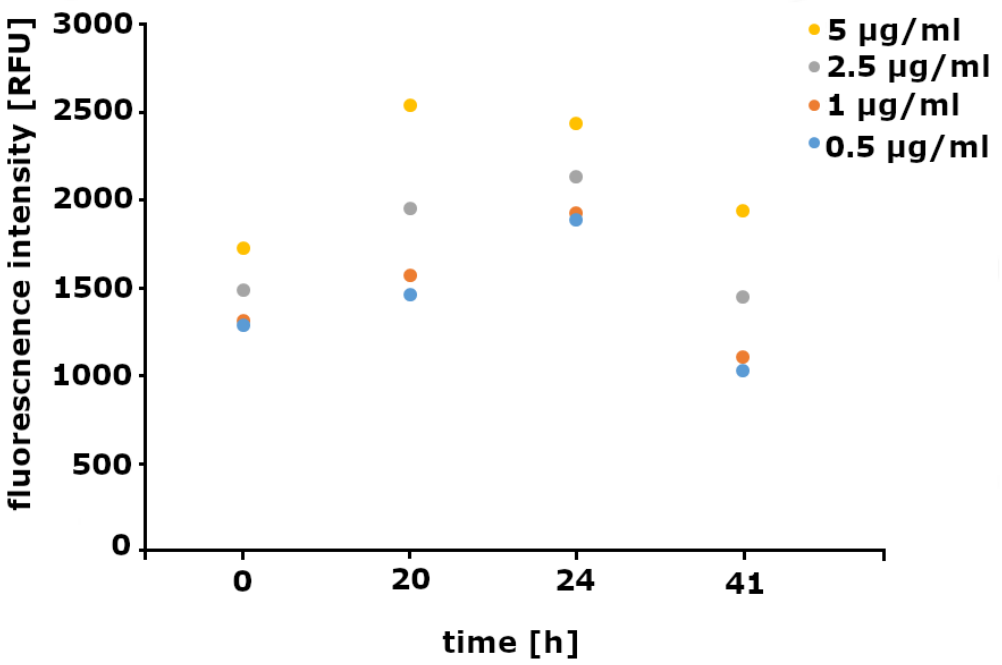

Fig. 3.6 Concentration dependent fluorescence increase of GLAST-1 internalization in astrocytes. *Cells were seeded at 30,000 per well in a 24-well plate and incubated for 3 days before treated with various concentrations of antibody-dye-conjugate (0.5-5 µg/ml). Dye-Antibody-Ratio: 4. At timepoints 0, baseline measurement was done. Mean values of three wells per condition and time point are shown.*

A concentration and time dependent increase of fluorescence intensities is well observed as well as an increase in fluorescence over a longer period due to slow antibody internalization or low antibody binding properties (Nath *et al.*, 2016).

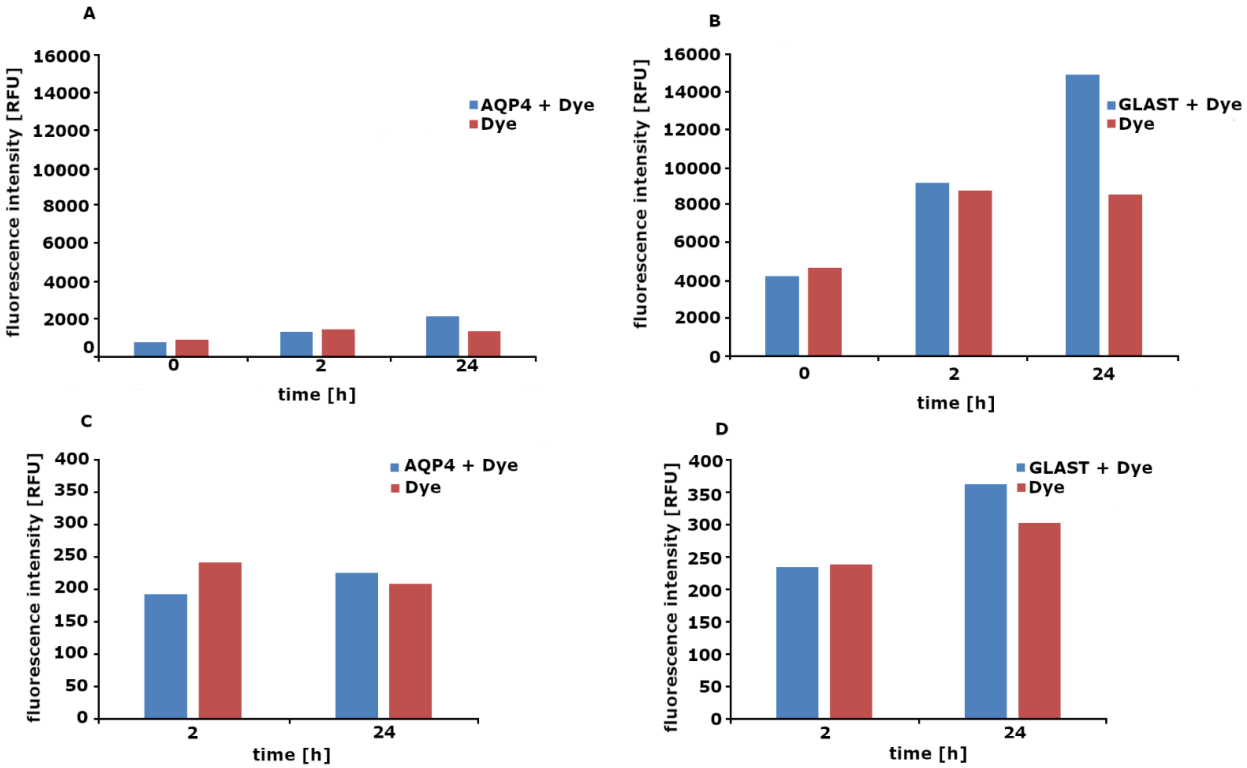

Fig. 3.7 Comparison of two antibodies on their ability to be internalized in astrocytes by pHAb reactive dye measurement. *Primary astrocytes were seeded at a density of 30,000 cells per well in a 96-well plate. Cells were either treated with 1 µg/ml of an antibody-dye conjugate (blue) or the dye alone in the corresponding concentration to the antibody conjugate (red). Plates were measured in medium after 0, 2- and 24-hours of incubation.* ***A*** *The antibody conjugate consisted of Aquaporin 4 (DAR: 3.3) in* ***B*** *the conjugate consisted of GLAST-1 (DAR:19.34). Two wells per condition, mean values of one experiment are shown.* ***C*** *and* ***D*** *Supernatant was collected in fresh tubes and wells were washed twice with PBS and measured in PBS after 2 and 24 hours.*

Striking, both antibody-conjugates (red bars) tend to have higher fluorescence intensities over time in comparison to the corresponding controls (blue bars). Whereas the effect of AQP 4 (fig. 3.7 A) is only small, the effect of the GLAST-1-conjugate (fig. 3.7 B) is almost double of that from the control after 24 hours.

Again, there is an increase already after 2 hours of incubation, but intensity even increases up to 16,000 RFU after 24 hours. Though the DAR of GLAST-1 used in this assay is extremely high,

there is a clear difference between the dye alone treatment and antibody-dye treatment except for the baseline measurement. This indicates that at the beginning of the experiment, little fluorescence was measured when the dye was applied to cells.

Plates were additionally measured in PBS after 2 and 24 hours when washed twice with PBS, to remove the unbound antibody conjugates and dyes (fig. 3.7 C and D). The supernatant containing the antibody-conjugates were collected in fresh tubes and applied again after the measurement. The overall values of PBS measured wells are much lower compared to measurements made in medium. Nevertheless, the same picture concerning GLAST-1 higher intensities remains compared to AQP4 and the dye-treatment alone. Whereas the effect between the dye and GLAST-conjugate is not as high as when measured in medium (fig. 3.7 B). Furthermore, both antibodies result in higher intensities after 24 hours compared to the 2 hours measurement. For additional controls and to verify the results, another experiment was performed. As a negative control, intravenous IgGs (IVIg; Octagam 10%, Octapharma) were conjugated with the dye and applied to cells as well. Astrocytes should not react to exposure with IVIgs. Furthermore, a different antibody against GLAST-1 (GLAST-1 from Santa Cruz (Sc)) from another company was also tested (fig. 3.8).

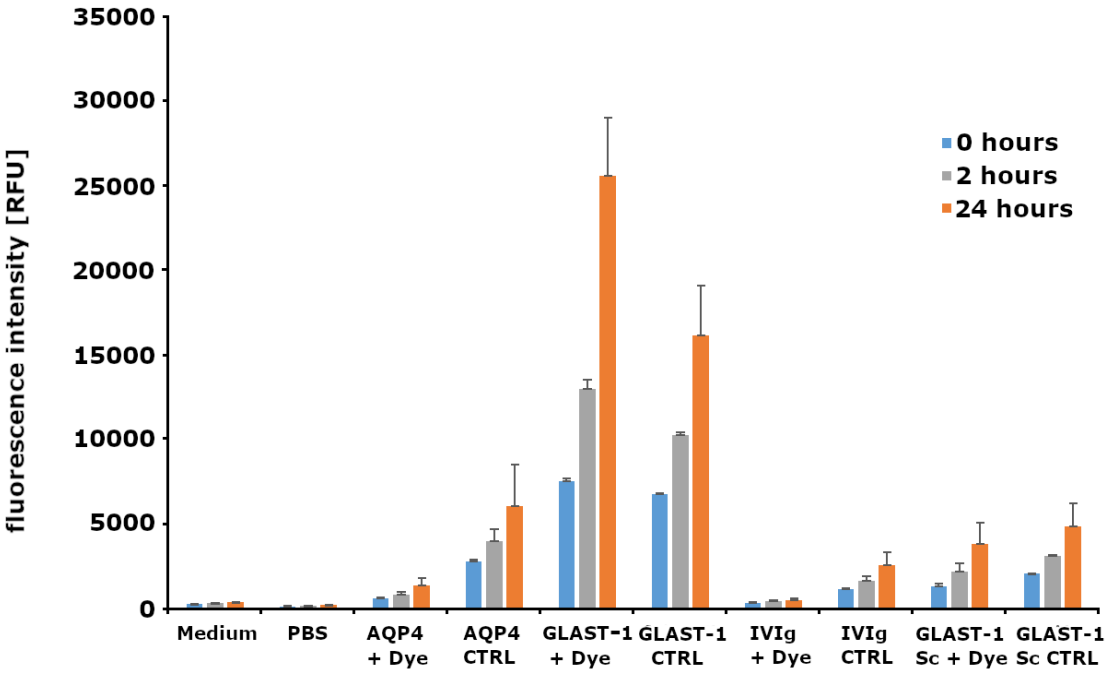

Fig. 3.8 High DARs result in higher intensities when antibodies were applied at the same concentration. *Astrocytes were seeded at a density of 10,000 cells per well in a 96-well plate. Cells were treated with 5 µg/ml of various antibody-dye conjugates and corresponding controls. DARs are summarized in tab. 9. Plate was measured at timepoints 0-, 2- and 24-hours in medium.*

Clearly, GLAST-1 conjugates reached higher intensities up to 24 hours of incubation on astrocytes. Compared to AQP4 and GLAST-1 Sc conjugates. Medium and PBS background signals were almost not detectable. As a control, conjugated IVIg was added to the cells as well. The conjugate did not result in significant fluorescent signals at none of the time points. Interestingly, antibody-controls obtained higher signals than antibody-conjugates of AQP4, IVIG and GLAST-1 Sc but not of GLAST-1, indicating that the signal is specific for the internalization of the antibody. The reason that the control conditions themselves exert fluorescent signals could be explained by the fact the control is produced: the amount of dye that was used for the conjugation of each individual antibody was added to an amount of medium (e.g. 1.2 µl dye in 100 µl medium). This stock solution was further diluted according to each antibody-conjugate. The amount of dye should be the same for the antibody and the controls. But since individual antibody-conjugates have been purified after conjugation using Zeba™ columns (in the case of IVIg and AQP4) controls could contain more dye molecules, though

dyes alone should not result in detectable signals since the medium has a neutral pH (Nath *et al.*, 2016).

Both GLAST-1 antibody-conjugates were not purified after conjugation since it was shown that purification did not have an impact on the measurements since only internalized conjugates could be detected by the increase in fluorescence signal (Nath *et al.*, 2016). That could be an explanation why GLAST-1 Sc-conjugates and the control nearly reached similar intensities. However, control signals of all antibodies increase over time whereas the pH of the medium should not change between the time points in such a great extent. Nevertheless, GLAST-1 conjugate almost reached double of the intensity of the corresponding control.

Table 3.1: Antibody-dye conjugates and corresponding DARs to fig. 3.8.

Antibody-dye conjugate	DAR
AQP4	3.3
GLAST-1	14.2
IVIG	5.02
GLAST-1 Sc	2.36

Since GLAST-1 internalization seemed to be stronger than AQP4 and the GLAST-1 antibody from Santa Cruz, following experiments were performed with this antibody. However, some of the experiments were also performed with AQP4 as a comparison. In a following experiment, GLAST-1 and the glutamate transporter 1 (GLT-1, also known as EAAT2) were conjugated with the pHAb reactive dye and applied to cells at different dilutions (1:10, 1:50, 1:500, 1:1000). GLT-1 is a cell surface transporter that is also expressed by astrocytes and was tested as a possible target for ablation experiments. Internalization was measured in PBS at 0 and after 24 hours of incubation (fig. 3.9). Dilutions of GLAST-1 reached highest fluorescence intensities after 24 hours at 1.5 and 0.3 µg/ml concentration (yellow bars). Lower concentrations of both antibody-conjugates only had little differences between 0 and 24 hours. GLT-1 intensities also increased after 24 hours (orange bars) at the highest concentrations compared to the starting point (blue bars).

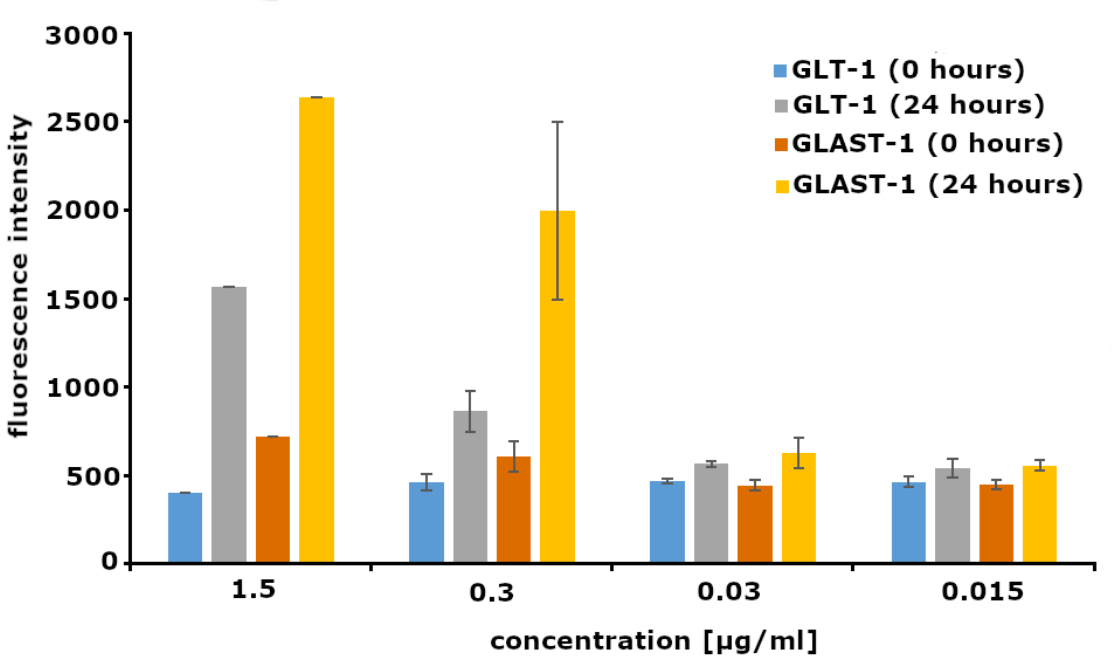

Fig. 3.9 Internalization assay of GLAST-1 and GLT-1 reveals that GLAST-1 internalization is strongest after 24 hours at a concentration of 1.5 µg/ml. *Primary astrocytes were seeded at a density of 5,000 cells per well in a 96-well plate and were cultivated for 6 days. phAb-reactive dye-conjugated antibodies GLT-1 (DAR: 13.54) and GLAST-1 (DAR: 19.34) were added to the wells in various dilutions (1:10: 1.5 µg/ml, 1:50: 0.3 µg/ml, 1:500: 0.03 µg/ml and 1:1000: 0.015 µg/ml). The plate was measured after 0 and 24 hours in PBS. Mean values ± SD of one experiment with triplicates are shown except for 1.5 µg/ml, here value of one well is shown.*

To summarize this part of the thesis, internalization of different antibody-dye conjugates revealed GLAST-1 as a promising candidate to be further tested in ablation studies on primary astrocytes. Though some of the results are partly contradictory and the mechanism of the internalization needs to be further elucidated, there is a consistency regarding GLAST-1 signals that exceeded the ones from the other conjugates in almost all experiments shown here.

3.2.2 Immunoablation of astrocytes *in vitro* using toxin-coupled antibodies

For the immunoablation of astrocytes, GLAST-1 on the cell surface was targeted with a suitable primary and secondary antibody. In first experiments, an excess of the secondary antibody was used in order to make sure, that there is no competition between conjugated and free primary antibodies. Both antibodies were diluted in culture medium (GLAST-1 1:1000 ~ 0.4 µg/ml and various concentrations of Rab-ZAP) and incubated for 30 minutes before added to the wells. Cell viability was measured after 72 hours by MTT assay (fig. 3.10).

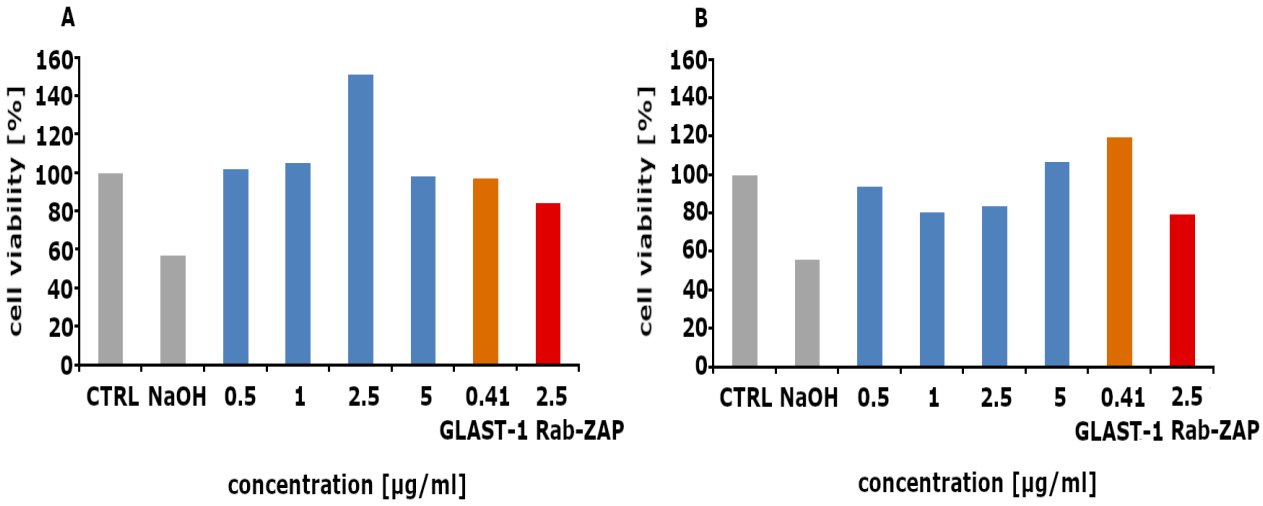

Fig. 3.10 Cell viability assessment after treatment of primary astrocytes with antibody complex. ***A*** *10,000 cells/ well and* ***B*** *5,000 cells/ well were seeded in a 24-well plate and incubated for 4 days before treatment with GLAST-1 (1:1000; 0.414 µg/ml) and various concentrations (0.5, 1, 2.5, 5 µg/ml) of Rab-ZAP and controls (untreated and 1 M NaOH) started. Plates were incubated for additional 3 days. MTT assay was performed to measure cell viability.*

Both cell densities respond equally to the high concentration of the secondary antibody alone, even higher than when both antibodies were combined at 5 µg/ml. In contrast, viability remains comparable to untreated cells, whereas cells treated with 1 M NaOH showed a lower viability than all other conditions, but also not as low as expected, revealing that the assay itself might not be performed properly. Strikingly, when the experiment was repeated with more cells and wells/ condition, cells treated with 1 M NaOH showed a decreased viability of up to 92 % and a concentration dependency due to the antibody complex (fig 3.11). But also,

treatment with both antibodies alone resulted in decreased viability. In a concentration dependent manner, the antibody complex decreased cell viability up to 54 % at 5 µg/ml Rab-ZAP and a dilution of 1:1000 GLAST-1.

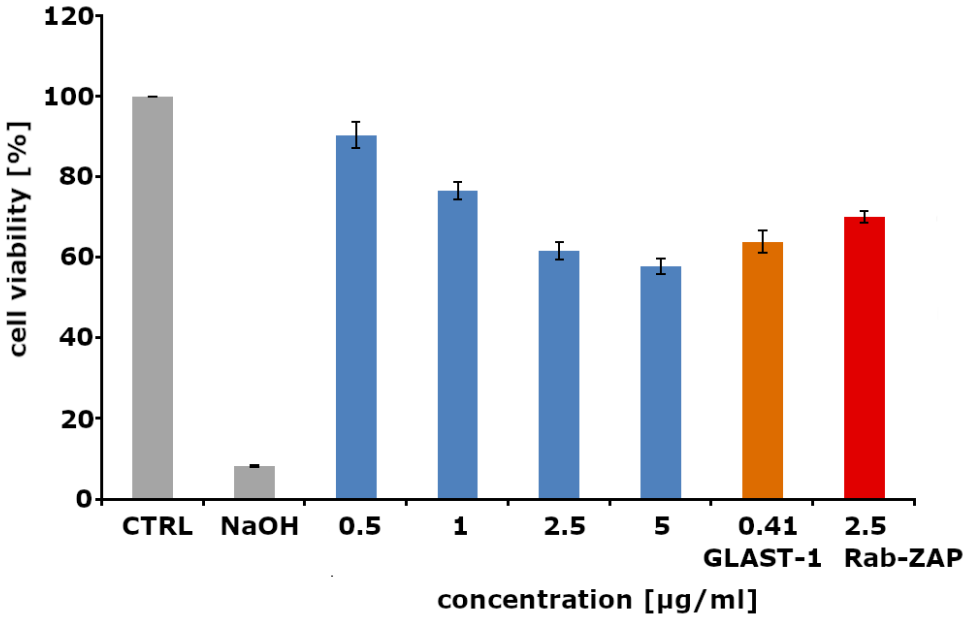

Fig. 3.11 Cell viability assessment after treatment of primary astrocytes with antibody complex. *Primary astrocytes were seeded at a density of 100,000 cells/ well in a 48-well plate with 6 wells per condition and incubated for 24 hours before treatment with the antibody complex at various concentrations (0.5-5 µg/ml) occurred. Thereby, the primary antibody (GLAST-1) was constantly applied at 1:1000 (0.414 µg/ml). As controls, untreated cells, 1 M NaOH and both antibodies alone were applied to cells and incubated for additional 3 days before MTT assay was performed.*

In further experiments, the complex of antibodies was diluted at a ratio of 1:1 and incubated 30 minutes before added to the medium of cells. When higher concentrations (8 µg/ml) of the antibody complexes were used, viability of astrocytes decreased even more compared to controls (fig. 3.12).

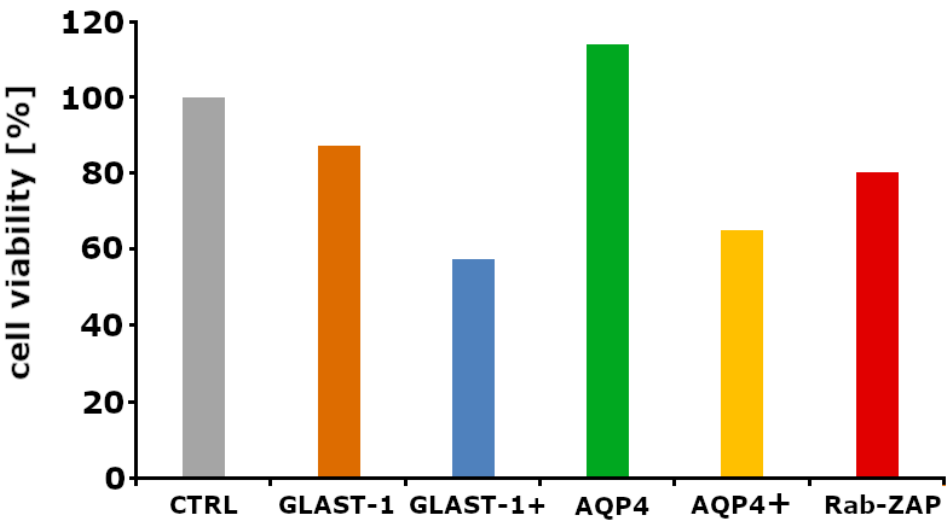

Fig. 3.12 Cell viability assessment after treatment of primary astrocytes with different antibody complexes. *Cells seeded at a density of 10,000 cells per well in a 96-wells plate. Cells were treated with a combination of GLAST-1 (8.3 µg/ml) and Rab-ZAP (8.3 µg/ml), as well as Aquaporin 4 (8.3 µg/ml) and Rab-ZAP (8.3 µg/ml) and all three antibodies alone, whereas the concentration of the toxin-coupled antibody was 3.3 µg/ml. Untreated cells and 1 M NaOH served as additional controls. Cells were incubated for 72 hours and MTT assay was performed with 6 wells per condition.*

But also treatment with a lower concentration (3.3 µg/ml) of the toxin-coupled antibody alone resulted in decreased viability of astrocytes (69 %).

Since the effects were not as high as expected and due to limited availability of antibodies, the incubation and treatment time with lower concentrations was adapted. This time, cells were treated three times every second day and incubated for a total of 7 days before MTT assay was performed (fig. 3.13). Because of the long incubation time, the cell density was lowered to 6,000 cells/ well. All antibodies were diluted in a ratio of 1:1 and pre-incubated at room temperature.

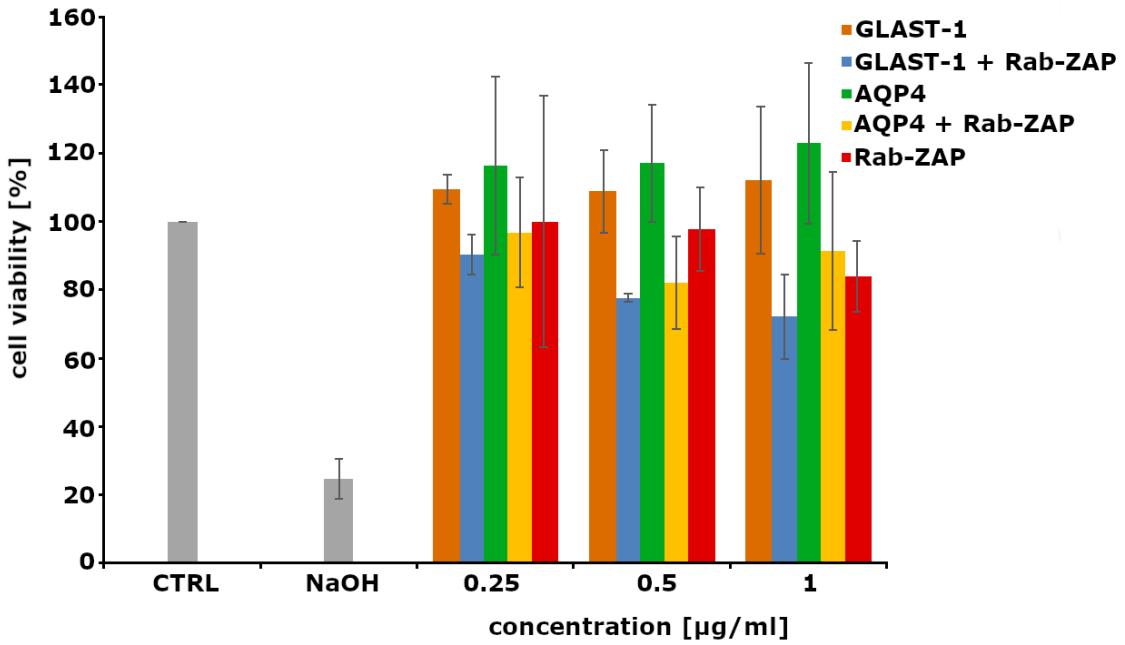

Fig. 3.13 Effect of GLAST-1-toxin-conjugate treatment of astrocytes is stronger than AQP4-toxin-conjugate. *Astrocytes were seeded at a density of 6,000 cells/ well and treated with different concentrations of the antibody complex for 6 days. As positive control, cells were treated with 1M NaOH. As additional controls, cells were either treated with primary (GLAST-1) or secondary antibody (Rab-ZAP) alone. Treatment was repeated every second day. On the 7th day, cell viability was measured using MTT-assay. Mean values ± SD are shown from two experiments.*

Interestingly, the primary antibodies in combination with the toxin-coupled secondary antibody decreased cell viability after 6 days of treatment up to 35% at the highest concentration of 1 µg/ml whereas controls only slightly decreased cellular survival. Though standard deviations are quite high, there is a clear difference between the control and treatment conditions. Aquaporin 4 showed similar effects on the cell viability in combination with Rab-ZAP secondary antibody, whereas the effect is not as strong as with GLAST-1. Therefore, the following experiments were solely performed with GLAST-1.

GLAST-1 (orange bars) itself seems not to be toxic to astrocytes except when applied at high concentrations (5 µg/ml). In a concentration dependent manner both the antibody complex (blue bars) and Rab-ZAP (red bars) alone decreased cell viability *in vitro* (tab. 3.2). Thereby, Rab-ZAP treatment alone was enough to reduce cell viability down to 28.04 % ± 5.82 % at a concentration of 5 µg/ml.

Table 3.2: Cell viability assessment of astrocytes after treatment with primary and secondary antibodies. *Astrocytes were seeded at a density of 6,000 cells/ well and treated with different concentrations of the antibody-complex for 6 days. As positive control, cells were treated with NaOH. As additional controls, cells were either treated with primary (GLAST-1) or secondary antibody (Rab-ZAP) alone. Treatment was repeated every second day. On the 7th day, cell viability was measured using MTT-assay. Untreated and cells treated with 100 mM NaOH served as controls. Cell viability is shown in % as mean values ± SD are shown from one experiment.*

Concentration [µg/ml]	CTRL	NaOH	GLAST-1	GLAST-1 + Rab-ZAP	Rab-ZAP
	100 ± 0	10.61 ± 0.67			
1			94.68 ± 5.82	42.33 ± 1.70	40.13 ± 2.14
2.5			108.51 ± 11.68	31.31 ± 4.14	32.27 ± 3.72
5			96.83 ± 21.95	24.56 ± 1.46	28.04 ± 5.82

3.2.3 Immunoablation of astrocytes *ex vivo*

Since low concentrations of the antibody-complex showed little effects on cellular survival *in vitro* even over a longer period of treatment, the same experiments with higher concentrations *ex vivo* using slice cultures were performed. Astrocytes in slice cultures form a dense network (fig. 3.14 A) that is evenly distributed. With increasing antibody concentration, the number of GFAP-positive cells diminished (fig.3.14), whereas the cell architecture and structure of neurons remained. Even the highest concentration (5 µg/ml in D) was not enough to deplete all astrocytes from the slices.

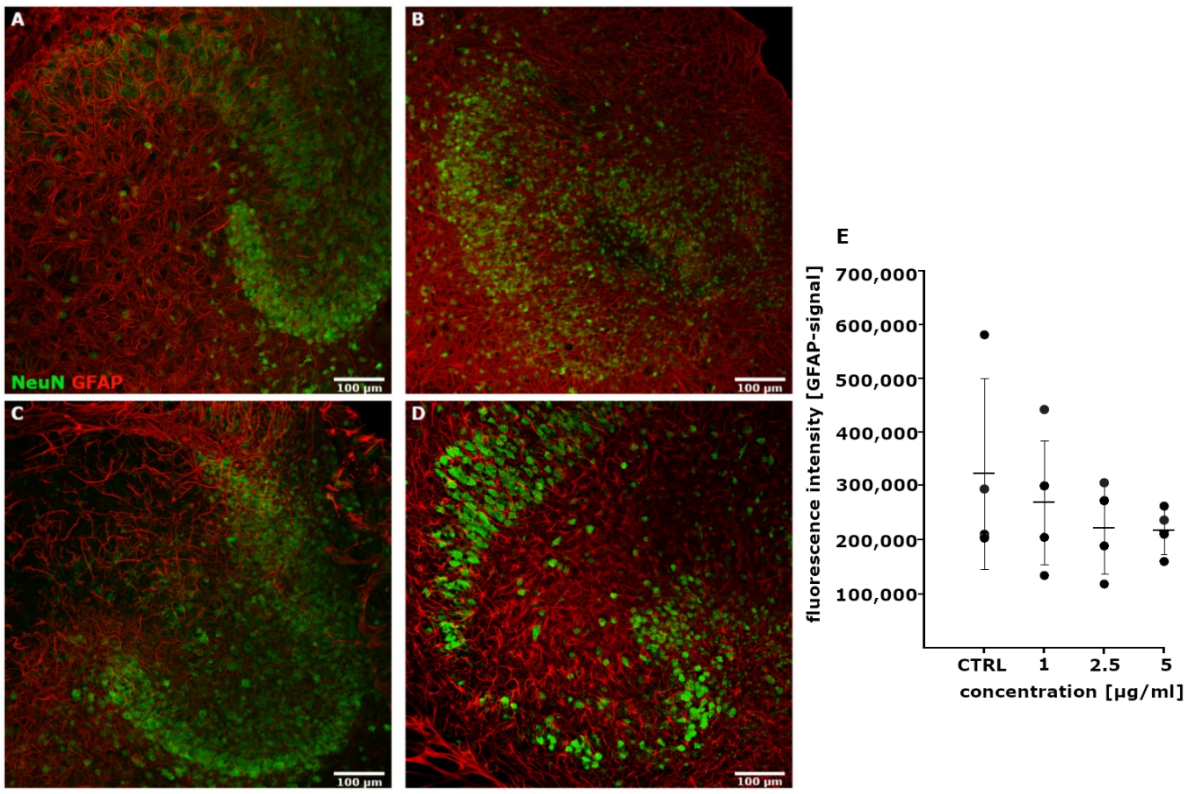

Fig. 3.14 Immunoablation in OHSCs using GLAST-1 and Rab-ZAP antibodies is concentration dependent. *OHSCs were cultured for 6 days before treatment with various concentrations of GLAST-1 and Rab-ZAP antibodies started. Antibodies were diluted in culture medium and incubated at RT for 30 minutes prior to treatment. Untreated slices served as controls. Representative images are shown.* ***A*** *Control slice;* ***B*** *1 µg/ml;* ***C*** *2.5 µg/ml and* ***D*** *5 µg/ml of antibody complex. Slices were cultivated additional for 7 days with 3 treatments and stained for neurons (NeuN; green) and astrocytes (GFAP; red). Images were taken with a Leica SP8 confocal laser scanning microscope and an 20x/ 0.70 objective with a zoom of 0.75.* ***E*** *shows individual fluorescence intensities of GFAP-signal of 4 slices per condition. Black line indicates mean ± SD.*

Fig. 3.14 E shows the individual GFAP intensity of 4 slices per condition after the treatment with 1, 2.5 and 5 µg/ml of GLAST-1 and Rab-ZAP. With increasing concentration, the standard deviation and spreading of the individual slices strongly reduces as well as the mean intensity, which could be an indicator of reduced GFAP-positive cells.

Nevertheless, GFAP signal is still detectable in the images. Possibly, not all astrocytes have been eliminated using this antibody-toxin conjugate indicating that there are possible different types of astrocytes in the slice cultures.

Due to the high amount of antibody that is needed to treat one well containing slices, higher concentrations were not applicable. Therefore, a different approach was implemented that is described in the following paragraphs.

3.2.4 Depletion of astrocytes using L-alpha aminoadipic acid *in vitro*

For the second approach, the known gliotoxin L-alpha aminoadipic acid (Lα-AAA) was used. In the late 70s and early 80s, a couple of research was done with this compound and several studies were published concerning the astrocyte-specific-toxic action. Interestingly, since the late 90s, the use of Lα-AAA vanished. Most research was done *in vivo* by direct injection into cerebral regions (Olney *et al.*, 1980). Because satisfying investigation of astrocytes *ex vivo* is lacking, there is a need to investigate its putative effect on primary cells and on slice cultures. Direct injection of Lα-AAA was found to be a potent way of eliminating astrocytes region-specific. To find a concentration that is sufficient for slice cultures, first experiments on primary astrocytes were performed with low (0.125 mM) to high (10 mM) milli molar concentrations.

Cell viability of astrocytes was assessed using celltiter Glo (Promega, Madison, USA), herein the ATP production of viable cells is a measure for viability. With increasing concentration of the gliotoxin (light green bars), cell viability of primary astrocytes decreased compared to untreated controls (grey bar) (fig. 3.15). Remarkably, the effect on the viability is not observed until a concentration of 5 mM, which is low in contrast to direct injections (20 µg/µl) (Khurgel *et al.*, 1996). With 7.5 mM (29.35 % ± 4.54 %) and 10 mM (12.02 % ± 3.69 %) cell viability went down to 10 % with a steep decrease from 5 (78.61 % ± 5.01 %) to 10 mM (12.02 % ± 3.69 %) which is more than double.

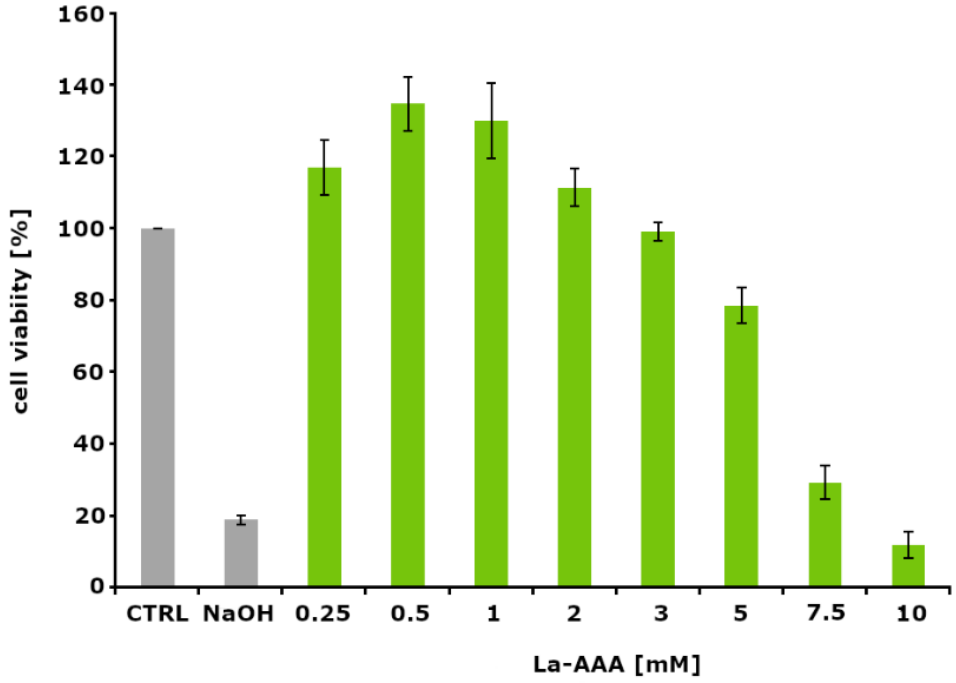

Fig. 3.15 Treatment of astrocytes with Lα-AAA results in concentration dependent cell death. *Primary astrocytes were seeded at a density of 10,000 cells per well in a 96-well plate and incubated for 24 hours before treatment with various concentrations of Lα-AAA started and cultivated for 72 hours. Cell viability was assessed using celltiter Glo (Promega). Untreated cells and cells treated with 100 mM NaOH served as controls. Mean values ± SD of one experiment with six replicates per condition are shown.*

Since, Lα-AAA is only slightly soluble in water (2 mg/ml) and when solved, the pH drops to a very acidic level (pH 1) a stock solution of about 12 mM could be prepared and a pH of 6-7 was achieved by the addition of 1 M NaOH. For the dilutions used in fig. 3.15 almost half of the culture medium was replaced by the toxin-solution and even more when higher concentrations were applied (7.5 and 10 mM). Additionally, viability of cells treated with 10 mM Lα-AAA even underscores the viability of cells treated with 100 mM NaOH (18.90 % ±1.36 %). Therefore, it was necessary to verify that the effect on the viability derived from the drug itself and not because of the replaced culture medium (fig. 3.16).

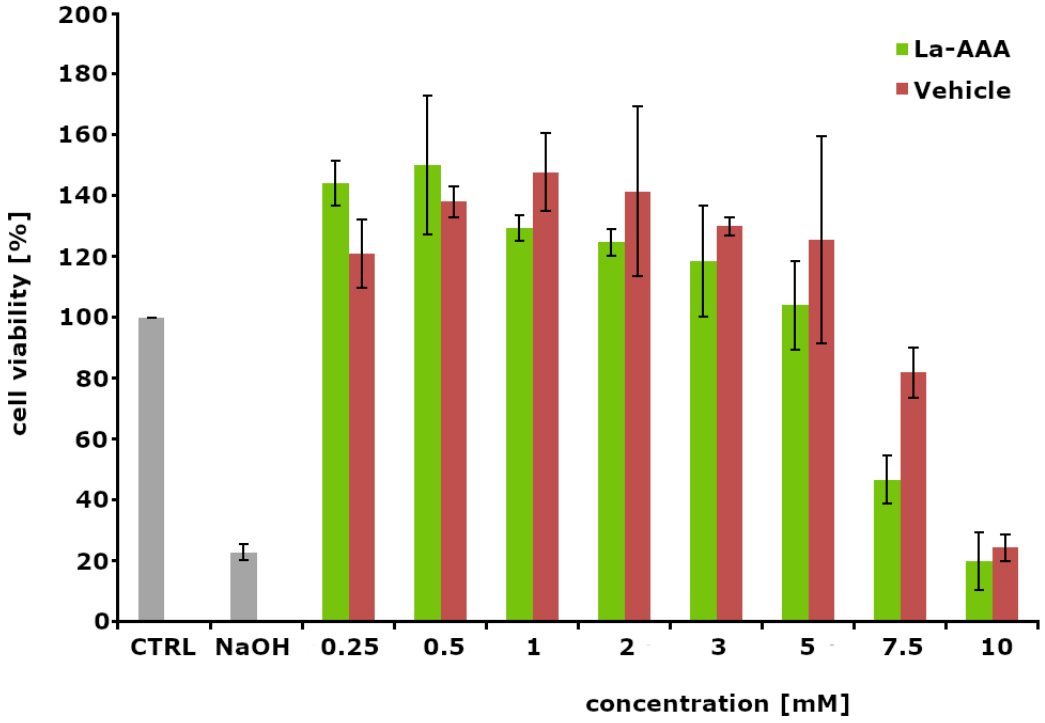

Fig. 3.16 Treatment of astrocytes with Lα-AAA and corresponding vehicle control. *Primary astrocytes were seeded at a density of 6,000 cells per well 6 days prior to treatment with various concentrations of Lα-AAA (light green bars) as well as corresponding concentrations of the vehicle (aqua bidest. + 1 M NaOH, pH 6-7 with addition of HCL; red bars). Untreated cells and cells treated with 100 mM NaOH served as controls (grey bars). Cells were treated for 3 days, before celltiter Glo was performed. Mean values ± SD of one experiment with six replicates per condition are shown.*

Again, cell viability decreased with increasing drug-concentrations (light green bars). The same is true for the vehicle treated cells (red bars). Interestingly, at 7.5 mM Lα-AAA and vehicle, there is a clear difference towards a more decreased viability when cells were treated with the toxin. This effect is lost when cells were treated with 10 mM of both conditions. Moreover, the effect of the drug at 10 mM (20.26 % ± 9.44 %) again underscores the effect of 100 mM NaOH (23.11 % ± 2.65 %), whereas the vehicle is marginally higher (24.68 % ± 4.40 %). Thereby, the concentration of NaOH in the toxin-stock solution and vehicle stock solution is 12 mM and therefore much lower, indicating that the effect on the viability could be due to the drug itself and the replacement of the culture medium.

To solve this question, an additional experiment was performed with addition of an extra control. Cells were treated with different concentrations of the toxin, as well as the vehicle and aqua bidest. alone (fig. 3.17).

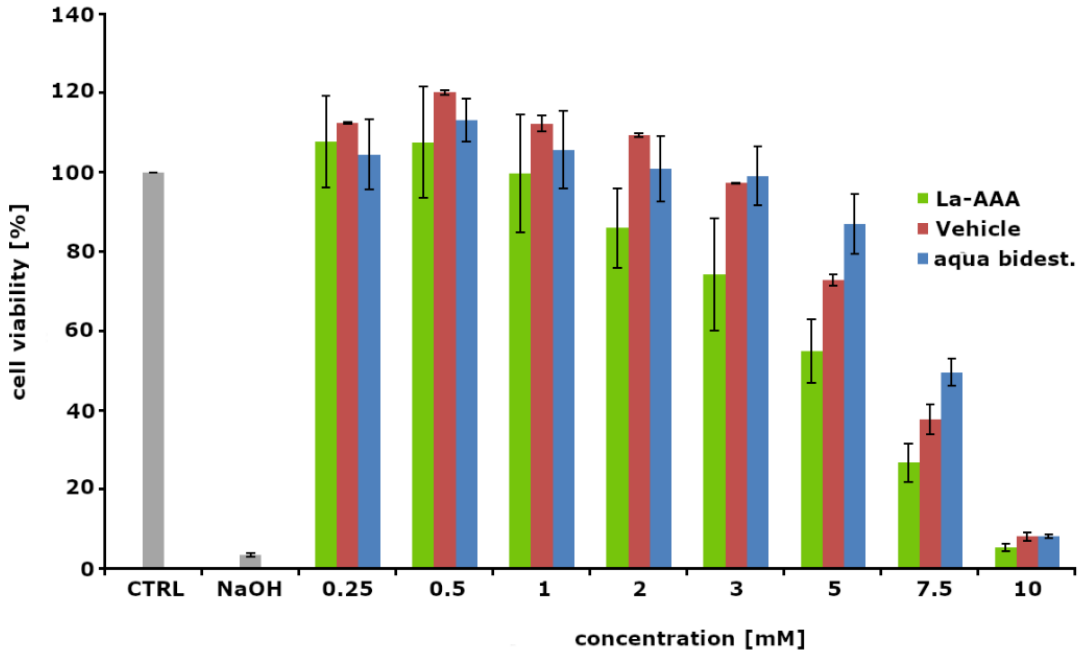

Fig. 3.17 Treatment of astrocytes with Lα-AAA, vehicle control and volume replacement control. *Primary astrocytes were seeded at a density of 10,000 cells per well 24 hours prior to treatment with various concentrations of Lα-AAA (light green bars) as well as corresponding concentrations of the vehicle (aqua bidest. + 1M NaOH, pH6, red bars) and aqua bidest. (blue bars). Untreated cells and cells treated with 100 mM NaOH served as controls (grey bars). Cells were treated once and incubated for 5 days, before celltiter Glo was performed. Mean values ± SD of one experiment with six replicates per condition are shown.*

Clearly, the replacement of culture medium has a detrimental effect on cellular survival (blue bars), but only in high concentrations. Still, Lα-AAA (10 mM) treated cells (5.53 % ± 0.92 %) underscore the viability of cells treated with the vehicle (8.20 % ± 0.99 %) or aqua bidest. (8.30 % ± 0.42 %). However, the same concentration dependence regarding the decreasing viability is observable. To examine an EC50 concentration, more experiments were necessary. Therefore, the range between 1 and 6 mM was chosen as treatment conditions and the number of treatments and incubation times were adapted (fig. 3.18 A and B).

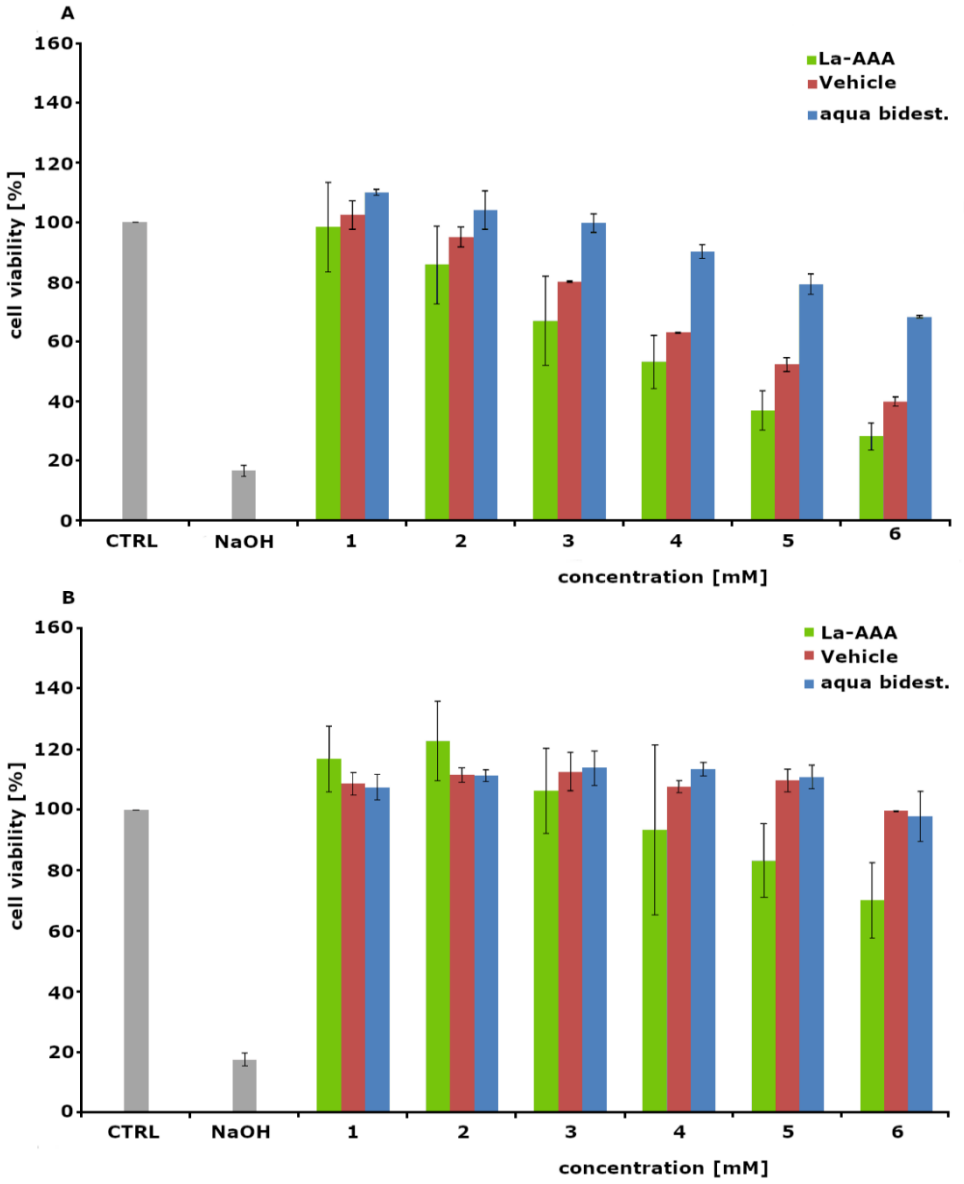

Fig. 3.18 Number of treatment and incubation times matter in primary astrocytes treated with Lα-AAA. *Primary astrocytes were seeded at a density of 10,000 cells per well in 96-well plate 24 hours prior to treatment. Cells were treated three times and incubated for a total of 6 days (A) or twice and incubated for 3 days (B) with Lα-AAA (green bars) and the vehicle (red bars) and corresponding controls (blue bars). Untreated and cells treated with 100 mM NaOH served as additional controls (grey bars). Mean values ± SD of one experiment with six replicates per condition are shown.*

There is an overall stronger effect observable when cells were treated three times every second day (fig. 3.18 A) compared to two treatments in a row and a shorter overall incubation time (B). Nevertheless, concentration dependence is also recognizable in both experiments.

When cells were treated three times with the toxin, cell viability almost decreased to 50 % at 4 mM (53.22 % ± 8.93 %), though the controls reached much higher results (63.02 % ± 0.03 % (red bar) and 90.24 % ± 2.28 % (blue bar)). This is not the case when cells were treated twice on two days in a row and incubated for only 3 days in total (B). Here, an EC50 is even not obtained at a concentration of 6 mM (70.16 % ± 12.43 %). Again, revealing that duration of treatment as well as the concentration has an impact on the effectiveness of the drug.

Because of the effect concerning the replacement of culture medium and the purpose to treat slices where much higher volumes are needed; lower concentrations were tested with more incubation times and more treatments. Primary astrocytes treated twice with the gliotoxin Lα-AAA showed a concentration dependent decrease in ATP-production in comparison to vehicle-treated cells even at lower concentrations (fig. 3.19 A). Though the effect of the drug at 2 mM (76.45 % ± 9.83 %) compared to fig. 3.18 A (2 mM: 85.72 % ± 12.92 %) is marginal, there is a consistency, whereas these cells were treated one time less. This concentration dependence was also shown to be confirmed again with higher concentrations over a treatment duration of 7 days with three repeated treatments (fig. 3.19 B). Again, the EC50 is about 5 mM (fig. 3.19 B: 43.26 % ± 2.45 %) or even lower according to fig. 3.18 A (36.99 % ± 6.63 %). Nevertheless, in higher concentrations the replacement of medium by the solution itself influences viability (blue bars). Interestingly, with both Lα-AAA preparations cell viability first increases and overcomes the viability of untreated cells in the lower millimolar concentrations. Whereas the viability of cells treated with 2 mM (76.45 % ± 9.83 %) of Lα-AAA is about 80 % in A, viability of cells treated with 2.5 mM is higher (95.32 % ± 6.05 %) in B even if these cells were treated three times instead of twice. This discrepancy could be explained on the one hand by the fact that in A three plates were used for the evaluation which is reflected by the higher standard deviation. On the other hand, composition of the cell culture itself might play a role since experiments were done with different cell preparations.

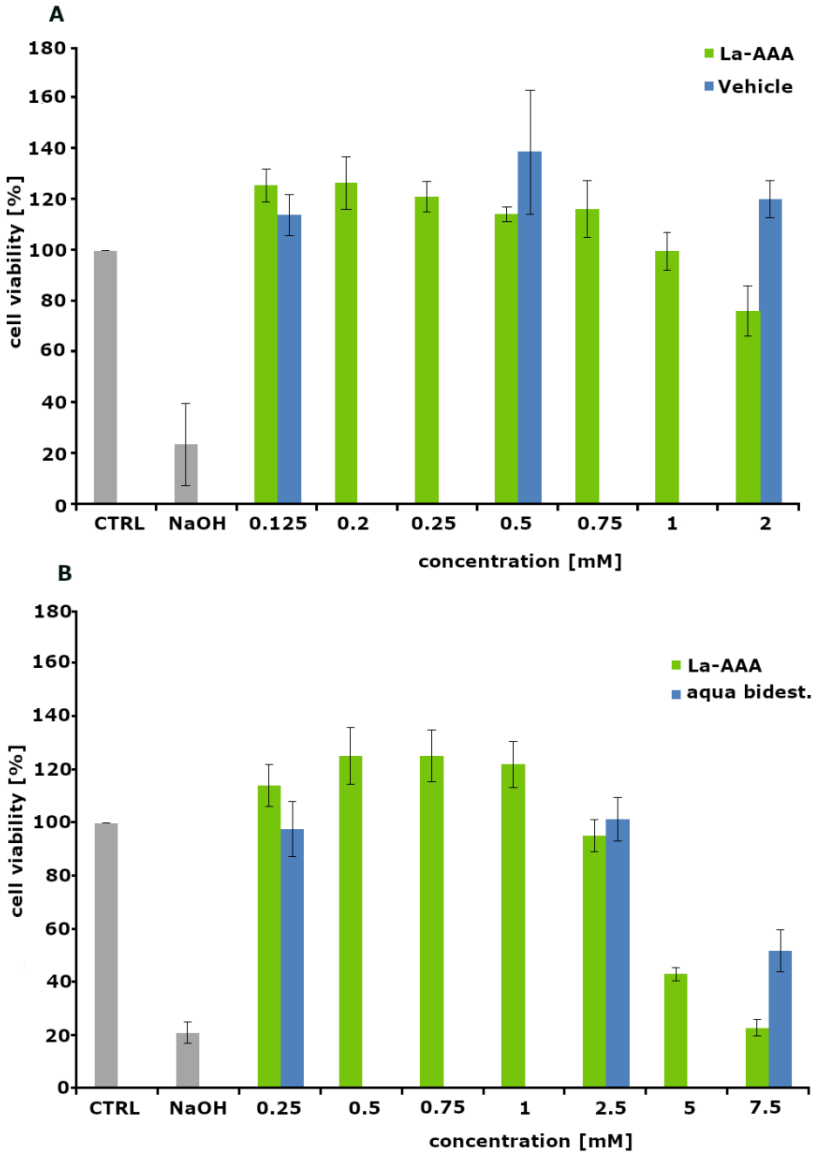

Fig. 3.19 Correlation between number of treatments and concentration of Lα-AAA. **A** *Primary astrocytes isolated from embryonic mice were seeded at a density of 6,000 cells per well and cultured for 48 hours prior to treatment. Cells were treated twice with various concentrations of Lα-AAA (H_2O + NaOH, pH 7.4; light green bars) and vehicle (H_2O + NaOH, pH 7.4; blue bars). After 5 days of incubation, celltiter Glo (Promega) was performed. Untreated cells and cells treated with 100 mM NaOH served as controls. Mean values ± SD of three plates are shown.* **B** *Primary astrocytes isolated from mixed glia cultures were seeded at a density of 6.000 cells per well and cultured for 24 hours prior to treatment. Cells were treated three times with various concentrations of Lα-AAA (H_2O + NaOH, pH 7.4; light green bars) and vehicle (aqua bidest.; blue bars). After 7 days of incubation celltiter Glo (Promega) was performed. Untreated cells and cells treated with 100 mM NaOH served as controls. Mean values ± SD of one experiment with six replicates per condition are shown.*

The results show that there is a correlation between cell density, incubation time and number of treatments. But they also show that the differences in pH did not detrimentally affect the efficacy of the drug. Since there is always a concentration dependent decrease in viability, whether a pH of 6 (fig.3.17) or between 6-7 (fig. 3.16) or even 7.4 (fig. 3.19) was used. In former experiments, when pH was not adjusted to almost neutral (pH 1-2), culture medium shifted towards acidic (yellow colour) and was not used for treatment. The effects of t high pH are seen when cells were treated with 1M or 100mM NaOH alone.

3.2.5 Depletion of astrocytes using L-alpha amino adipic acid *ex vivo*

According to the *in vitro* experiments, the LD50 of Lα-AAA is about a concentration of 4-5 mM and exerts the greatest effect after repeated treatments and longer incubation times. These findings were transferred onto *ex vivo* experiments. First, slices were treated with a dilution of 5 mM for 24 hours based on clodronate findings. Afterwards, immunofluorescence staining for neurons, astrocytes and overall cellular nuclei was performed. Images were taken with a Zeiss Axio Observer fluorescence microscope at a magnification of 5x (fig. 3.20).

As described in detail in 2.2.10, different solutions of Lα-AAA were prepared with different solvents (see appendix for results). The following results were obtained with the treatment of slices with Lα-AAA dissolved in aqua bidest. and the adjustment of pH with 1M NaOH. During the fixation process with 4% PFA, most of the slices already detached from the membrane inserts. Free floating slices cannot be stained using the procedure described in 2.2.16. Nevertheless, staining was continued with the membranes and analysis showed that the cellular architecture is severely destructed by the compound, but with the addition that more neurons could be stained than astrocytes. Clearly, Lα-AAA has an impact on the viability of neurons as well in slices.

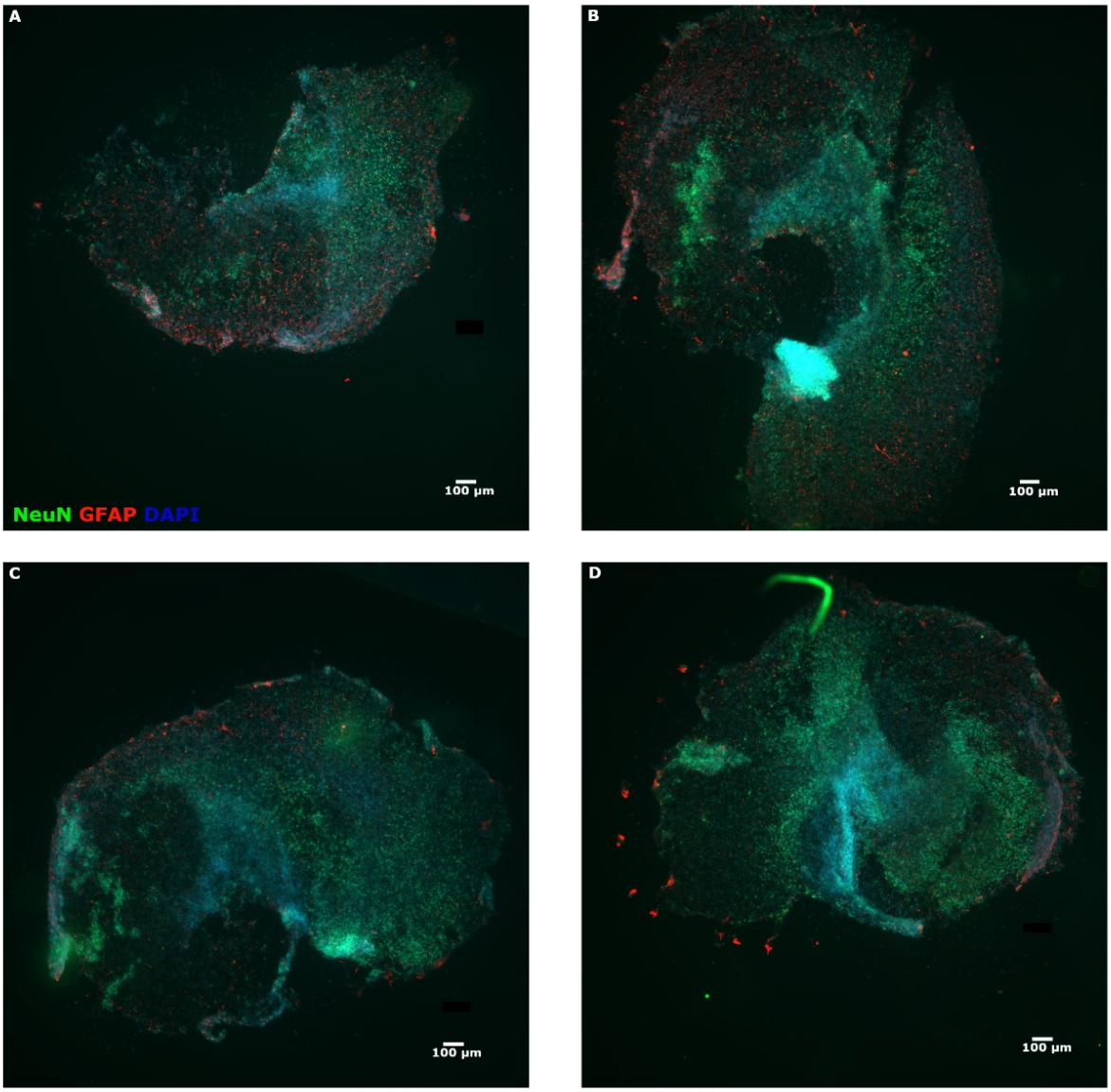

Fig. 3.20 5 mM Lα-AAA leads to disruption of cellular architecture. *Slices were cultivated for 6 days and treated with 5 mM Lα-AAA for 24 hours. After fixation, immunofluorescence staining was performed; neurons (NeuN, green), astrocytes (GFAP, red) and nuclei (DAPI, blue). Images were taken with a Zeiss Axio Observer fluorescence microscope and 5x/0.16 plan/ neofluar objective.*

Due to the high damage that the compound exerted on the slices when administered via culture medium, a 5 mM solution was diluted in PBS and applied to the slices by dropping 2 µl on top of each slice. This technique was based on amyloid-beta application. The dropping method decreased volume replacement enormously. The slices remained intact and could be stained by immunofluorescence (fig. 3.21). In more detail, astrocytes remained as well according to GFAP signal and revealing that the depletion was not successful.

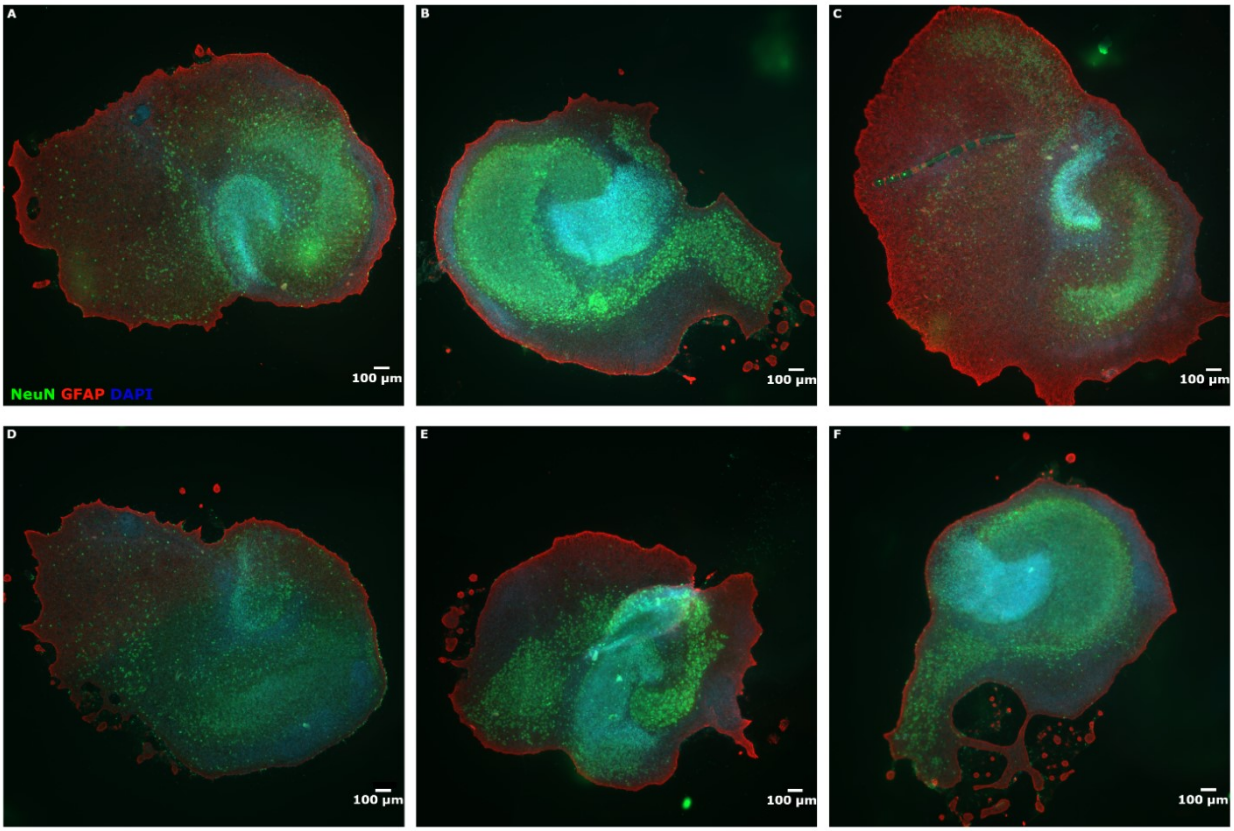

Fig. 3.21 5 mM Lα-AAA was applied to slices by dropping the solution on top of each slice. *A dilution of 5 mM Lα-AAA in PBS was prepared and 2 µl were dropped on top of each of the six slices per well and incubated for 24 hours before immunofluorescence staining was performed; neurons (NeuN, green), astrocytes (GFAP, red) and nuclei (DAPI, blue). Images were taken with 5x/0.16 plan/ neofluar objective.*

Since a single treatment with 5 mM of the compound had detrimental effects even on the viability of neurons and the application of the compound by direct dropping on the tissue had no effects, more concentrations and numbers of treatments were tested. While low concentrations had little effects *in vitro* on astrocyte viability, a single treatment of slices with 0.5 mM and 1 mM (fig. 3.22 D and E) resulted in reduced GFAP signal *ex vivo*.

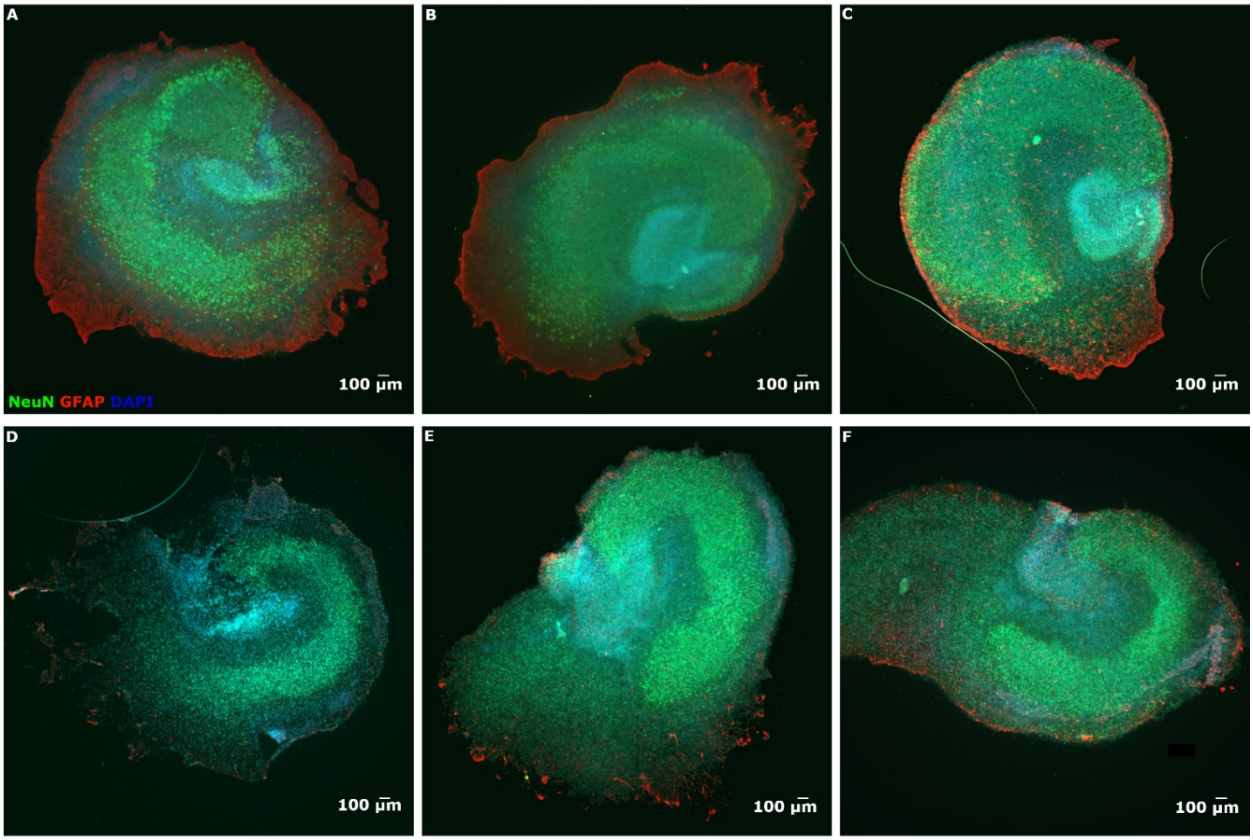

Fig. 3.22 Lα-AAA treatment in OHSC is concentration dependent. *Slice cultures were treated once with various concentrations of La-AAA in culture medium and cultivated for 2 days.* ***A*** *untreated;* ***B*** *0.1 mM;* ***C*** *0.25 mM;* ***D*** *0.5 mM;* ***E*** *1 mM;* ***F*** *1.5 mM. Immunofluorescence was performed (NeuN, green; GFAP, red; DAPI, blue). Representative images are shown.*

Again, slices did not seem vital at all (fig. 3.22 D), especially regarding the dentate gyrus. Interestingly, GFAP signal diminished with increasing Lα-AAA concentration, but this was not true for all slices from one condition. Some of the slices treated with 0.25, 1 and 1.5 mM appeared to be damaged.

Therefore, additional experiments were performed with lower concentrations but higher treatment events (fig. 3.23). Surprisingly, three repeated treatment did not result in efficient reduction of GFAP signal compared to control slices (A).

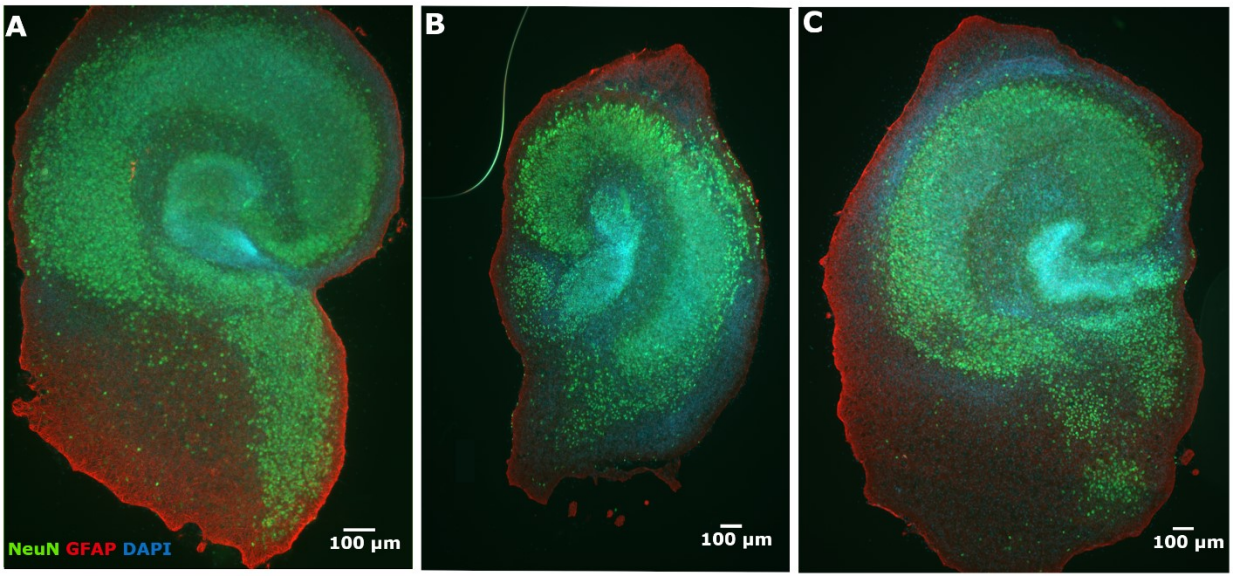

Fig. 3.23 Low concentrations of Lα-AAA have no direct effects of viability in OHSC. *Slice cultures were treated three times with various concentrations of Lα-AAA in culture medium and cultivated for 7 days.* ***A*** *untreated;* ***B*** *0.0625 mM;* ***C*** *0.125 mM. Immunofluorescence was performed (NeuN, green; GFAP, red; Dapi, blue). Representative images are shown.*

In low concentrations, even repeated treatment for a duration of 7 days was not enough for the depletion of at least half of all astrocytes in slice cultures (Fig. 3.23). Nevertheless, cell architecture remains intact. When treated for a shorter period but with higher concentrations, astrocytes are mostly depleted, but also the cell architecture is severely disrupted again (fig. 3.24).

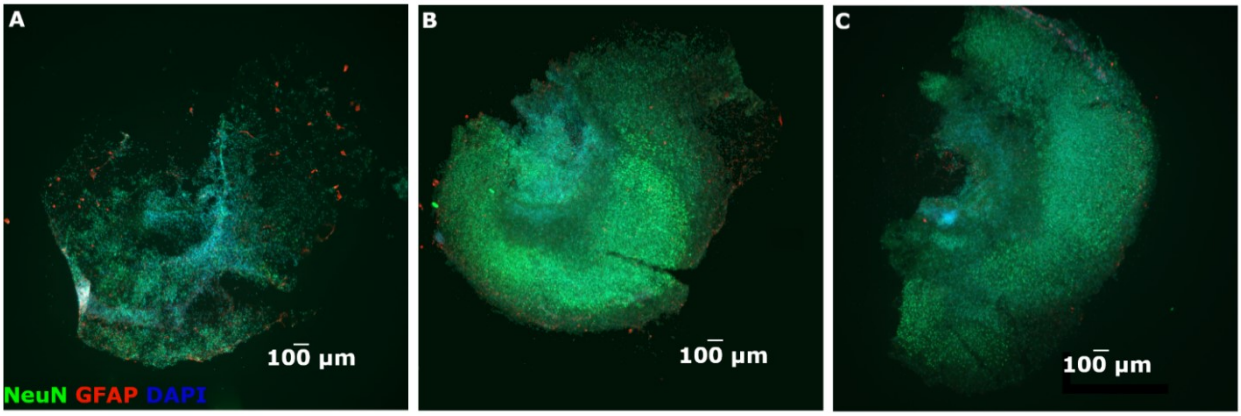

Fig. 3.24 La-AAA treatment in OHSC. *Slice cultures were treated twice with various concentrations of La-AAA in culture medium and cultivated for 5 days.* ***A*** *0.25;* ***B*** *0.5 mM;* ***C*** *1 mM. Immunofluorescence was performed (NeuN, green; GFAP, red; DAPI, blue). Representative images are shown.*

To summarize this part, treatment of slices with Lα-AAA at various concentrations, incubation times and numbers of treatments was not successful in depleting astrocytes in slice cultures *ex vivo*. There is a huge variance between the different experiments and even within one experiment, since single slices showed the desired result that could not be validated by repeated experiments.

The following paragraph shows experiments that were done with the murine oligodendrocyte precursor cell line *Oli-neu*.

3.3 Oligodendrocytes

3.3.1 Immunoablation of oligodendrocytes

For the immunoablation of oligodendrocytes, *Oli-neu* cells (fig. 3.25) were seeded and treated with different concentrations of the primary antibodies GPR17 (Fig. 3.26) and Claudin-11 and a suitable secondary antibody coupled with saporin (Advanced Targeting Systems, USA). These experiments were done analogously to the astrocyte immunoablation experiments. Because isolated primary oligodendrocytes as described in 2.2.2 did not grow up to numbers that could be seeded and assayed the cell line *Oli-neu* was used. However, a few stainings could be made (see appendix fig. 6.2). *Oli-neu* cells were broadly seeded and began to spread in culture (fig. 3.25 A). For cell viability measurements, cells were first seeded at different densities, to examine the most suitable cell number. Cells were cultivated for 48 hours and then treated with a combination of Claudin-11 and Rab-ZAP antibodies twice for a total of 5 days. MTT-assay was performed (fig. 3.25 B). Overall, a density of 2,000 cells per well is impractical. Cells seeded at a density of 4,000 and 6,000 mostly yielded similar results except for the treatment condition of 5 µg/ml antibody complex. Therefore, following experiments were performed with 6,000 cells per well. Nevertheless, an effect of the antibody complex is obvious, since all three concentrations decrease cell viability up to 10 % (5 µg/ml).

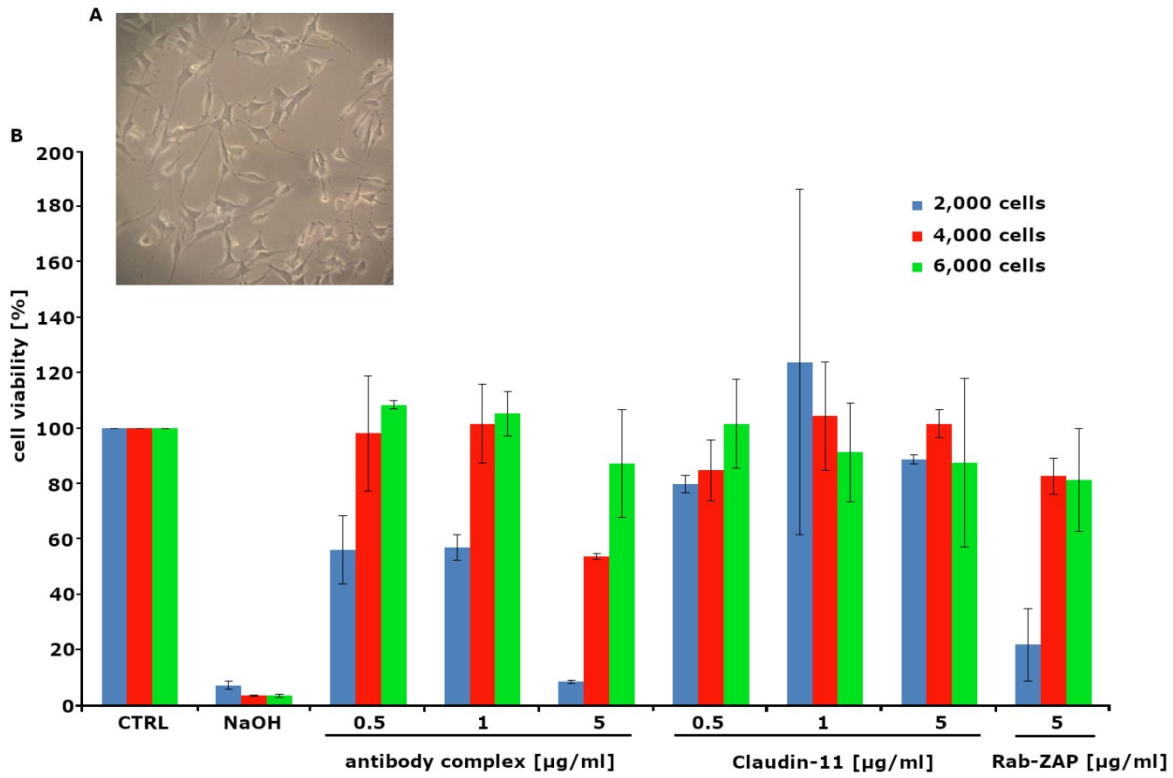

Fig. 3.25 Cell viability assessment of *Oli-neu* cells after treatment with Claudin-11-toxin-conjugate. A *Oli-neu cells (p 28) were seeded at a density of 6,000 cells per well into 96 well plates for 48 hours and pictures using a brightfield microscope were taken.* **B** *Different densities (2,000-6,000 cells/ well) of Oli-neu cells were seeded into 96-well plates and cultured for 48 hours. On the 3rd day of incubation, cells were treated with various concentrations of an antibody-complex containing Claudin-11 and Rab-ZAP for a total of 5 days with two treatments. MTT-assay was performed to measure cell viability. Untreated, cells treated with 100 mM NaOH and the primary (Claudin-11) or secondary (Rab-ZAP) antibody alone served as controls. Mean values ± SD from triplicates of one experiment are shown.*

Furthermore, cell viability was also assessed after cells were treated with another antibody complex (fig. 3.26 A). In this case, as primary antibody the GPR17 and suitable anti-goat-saporin (Gab-ZAP; ATS) were diluted in culture medium at different concentrations (0.25 – 10 µg/ml) and incubated 30 minutes before treatment at room temperature. Treatment was done twice and for a total of 7 days. The antibody complex only slightly decreased cell viability in comparison to the control conditions (both antibodies alone). Cells treated with 10 µg/ml of both antibodies together resulted in a remaining viability of 32.73 %. When cells were solely treated with Gab-ZAP, viability already decreased to 71.21 % at 0.5 µg/ml. Since high treatments of cells with both antibodies alone were not applicable, the experiment was repeated with a different antibody complex and corresponding controls (fig. 3.26 B). Whereas viability of cells treated with GPR17 and Gab-ZAP decreased to 32.73 %, the effect of the antibody complex consisting of Claudin-11 and Rab-ZAP decreased viability to 26.86 % at 10 µg/ml. Herein, the corresponding primary antibody control Claudin-11 (23.39 %) underscored the viability of the complex while the secondary antibody Rab-ZAP (41.88 %) did not. Due to lacking standard deviations concerning high antibody controls, only a comparison between the mean values can be made. In general, except for the highest concentration of 10 µg/ml, both antibody complexes were not able to decrease viability of cells to 50 %. In both situations, primary and secondary antibodies alone had stronger effects than the complexes.

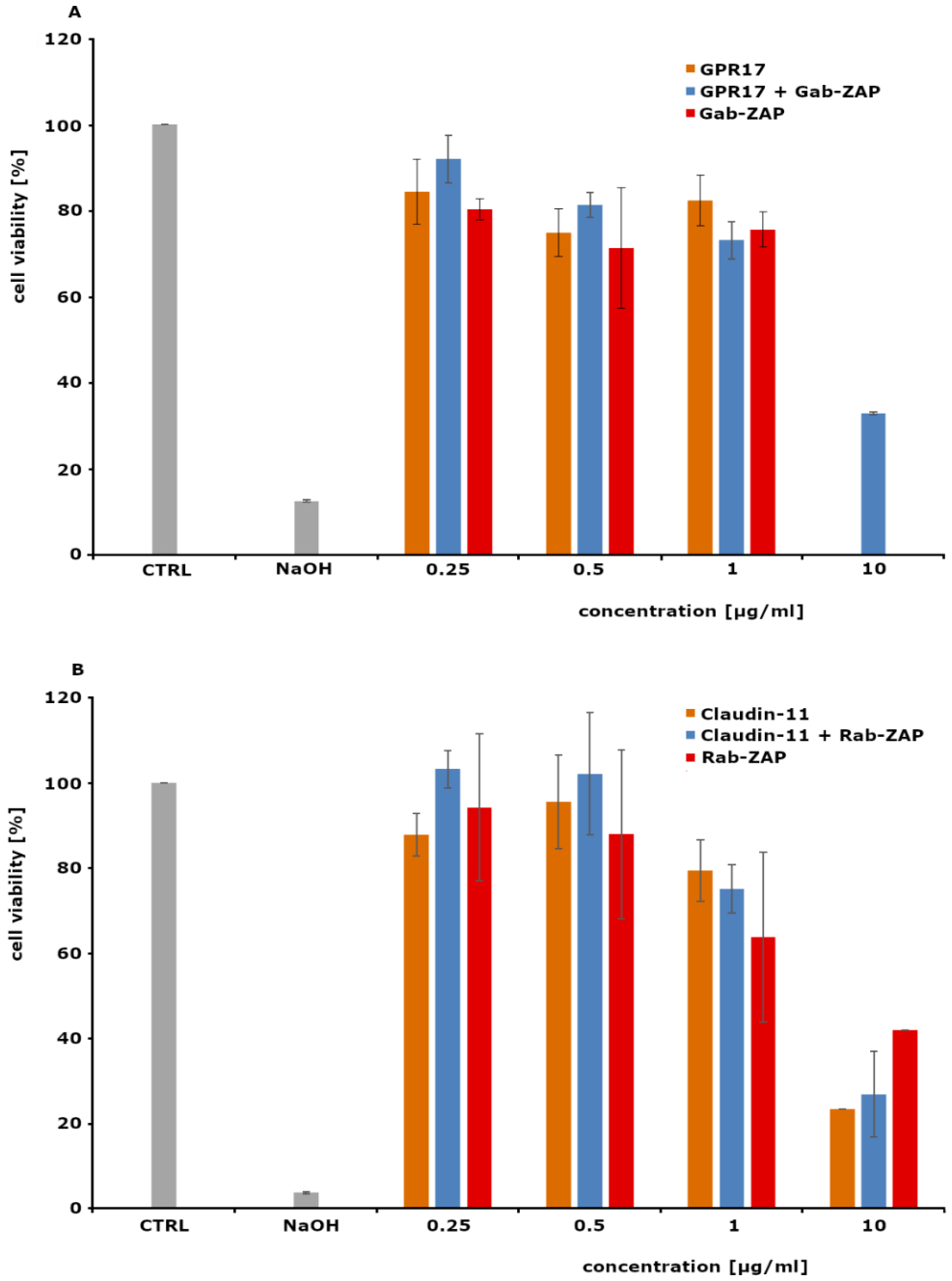

Fig. 3.26 Cell viability assessment of *Oli-neu* cells after treatment with two antibody-toxin-conjugates. *Oli-neu cells were seeded at a density of 6,000 cells per well in 96-well plates and cultured for 48 hours. Cells were treated twice with various concentrations of an antibody complex (**A** GPR17 and Gab-ZAP; **B** Claudin-11 and Rab-ZAP; blue bars) after a total of 7 days of incubation MTT-assay was performed.1 M NaOH and cells treated either with the primary or the secondary antibody alone, served as controls. Mean ± SD values of triplicates from one experiment are shown.*

Since, 1 µg/ml had a weak and 10 µg/ml showed a strong effect on the viability of *Oli-neu* cells, the effect of 5 µg/ml was examined (fig. 27). Again, treatment of cells with high concentrations of the antibody complex (blue bars; 11.96 % ± 7.76 %) but also of the primary antibody (orange bars; 26.28 % ± 11.61 %) alone resulted in severely decreased viability. Interestingly, treatment with the secondary antibody alone (red bars) did not result in high reduction of cell viability indicating that the effect of the complex could be specific or derived mainly from the primary antibody alone.

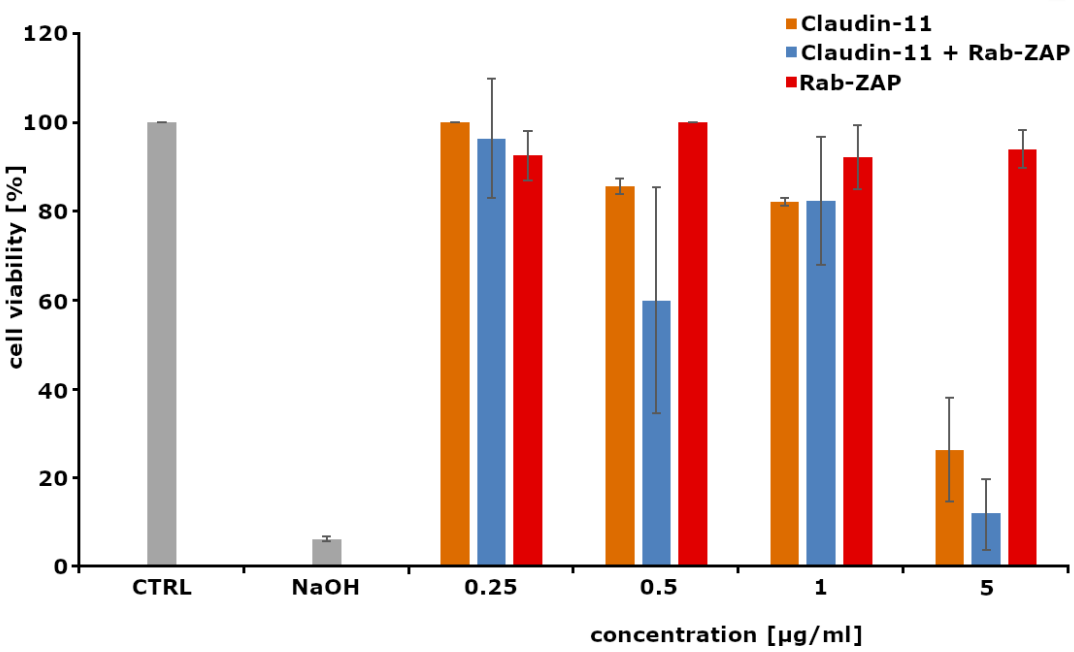

Fig. 3.27 Toxicity assessment of anti-claudin-11 antibody on *Oli-neu* cells. *Oli-neu cells were seeded at a density of 6,000 cells per well and incubated for 48 hours before treatment with antibody complex (Claudin-11 and Rab-ZAP; blue bars) as well as corresponding controls started. Cells were treated twice, ATP-measurement was performed after 7 days of incubation. Untreated cells and cells treated with 1 M NaOH served as controls. Mean values ± SD of one experiment with triplicates are shown.*

Claudin-11 antibody is provided in a solution containing 0.1 % sodium azide (NaN_3 ; 15 mM) which itself is toxic to cells (Kho *et al.*, 2017). To examine whether the presence of NaN_3 has an impact on the cell viability of *Oli-neu* cells, different dilutions of NaN_3 corresponding to the antibody complex concentrations were made. Cells were treated twice, and an ATP-assay was performed (fig. 28). Clearly, NaN_3 contained in 5 (46.54 % ± 11.77 %) and 10 µg/ml (20.43 % ± 2.57 %) dilutions is toxic to cells itself. That is resembling the results from the MTT-assay (fig. 3.26 and 3.27).

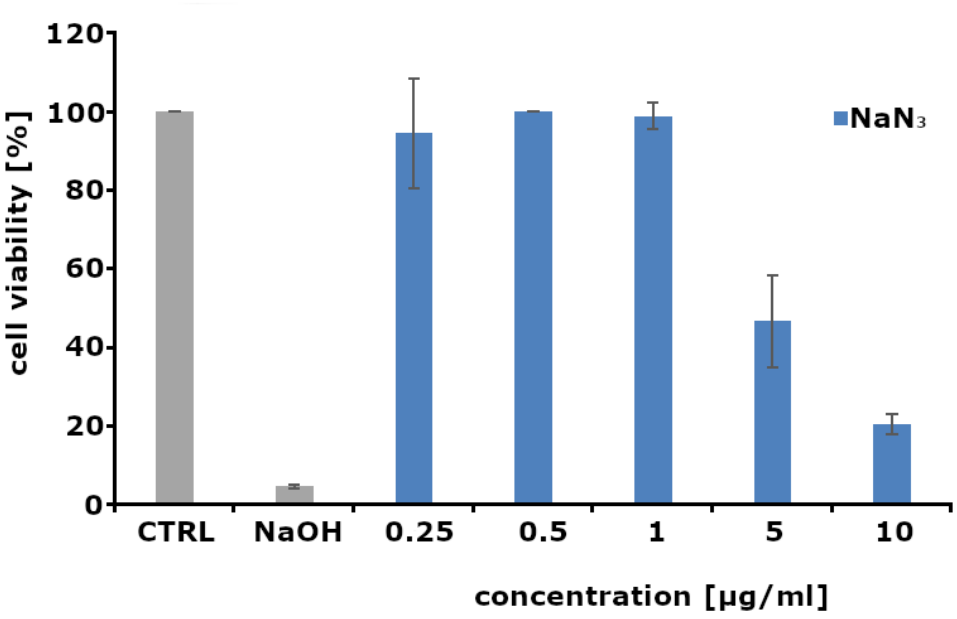

Fig. 3.28 Dilutions containing sodium azide (NaN_3) are toxic to *Oli-neu* cells. *6,000 cells per well were seeded and incubated for 48 hours before treatment with different dilutions of NaN_3 started. First a stock solution of PBS containing 0.1 % (15 mM) NaN_3 was prepared. Afterwards, different dilutions correlated to the concentrations used in previous experiments were prepared in culture medium. Thereby, 0.25: 0.015 mM; 0.5: 0.03 mM; 1: 0.06 mM; 5: 0.3 mM; 10: 0.6 mM refer to concentration of NaN_3. Cells were treated twice and incubated for a total of 7 days before celltiter Glo was performed. Untreated cells and cells treated with 1 M NaOH served as controls (grey bars). Mean values ± SD of one experiment with six replicates are shown.*

To remove NaN_3 from the Claudin-11 solution, the antibody was dialyzed in PBS using a vivaspin column (2 ml, 10,000 MWCO; Sartorius, Göttingen, Germany). *Oli-neu* cells were seeded at a lower density but for a longer time compared to previous experiments (fig. 3.29). Treatment occurred twice in one week. Cells treated with Claudin-11 (orange bars) alone, showed similar viabilities between concentrations. Overall, Claudin-11 alone has no effect on *Oli-neu* cells compared to previous experiments. The antibody complex (blue bars) on the contrary, showed a concentration dependence when mean values were compared. Regarding the high standard deviations at 0.5 (76.48 % ± 26.13 %) and 1 µg/ml (78.11 % ± 22.08 %) some cells seem to be less viable than when treated with 5 µg/ml (63.70 % ± 9.99 %). In addition, treatment with Rab-ZAP (red bar) alone, resulted in the lowest viability (57.16 % ± 11.73 %) compared to the other conditions except for when cells were treated with 100 mM NaOH (2.54 % ± 0.28 %).

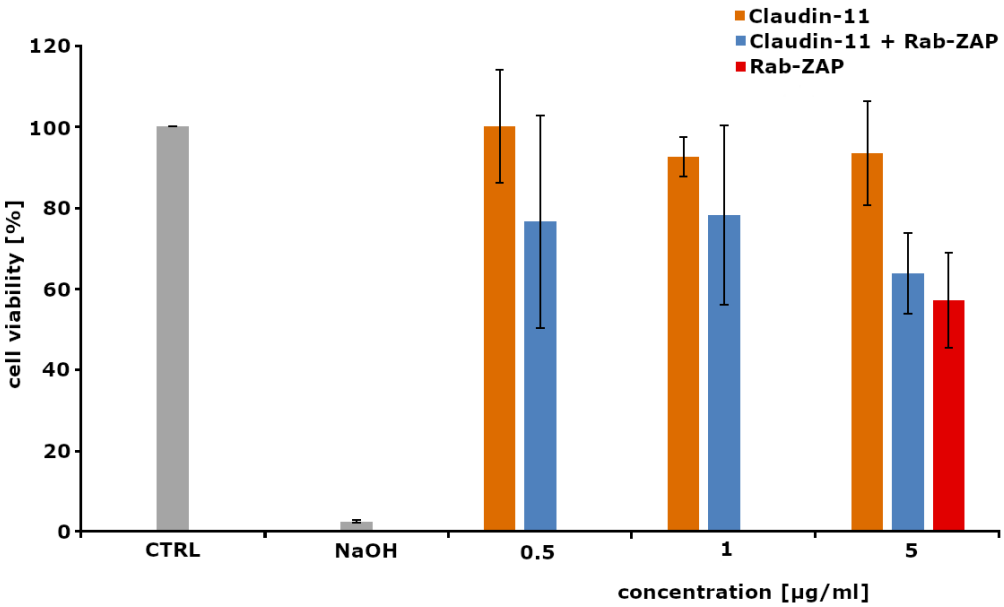

Fig. 3.29 Dialyzed Claudin-11 antibody is not toxic to *Oli-neu* cells anymore. *3,000 cells per well were seeded and incubated 5 days prior to treatment with antibody complex (Claudin-11 (dialyzed in PBS) and Rab-ZAP; blue bars). Cells were treated twice and incubated for a total of 10 days before MTT-assay was performed. Untreated cells, cells treated with 100 mM NaOH and with both antibodies alone served as controls. Mean values ± SD of one experiment with triplicates are shown.*

The differences between fig. 3.27 and fig. 3.29 regarding cell viability after treatment of cells with 5 mg/ml could be derived from the different cell densities that were initially plated. In more detail, 6,000 cells were plated in fig. 3.27 and incubated for 48 hours, whereas 3.000 were plated but incubated for 5 days prior to treatment in fig. 3.29. Also, the cultivation time differed since in the first situation cells were incubated for a total of 9 days, cells in the latter set up were incubated for 10 days. Assuming a constant growth rate for both plates, nearly the same number of cells should be present at the end of both experiments whereas at the start of treatment there were less cells in fig. 3.27 compared to fig. 3.29. Hence, more cells per condition could be responsible for a reduced effect of the antibody complex as observed in here. Such an effect was also monitored in fig. 3.25 when different cell densities responded differently to the treatment. However, regarding the high standard deviations for the antibody complex treatment at 0.5 and 1 µg/ml as well as the decrease of cell viability when treated with Rab-ZAP alone, further investigations needed to be done regarding the usefulness of this cell line for this kind of experiments.

3.3.2 Characterization of oligodendrocytes *in vitro* and *ex vivo*

Because the results in the previous section were contradictory a more detailed characterization of *Oli-neu* cells for the usefulness for immunoablation experiments was done. To characterize *Oli-neu* cells, cells were seeded on chamber slides and cultivated for several days before immunofluorescence staining for oligodendrocyte specific markers was performed. Cells were stained with anti-GPR17 antibodies (red) (fig.3.30 A, B and C). Additionally, in C also nuclei were stained using DAPI (blue). *Oli-neu* cells could successfully be stained with the GPR17 antibody that was previously used in immunoablation experiments. Furthermore, two oligodendrocyte precursor-specific markers were used: Oligodendrocyte marker 4 (O4; fig. 3.30 D) and Neuron/ glial antigen 2 or melanoma-associated chondroitin sulfate proteoglycan (NG2/MCSP; fig. 3.30 E). Both antibodies were found to stain a portion of the cultured *Oli-neu* cells. The number of GPR17-positive cells is quite high even after 12 days of culture indicating that the cells have not developed to a great extent over time.

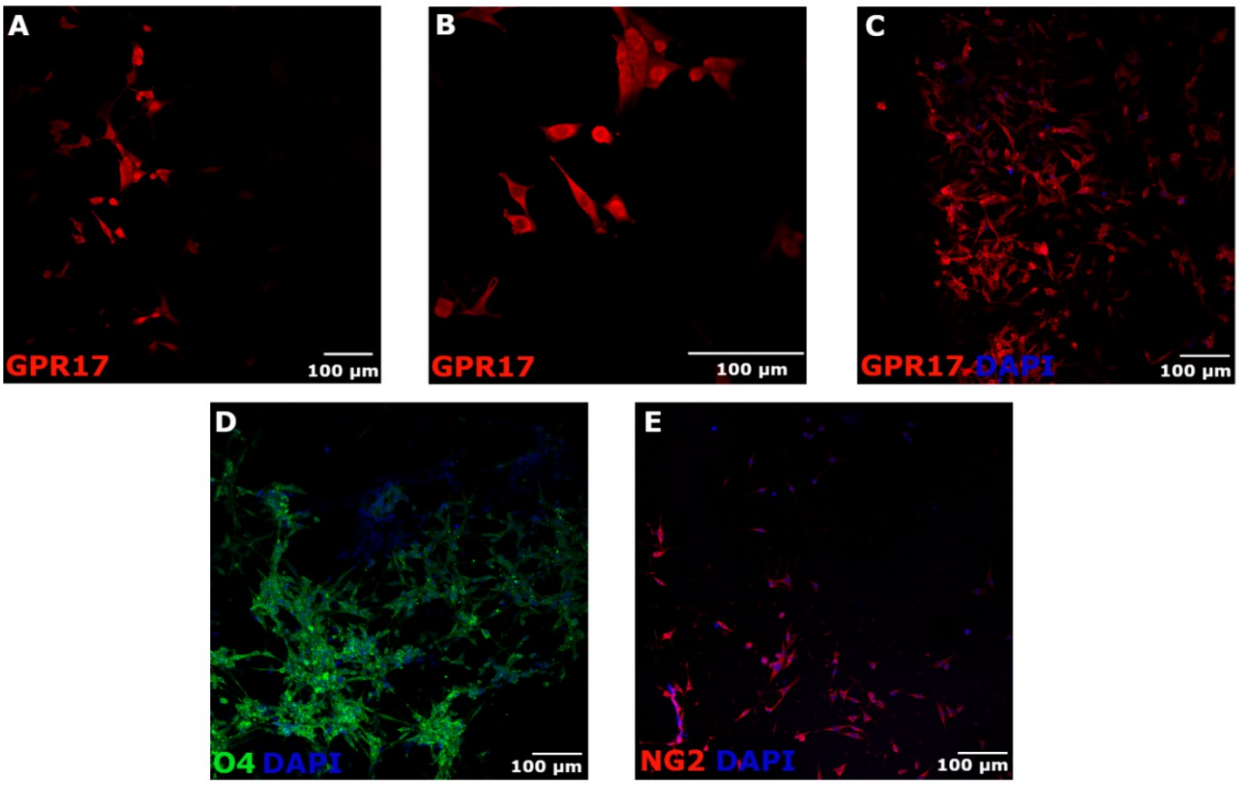

Fig. 3.30 GPR17-positive *Oli-neu* cells *in vitro*. *Oli-neu cells were seeded at a density of 10,000 cells per chamber on PDL-coated chamber slides cultivated for 12 days and stained with specific markers. Images were taken with a Leica SP8 LSM with an 20x/0.70 dry objective and a zoom of 0.75. Primary and secondary antibodies were diluted 1:200 and incubated for 1 hour each.* ***A*** *Cells were stained with anti-GPR17 antibody and anti-goat-AF555 antibody (red).* ***B*** *Cells in image A at a 20x magnification with a zoom of 1.77.* ***C*** *Cells were stained with anti-GRP17 antibody (red) and DAPI (blue).* ***D*** *Cells were stained with oligodendrocyte marker 4 (O4) and anti-mouse-AF488 (green) and DAPI (blue).* ***E*** *Cells were stained with anti-NG2 antibody and anti-rat-AF594 (red) and DAPI (blue).*

The addition of several factors can induce differentiation/ maturation processes of progenitor cells *in vitro*. The cyclic nucleotide derivate dbcAMP can activate cAMP-dependent protein kinases and induce differentiation of oligodendrocyte progenitor cells derived from mixed glial cultures (Raible and McMorris, 1993) and human potent stem cells into dopaminergic neurons (Xia *et al.*, 2016). Here, the compound was used to induce differentiation of *Oli-neu* cells.

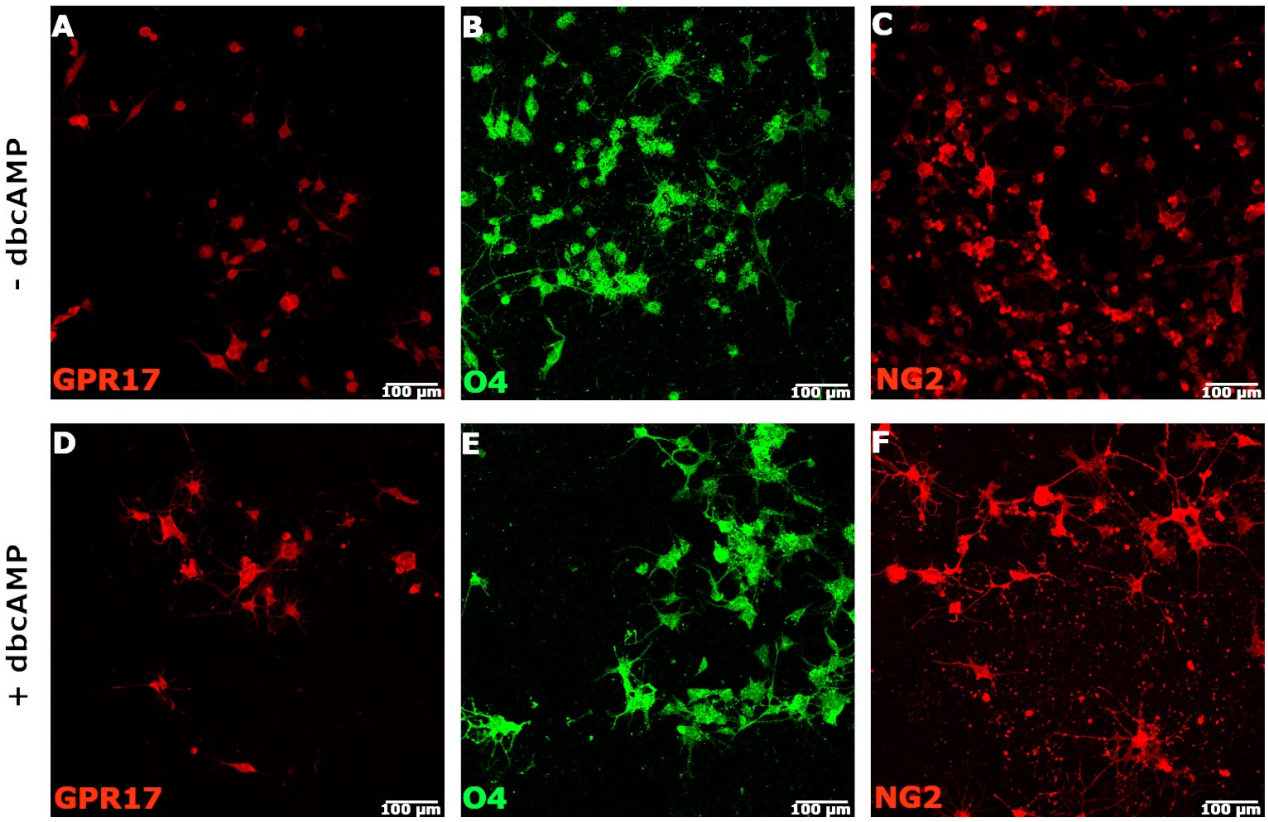

Fig. 3.31 *Oli-neu* cells were treated with dbcAMP to induce differentiation. *Oli-neu cells were seeded on chamber slides and cultivated for 5 days. Half of the cells were treated with 1 mM dbcAMP (D-F) and cultivated for another 5 days.* ***A*** *+* ***D*** *anti-GPR17,* ***B*** *+* ***E*** *anti-O4,* ***C*** *+* ***F*** *anti-NG2. Antibodies were diluted 1:400 each, secondary antibodies were applied at a dilution of 1:1000. Images were taken with a CLSM at a magnification of 20x.*

The addition of dbcAMP to the culture medium of *Oli-neu* cells led to a slight decrease of GPR17-signal (fig. 3.31 D). GPR17 was found to be reduced after longer incubation times due to maturation processes (Viganò *et al.*, 2016). *Oli-neu* cells were treated for 5 days before fixation and staining was performed.

Cells were stained with anti-NG2, anti-GPR17 and anti-O4. There is a reduction of NG2-positive cells under dbcAMP treatment compared to non-treated cells (fig. 31 C and F). Moreover, *Oli-neu* cells treated with dbcAMP seemed to undergo morphological changes as they appear more branched (fig. 31 E and F) compared to non-treated cells.

All three proteins could be stained in ten days old slice cultures (fig. 3.32). NG2 and O4-positive cells were detected in one individual slice (A). Additionally, GPR17 cells could also be targeted (B) though staining was not as strong as the other ones. Which is like *in vitro* staining where there were also less GPR17-positive than O4-positive cells detected.

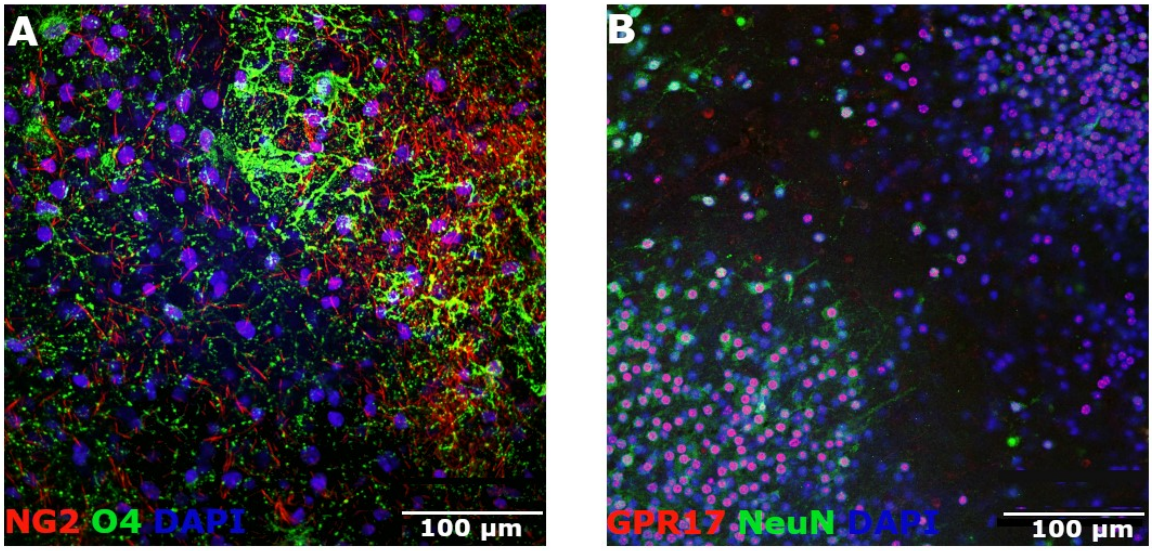

Fig. 3.32 OHSCs were stained with different oligodendrocyte-specific markers. *Slices were cultivated for ten days, before fixation and staining procedure was performed. Images were taken with a CLSM and an 40x/1.30 oil objective and a zoom of 0.75.* ***A*** *Slices were stained with anti-NG2 (red), anti-O4 (green) and DAPI (blue).* ***B*** *Slices were stained with anti-GPR17 (red), anti-NeuN (green) and DAPI (blue).*

Due to unpredictable events including the corona situation, immunoablation experiments of oligodendrocytes *ex vivo* could not be started.

4. Discussion

The present thesis provides evidence for the importance of astrocytes for the maintenance of cell architecture in organotypic hippocampal slice cultures and provides first evidence for the possibility of transporter-mediated internalization of antibodies.

To understand and characterize the role of glial cells in neuroinflammatory processes of neu-rodegenerative diseases, it is crucial to establish a model system that displays the pathol-ogy of the disease and allows the individual study of cells. In a previous study, we established a model system of AD displayed by Aβ-toxicity and it was shown that microglia could success-fully be depleted using the bisphosphate clodronate and that the depletion resulted in en-hanced Aβ-induced cytotoxicity. Moreover, microglia remained a ramified morphology and the mechanism behind the protection against Aβ-induced toxicity was proven to be phagocy-tosis (Richter *et al.*, 2020). Here these results were confirmed regarding the ability to suffi-ciently deplete microglia from slice cultures (fig. 3.2), whereas it was difficult to deplete *BV-2* cells *in vitro* (fig. 3.1). Cell lines react different since they are not a physiological system due to their genetic modification towards immortality (Henn *et al.*, 2009). It is not surprising that *BV-2* cells were more robust against clodronate treatment in this context and showed less cell death compared to primary microglia in the slices.

Treatment of slices with monomeric and oligomeric $A\beta_{42}$ did not result in enhanced cell death as revealed by immunofluorescence (fig. 3.3 B and C) compared to control (A). These findings are in line with the results obtained in a previous study from the working group. In this study, cell death by Aβ-application was induced only in slices where microglia have been depleted. These results indicate that microglia display a crucial role in the context of Aβ-induced cytotoxicity *ex vivo*. Mechanisms of this protection have been discussed in our publication (Richter *et al.*, 2020).

There is still a lack of a system to study the individual role of astrocytes and oligodendrocytes *ex vivo*. In this study, two ways to investigate the role of astrocytes and oligodendrocytes using primary cells, cell lines and slice cultures was examined.

4.1 Finding the right antibody complex for immunoablation

To investigate the role of astrocytes, first experiments were done with isolated primary murine cells. For the ablation of astrocytes, a technique that was described by Higgins et al. was utilized (Higgins *et al.*, 2015). The authors used antibody constructs in combination with toxins to specifically target tumor cells for ablation. This technique is widely used in tumor therapy and was adopted in the present study for specific ablation of primary astrocytes in culture. An antibody complex consisting of primary antibodies against surface proteins e.g. receptors, transporters or channels especially expressed on astrocytes and an inherent secondary antibody attached to saporin molecules was designed. Therefore, three different primary antibodies against antigens (GLT-1, GLAST-1 and AQP4) were investigated upon their ability to bind to cell surface proteins of astrocytes and to be internalized in order to be useful for further studies (fig. 3.5 – 3.9). GLAST-1 is a glutamate aspartate transporter and was found to be expressed to a lesser extent in hippocampal astrocytes, but more prominently in Bergmann glia (Storck *et al.*, 1992). However, immunofluorescence staining of isolated cells here revealed that primary astrocytes expressed GLAST-1 proteins and that these cells had a flat polygonal shape (see appendix fig. 6.1 A).

AQP4 is a water channel distributed throughout the cerebellum, the hippocampus and ependymal cells (Jung *et al.*, 1994) and thus exerts its function in the regulation of water balance. Glutamate transporter 1 (GLT-1 also referred as EAAT2) is expressed on astrocytes to a lesser extent than GLAST-1. AQP4 and GLT-1 coexist in a “macromolecular complex” (Hinson *et al.*, 2008). In neuromyelitis optica (NMO) autoantibodies against AQP4 led to the internalization of the transporter and reduction of GLT-1 and impaired glutamate homeostasis (Hinson *et al.*, 2012). Thus, indicating that internalization of transporters after the binding of antibodies directed against them is a rare but observed event.

Among the here tested antibodies, GLAST-1 was found to be a promising candidate, since fluorescence intensities as a measure of internalization, increased to a higher extent over time compared to AQP4 (fig. 3.5 A and B). With the highest rate of intensity after 24 hours. Though intensity of the control (dye alone in medium) also increased over time. When plates were washed in PBS and measurement was also done in PBS, values per se were lower but the same remained regarding higher intensities of GLAST-1 after 24 hours if incubation was compared to control and AQP4 (fig. 3.5 Ca and D). This time the intensity of the control-treated cells

again was also high but did not reach the intensity of the antibody-dye conjugate. Whereas all three proteins are found in the plasma membrane of astrocytes (Jung *et al.*, 1994; Nielsen *et al.*, 1997) the binding and internalization ability differed. The two glutamate transporters (GLT-1 and GLAST-1) showed similar effects concerning internalization (fig. 3.7). But because, GLAST-1 fluorescence intensity exceeded that of GLT-1 at the highest concentrations, GLT-1 was not used in the other experiments. Internalization of macromolecules like proteins e.g. antibodies usually is mediated through cell surface receptors. Binding of antibodies to these receptors, results in endocytosis and transport of the endocytic vesicle to endosomes and lysosomes where degradation processes will take place (Peters and Brown, 2015; Parslow *et al.*, 2016). However, evidence indicates that endocytosis is also mediated through different surface proteins as was shown by the internalization of Mab against tumor surface antigens (Matzku *et al.*, 1988). Recent studies regarding tumor specific Mab-targets for drug delivery (antibody-drug-conjugate; ADC) identified a member of the solute carrier family (SLC) as a promising candidate for pancreatic and prostate epithelial tumor target (Mattie *et al.*, 2016). The choline transporter like protein (CTL4) is targeted by an ADC since this kind of transporter is upregulated in tumor cells and therefore can be used to specifically target diseased cells. It was also shown that the conjugate was internalized and brought to the lysosome after 24 hours which is the favored organelle for the antibody-dye conjugate investigated here (Mattie *et al.*, 2016). This type of ADC is now in phase I clinical trial (Coveler *et al.*, 2016; McHugh *et al.*, 2019). Though the exact mechanism is missing, internalization in these studies is not dependent on receptor mediated endocytosis. A similar phenomenon was described by the group of Pulaski. In their study, the authors found that binding of an 5D3 antibody to an ABCG2 transporter on A549 cells resulted in the transporter's internalization and partial translocation to early endosomes, lysosomes or back to the plasma membrane in order to be recycled (Studzian *et al.*, 2015). This was the first study that demonstrated ABCDG2-transporter internalization after antibody-binding. Translocation of membrane proteins e.g. glucose transporters/ receptors is well known (Rahbek-Clemmensen *et al.*, 2014). It was shown that the serotonin transporter (SERT) as well as the dopamine (DAT) (Loder and Melikian, 2003) and glycine transporter 2 (GLYT2) (Fornés *et al.*, 2008) – also members of SLCs- undergo internalization and are mostly directed to early endosomes for degradation rather than recycled. Transcytosis of macromolecules was already investigated and shown by others (Matzku *et al.*, 1988; Megias *et al.*, 2000). Also in astrocytes, macromolecules like serum

albumin (BSA) have been found to be transported through the cell cytoplasm (Juurlink and Devon, 1990). Though BSA is a protein with a molecular weight (MW) of 65 kDa. But even greater proteins such as transferrin (79.5 kDa) and complexes of BSA and transferrin were found to be internalized by astrocytes by endocytosis. GLAST-1 itself has a MW of 60-64 kDa. One can speculate that antibodies bound to the transporter are internalized due to spontaneous transcytosis of the transporter itself, or forced by the binding process and brought to the lysosome for degradation purposes. The effect of anti-GLAST-1 antibody binding to the transporter *in vitro* was not investigated here. One possible consequence could be the disrupted function in glutamate uptake upon binding of the antibody-conjugate and subsequently the internalization process of the malfunctioning transporter for degradation purposes as was shown to happen with AQP4 and GLT-1 in NMO diseased astrocytes (Hinson *et al.*, 2012).

Here, the internalization of GLT-1, GLAST-1 and AQP4 after binding of commercially available antibodies in primary astrocytes was evaluated and regarded as a tool to identify a suitable candidate for further immunoablation studies *in vitro* and *ex vivo*.

4.2 Immunoablation of primary astrocytes *in vitro*

Due to the internalization experiments, GLAST-1 was used for the preparation of antibody-toxin conjugates and tested *in vitro* on primary astrocytes on its ability to specifically target and reduce GLAST-1 positive cells. Various concentrations of the antibody complex on primary astrocytes in cell culture over several incubation times were tested (fig. 3.10-3.14). Results show that there is a concentration dependence correlated with cell viability for the antibody-complex and the toxin-coupled secondary antibody alone. More likely, the concentration of the primary antibody is crucial to form a sufficient number of complexes. The viability only slightly decreased when treated with 1 and 2.5 µg/ml of Rab-ZAP and an unequal amount of GLAST-1 (0.41 µg/ml) (fig.10.8 B) although internalization revealed that a concentration of 0.3 mM of the GLAST-1 was enough for internalization.

Despite there are less cells seeded in fig. 3.10 B than in A, the effect of the antibody complex remained similar and was not detrimental. Whereas cell viability even exceeded untreated cells at 5 µg/ml Rab-ZAP + 0.41 µg/ml GLAST-1. But since even NaOH was not enough to kill

most of the cells, the assay itself might have not worked properly. When the experiment was repeated (fig. 3.11) with a higher number of cells, a concentration dependent decrease of viability was observed. But also when treated with GLAST-1 and Rab-ZAP alone, viability decreased. There is a variation between the different experiments. When cells were treated with an even concentration of both antibodies (fig. 3.12-14) the effect on the viability was concentration dependent. GLAST-1 treatment alone had only slight effects. Rab-ZAP treatment on the other hand resulted in severely decreased viability. These results are partly in line with the findings of Pilkington's group, since they observed a concentration dependence as well (Higgins *et al.*, 2015). But they did not observe that treatment with the toxin-coupled antibody alone had such an effect on the viability observed here. In a different study from the manufacturer that produces the toxin-coupled antibodies, cell viability is affected by the toxin at a concentration of 2.5 µg/ ml (Kohls and Lappi, 2000) which is similar to the results presented here. One explanation for the reduction of cell viability *in vitro* could be that the astrocyte culture isolated from a mixed glial cell culture that was used for experiments did not consist of 100% pure astrocytes (Kumamaru *et al.*, 2012). It is already known that primary cells isolated from tissue do not reach absolute purity (McCarthy and Vellis, 1980; Kirkley *et al.*, 2017). In addition, since individual experiments were performed with cells derived from several isolation processes, the actual number of cells and purity may vary. That is different to the studies mentioned above, since the authors used commercially available glioma derived cell lines. Remaining microglia in the cell culture could be responsible for the decreased cell viability due to toxin-treatment alone since they are capable of phagocytosis and could have died because of that. Therefore, the data from the antibody complex treatment seem to express the cell viability of astrocytes, since microglia do not express the primary target GLAST-1 (Kirkley *et al.*, 2017). Since both antibodies could form the complex during the pre-incubation period prior to treatment, only cells expressing GLAST-1 could be targeted by the complex in the cell culture. That excludes microglia. In addition, treatment with AQP4 resulted in similar findings (fig. 3.12 and 13).

In former publications, a distribution of GLAST-1-positive cells throughout the cortex has been evaluated (Perego *et al.*, 2000). In more detail, whereas GFAP could stain both types of astrocytes (fig. 6.1 B), GLAST-1 antibodies were able to stain polygonal flat cells, referred to as type 1 astrocytes. In the here used cell culture, most of the observed cells were type 1 astrocytes that displayed large cell bodies and made connections in form of processes with

surrounding cells, forming a layer after several days of incubation. But there were also cells with a small soma and thin processes that remained on top of the cell layer but were rather isolated. Of course, these cells could also contribute to the cell viability measurements but are not targeted by the antibody complex. Moreover, cultures containing neurons have a decreased amount of glutamate transporter 1 (GLT-1) expression whereas the expression of GLAST-1 is unaffected (Gegelashvili *et al.*, 1997). Since immunoablation was predominantly designed to be used in slice cultures where neurons are present, GLAST-1 was chosen to be the preferred antibody for ablation studies *ex vivo*.

Microglia could also be part of the explanation concerning the Lα-AAA results *in vitro*. Again, because the cultures used are not 100% pure, remaining cell viability signals can derive from remaining microglia in the culture that are not affected by the treatment themself (Takada and Hattori, 1986). Besides, presence of microglia was said to inhibit the toxicity of the compound (Brown and Kretzschmar, 1998). This was found to be proportional to the number of microglia present in the cultures and could explain why higher concentrations of Lα-AAA were used here and why there is also a discrepancy between the individual experiments presented in this study. On the one hand, microglia are able to release glutamate that could compete with the compound (Czeh *et al.*, 2011; Takaki *et al.*, 2012; Ridolfi *et al.*, 2013) and on the other hand, microglia could phagocytose the compound thereby lowering the actual concentration. In addition, Lα-AAA was found to be active on different types of astrocytes. In more detail, astrocytes type I are predominantly affected by the compound whereas type 2 astrocytes are mainly unaffected (Brown and Kretzschmar, 1998).

Due to a low concentration of the stock, the amount of the drug added to the wells exceeded 50% of total volume in the highest concentration (7.5 mM). Therefore, additional controls were applied to check whether the replacement of media by the drug-solution influences cell viability *in vitro*. Actually, the replacement did have an effect on the viability, but the effect of the drug was more intense and specific. These results slightly differ with experiments from isolated primary rat astrocytes (Bridges *et al.*, 1992), herein the authors found a concentration dependent decrease of cell viability due to Lα-AAA already after 48 hours of exposure with the highest decrease at a concentration of 1 mM. Whereas here, an EC50 was found to be achieved at 4 to 5 mM. Moreover, in previous studies results also indicated that the duration of treatment and concentration of the drug was important for consistent depletion of

astrocytes *in vitro* (Huck *et al.*, 1984). The authors observed a detrimental decrease of viability of nearly 97 % after 40 hours of incubation with 0.34 mM Lα-AAA. The observed effects here were obtained with even longer incubation times and higher concentrations compared to the older studies. An explanation for the discrepancy between the concentrations of former studies and the ones used here could derive from the fact that the presence of microglia in the culture leads to decreased effects of the drug (Brown and Kretzschmar, 1998) as explained earlier.

4.2 Immunoablation of astrocytes *ex vivo*

Since greater effects on the cell viability of astrocytes in cell culture were observed, same experiments on slice cultures were performed. Again, GLAST-1 was used as the primary target and treatment of slices occurred three times during a week. In the slice cultures even the highest concentration of 5 µg/ml was not sufficient to deplete all GFAP-positive cells. Besides, neuronal cells (NeuN-positive) were not affected by the antibody-complex and cell architecture remained intact, since neurons do not express GLAST-1 (Schmitt *et al.*, 1997; Perego *et al.*, 2000). Nevertheless, a trend with a concentration dependence was observable. Possible explanations for the incomplete depletion could be that the working concentrations were too low for the number of cells present in the slices that exceeds the amount in cell culture. On the other hand, the volume of the wells for the slice cultures is 1.2 ml and the slices are incubated on membrane inserts that are surrounded by the media. It may be that the antibody-complexes in the media are not equally distributed throughout the two days of treatment between the media changes, since the slices are not in constant movement, which is different to other culture methods (Gey and Gey, 1936; Hogue, 1947). Another reason could be that due to the presence of different types of astrocytes in the slices, not all types express GLAST-1 and because of that there are still GFAP-positive cells detectable (Rothstein *et al.*, 1994; Perego *et al.*, 2000; Tabata, 2015). According to GFAP-staining, predominantly type 1 astrocytes were observed in the cell culture. In contrast, most of the cells in the hippocampus are of the second type. As explained earlier, type 2 astrocytes do not express GLAST-1 on the cell surface.

Treatment of slices with the amino acid Lα-AAA resulted in detachment of cells from the insert, thus immunofluorescence staining was not possible, or slices appeared damaged under the microscope. In former publications, the toxicity of Lα-AAA was shown to not affect neurons when the compound was administered *in vivo* (Khurgel *et al.*, 1996; Nishimura *et al.*, 2000). But neurons in our preparations did not look vital at all in high concentrations of Lα-AAA. This was also observed *in vitro* when cells were treated with high molar concentrations (5 mM) which is comparable to the concentrations used here (Garthwaite and Regan, 1980). The effect on neurons could be due to the loss of structural maintenance by the depleted astrocytes. For the first time, this was shown to be an effect of the loss of astrocytes in the injection region by Lα-AAA of rat medial prefrontal cortex (Lima *et al.*, 2014). These results are in line with findings from McBean (McBean, 1994), who observed that glial cells are important for the integrity of neuronal cells and that manipulation of these cells could lead to toxic reactions in the central nervous system (Jäkel and Dimou, 2017). Furthermore, due to a loss of astrocytes in the slices, neurons can be affected by oxidative stress and impaired Ca^{2+} signaling (Sun *et al.*, 2018). Additionally, the start point of treatment seems important, since begin of treatment on the first day of cultivation had severe effects on neuronal survival compared to the treatment of older cultures (Huck *et al.*, 1984), which is different to clodronate treatment that is applied to slices on the day of preparation.

It was shown that directly injected Lα-AAA solutions were toxic to astrocytes in cerebral regions (Takada and Hattori, 1986; Nishimura *et al.*, 2000; Lima *et al.*, 2014) as well as the substantia nigra and locus coeruleus (Chang *et al.*, 1993) but not in the hippocampal formation (Saffran and Crutcher, 1987) of rodents. But more recent results showed that astrocytes could be depleted for at least 10 days *in vivo* by injection of Lα-AAA into the CA3 region of rat hippocampus (Sun *et al.*, 2018). This discrepancy could be due to different types of astrocytes present in the cerebral regions of the cortex as well as in the hippocampal formation itself (Testen *et al.*, 2019). According to a previous publication (Brown and Kretzschmar, 1998), Lα-AAA is toxic to type 1 astrocytes, but not to type 2 astrocytes which was observed to be more prominent in the slice cultures. Additionally, different ages of animals, that were used could contribute to the diverse outcome of experiments (Sun *et al.*, 2013).

To sum up the major differences regarding Lα-AAA treatment, from the studies mentioned compared with the results presented here, are (1) that most of the experiments from the past

were done *in vivo* whereas the experiments here were done *in vitro* and *ex vivo*. In addition, the cultivation method using membrane inserts has many advantages towards the former techniques, but in this case, it could be hindering. Also, the way of treatment differs (2), since most research was done by direct injection into cerebral regions and our experiments were done by application through media. Furthermore, a range of concentrations was tested (3) that are much higher than most of the studies used, since any effects in lower millimolar ranges were observed. The fourth difference is the solvent (4) that was used to solve the compound. Interestingly, there is no consistent protocol how to proper solve the amino acid-powder. Considerable trouble was caused when trying to solve it in aqua bidest. Since it is an amino acid, the pH dropped. In order to counteract this, the pH was adjusted to around 7.4 - 7.6 by adding NaOH to the solution. Because it was only possible to solve the compound to a final concentration of 2 mg/ml in water, this resulted in a molarity of 12.5 mM. Further attempts to solve the compound in culture medium, PBS or 1N HCL failed, since the addition of a proper amount of NaOH to raise the pH towards a physiological level led to precipitation of the powder and no proper working solution.

4.3 Immunoablation of oligodendrocytes *in vitro*

NG2 is a cell surface marker for oligodendrocyte precursor cells (OPCs) (Shoshan *et al.*, 1999; Zhu *et al.*, 2008) and was found to be present in the cell culture of *Oli-neu* cells (fig. 3.30 E). Oligodendrocyte marker 4 (O4) also is a cell surface marker of OPCs, but it also stains immature as well as mature and myelinating cells (Traiffort *et al.*, 2016). *Oli-neu* cells could be stained by this antibody *in vitro* (fig. 3.30 D). It seems that there is a mixture of different types of oligodendrocytes in the culture with a majority being O4-positive. As there are also NG2-positive cells, *Oli-neu* culture consists of mostly precursor cells as revealed by staining.

In contrary, cells could not be stained with anti-Claudin-11 antibody. Claudin-11 is a myelin-associated protein (Bronstein *et al.*, 2000b). Since *Oli-neu* cells were found to be mostly precursor and non-myelinating cells, it is not surprising that cells were lacking Claudin-11 staining. This could in part explain, why cells did not respond to treatment with Claudin-11 and Rab-ZAP (fig.3.25 and 3.26). The observed effect was low and found to be mostly derived from the presence of sodium azide (NaN_3) in the conservation-solution of Claudin-11 antibody (fig.3.26). Removal of NaN_3 resulted in less toxicity of Claudin-11 treatment alone (fig. 3.27).

Nevertheless, Claudin-11 was also found to be expressed in cultured oligodendrocytes before myelinating (Bronstein *et al.*, 2000a) and could contribute to some of the effects observed in viability assays. Moreover, cells could be stained with anti-GPR17 antibodies *in vitro*. GPR17 is expressed predominantly in OPCs that are non-myelinating and thus not mature (Mogha *et al.*, 2016), which is in line with the findings from the marker staining. GPR17 expression decreases with incubation time of cultures derived from neonatal rats already after 6 days in culture (Fumagalli *et al.*, 2011). This is in line with findings from the slice cultures, where staining of slices (fig. 3.32) reveals that there are still immature OPCs present even after ten days of culture, therefore GPR17 could still be detected. Primary oligodendrocytes were stained with anti-Proteolipid protein (PLP), anti-2',3'-Cyclic-nucleotide 3'-phosphodiesterase (CNPase) and anti-GPR17 antibodies (Appendix, fig. 6.2). CNPase is a cytoplasmic protein and a marker of mature oligodendrocytes, whereas PLP is a cell surface marker of mature but non-myelinating oligodendrocytes. Both markers also do target mature and myelinating cells, as PLP is involved in myelin formation and therefore expressed late in the development with a slight increase from day 6 *in vitro* and the peak at day 14 (Fumagalli *et al.*, 2011).

In order to investigate the different stages of oligodendrocyte differentiation *in vitro*, cells were treated with dbcAMP for 5 days (fig. 3.31). Cells treated with dbcAMP appear to have more branches compared to non-treated cells, thereby the O4 signal is slightly enhanced (fig. 3.31 E). This is in line with findings from Jung et al. who treated *Oli-neu* cells for at least 10 days before staining was performed (Jung *et al.*, 1995). They found that O4 signal is increased after treatment with dbcAMP and that cells develop multiple branches. Nevertheless, GPR17 signal was unaltered, but still cells could not be stained with Claudin-11, indicating that maturation was not completed until days 5 of treatment here.

4.4 Conclusion and future perspectives

The aim of the present study was to find techniques that can specifically discriminate astrocytes and oligodendrocytes from a dense-cell network like slice cultures. The ablation of specific cell types is crucial to investigate their specific role in neuroinflammation of neurodegenerative diseases and to better understand the individual effects of each cell type. The neuroprotection against Aβ-mediated toxicity by microglia was examined and summarized in a recent article (Richter *et al.*, 2020). Next to microglia, astrocytes and oligodendrocytes exert important functions in maintaining an environment that is necessary for the survival of neurons as well. Astrocytes play a crucial role in the (re-)uptake of neurotransmitters as glutamate from the synaptic cleft after the synaptic transmission (Maragakis and Rothstein, 2006; Liddelow *et al.*, 2017). Disturbances in this homeostasis can lead to glutamate- and excitotoxicity (Mahmoud *et al.*, 2019; Zhang *et al.*, 2019). Glutamate is taken up by various transporters on the surface of astrocytes (Rose *et al.*, 2018). Among others, two have been investigated here. GLAST-1 was found to be a promising candidate since internalization signals were strongest and treatment of slices responded in a concentration-dependent manner. To the best of my knowledge, this was the first work to demonstrate GLAST-1 internalization *in vitro* and immunoablation of astrocytes *ex vivo* using GLAST-1 as a target to specifically ablate astrocytes. These results are rather surprising since the internalization of transporters into cells after binding of antibodies is a rare event. The underlying processes for the internalization are of great interest since this method could be further developed for drug-delivery studies to different kinds of cells. This method could lead to a broader spectrum of ways for drug-targeting as it is already used in cancer treatment (Parslow *et al.*, 2016).

Moreover, the present study provides further evidence for the importance of astrocytes in maintaining the cell architecture in slice cultures, since depletion of astrocytes from slices resulted in a severely disrupted cytoarchitecture leading to neuronal cell death. Lα-AAA has been widely used *in vivo* to eliminate astrocytes region-specific (Khurgel *et al.*, 1996). Here, Lα-AAA treatment showed a concentration-dependence on the viability of isolated astrocytes *in vitro* and in some cases also *ex vivo*. Furthermore, preparation of Lα-AAA, duration of treatment as well as age of the slices seemed to be important. Preparation of Lα-AAA is difficult, since only few amounts of the drug are soluble in water yielding a low millimolar stock solution and it was shown that the replacement of medium by the drug itself had

consequences for the survival of astrocytes. Nevertheless, the effect *in vitro* was specific to the drug. *Ex vivo*, treatment of slices led to a destruction of cellular architecture and probably thereby to the death of neurons as well. These results indicate that astrocytes are important for the integrity of other cells and if depleted, the network can no longer be maintained. This is in line with the already known supportive functions of this kind of cells. Next to maintaining the metabolic environment, astrocytes seem to exert physical support by forming a network around and between neurons. Once this network is disturbed, environmental and pathogenic factors can affect neurons.

Regarding neurodegenerative diseases like AD, reduction of astrocytes could lead to enhanced vulnerability of neuronal cells towards malformed proteins and ongoing inflammatory processes thereby worsening the symptoms and further perpetuating the vicious cycle of inflammation and damage. However, in a few slices, neurons were still detectable using immunofluorescence whereas GFAP-signal was missing, indicating that astrocytes have been depleted but neurons stayed unaffected by the drug. Further investigations are needed to find the right concentration and duration of treatment of slices with Lα-AAA and additionally, solvents are required that are themselves not harming neurons but could be used to produce higher molar stock solutions.

For the depletion of oligodendrocytes, *Oli-neu* cells have been utilized and characterized by immunofluorescent stainings. According to the stainings, the cells of the cell line were found to be pre-mature to a greater extent. Two surface targets have been used for ablation studies here. Among them, the anti-Claudin-11 antibody showed greater effects on the viability than the anti-GPR17 antibody, whereas cells *in vitro* could not be stained with anti-Claudin-11 antibodies. Slices were also GPR17-positive but Claudin-11-negative based on immunofluorescence reactivity. The effect of the anti-Claudin-11 antibody was revealed to be due to the conservation solution containing sodium azide (NaN_3) which was proven to be toxic in low concentrations itself. After the removal of NaN_3, the effect of the anti-Claudin-11 antibody was observable but not significant enough for further experiments on slice cultures. These results indicate, that not all surface antigens and antibodies could be used as targets for toxin-delivery into glial cells. A screening of antibody-antigen candidates is crucial. Appropriate candidates that successfully have been internalized into the cells of interest should be

considered for the toxin conjugation. More investigations regarding the effect of GPR17 targeting *ex vivo* is needed since binding of this antibody was successful *in vitro* and *ex vivo*.

In conclusion, according to the results presented here, transporter-targeted toxin-delivery is a promising method for the specific ablation of astrocytes and oligodendrocytes. Hence the possibility that this kind of treatment could be extended for the treatment of various diseases as part of the personalized medicine care of individual patients not only regarding cancer treatment. In future studies, promising candidates for internalization should be used for ablation thereby taking into account that there are different types of astrocytes and various maturity levels of oligodendrocytes present in the slice cultures. OHSCs in this context exposed to be the appropriate model system for ablation studies. The slice cultures display all kind of cell types of interest at different activation states at once. Drug-based approaches have been successful in *in vitro* and *in vivo* studies but are not applicable for *ex vivo* examinations according to the set up here. After the ablation of specific cell types from slice cultures, slices should be treated with oligomer-enriched Aβ-solutions to examine their contribution to neuronal survival. To further investigate the role of the individual cell types in neuroinflammation in the AD model system, markers of inflammation such as cytokines could be measured in untreated and treated slices as well as in non-depleted and depleted slices which was already done for microglia and revealed insight into their neuroprotective action. This would lead to a better understanding of the interaction between the different glial cell types under AD-pathological circumstances. By understanding the mechanisms that lead to neuroinflammation, possible interventions could be designed to interrupt the inflammatory vicious cycle.

5. Summary

The etiology of Alzheimer's disease, the most common cause of dementia, is still under debate. On the molecular level, AD is characterized by the accumulation of the beta-Amyloid protein as well as neurofibrillary tangles. Additionally, evidence pinpoints to a crucial role of inflammatory processes in the progression of the disease. The cellular mechanisms leading to neuroinflammation and neuronal death observed in Alzheimer's disease are still unclear.

It has long been thought that the immune system of the brain is unique and separated from the blood and the remaining organism by the blood brain barrier. Actually, the central nervous system has a special set of defence mechanisms against pathogens and invaders that is distinct from the innate or adaptive immune system. Important players of this defence system are glial cells. Glial cells are non-neuronal cells that are subdivided into three cell types, including microglia, astrocytes and oligodendrocytes, with different modes of action and function. Astrocytes and microglia actively take part in the defence process, whereas oligodendrocytes seem to have a more supportive function. To understand and characterize the role of glial cells in neuroinflammatory processes, it is crucial to establish a model system that displays the pathology of Alzheimer's disease and allows the individual study of cells. It was already shown that microglia could successfully be depleted using the bisphosphate clodronate from organotypic hippocampal slice cultures. However, there is still a lack of a system to study the individual role of astrocytes and oligodendrocytes *ex vivo*. Here, two different approaches were tested on their ability to be useful in ablation studies of astrocytes and oligodendrocytes *in vitro* and *ex vivo*. For *in vitro* studies primary derived cells from either embryonic or postnatal mice were used. *Ex vivo* studies were exerted on murine organotypic hippocampal slice cultures that in general serve as an excellent model system to study cell to cell interactions and communications. The depletion of astrocytes by antibody-toxin conjugates was promising in vitro but lacking efficacy *ex vivo*. The cell surface transporter GLAST-1 was found to be a promising candidate, since internalization signals were strongest and treatment of slices responded in a concentration-dependent manner. Treatment of slices with the L-alpha-aminoadipic acid led to depletion of astrocytes and provides evidence for their impor-tance in maintaining cytoarchitecture and thereby influenc-ing the viability of neuronal cells. Antibody-toxin conjugates were also used for the ablation of *Oli-neu* cells *in vitro*. Among

them, a combination containing the antibody against the cell surface protein Claudin-11 showed greater effects on the viability than the combination of the receptor antibody GPR17. The underlying processes for the internalization are of great interest since this method could be further developed for drug-delivery studies to different specific cells. This method could lead to a broader spectrum of ways for drug-targeting as it is used in cancer treatment.

5.1 Zusammenfassung

Die Ätiologie der Alzheimer-Krankheit, der häufigsten Ursache einer Demenz, ist immer noch Gegenstand der wissenschaftlichen Diskussion. Auf molekularer Ebene ist die Alzheimer-Krankheit durch die Anhäufung des beta-Amyloid-Proteins sowie durch die Ansammlung neurofibrillärer Bündel gekennzeichnet. Darüber hinaus gibt es Hinweise auf eine entscheidende Rolle von Entzündungsprozessen beim Fortschreiten der Erkrankung. Die bei der Alzheimer-Krankheit beobachteten zellulären Mechanismen, die zu Neuroinflammation und neuronalem Tod führen, sind jedoch weitestgehend noch unklar.

Lange Zeit ist man davon ausgegangen, dass das Immunsystem des Gehirns einzigartig ist und durch die Blut-Hirn-Schranke vom Blut und dem übrigen Organismus getrennt ist. Tatsächlich verfügt das zentrale Nervensystem über eigene Abwehrmechanismen gegen Krankheitserreger und Eindringlinge, die sich vom angeborenen oder adaptiven Immunsystem unterscheiden. Wichtige Akteure dieses Abwehrsystems sind die Gliazellen. Gliazellen sind nichtneuronale Zellen, die in drei Zelltypen unterteilt werden, darunter fallen Mikroglia, Astrozyten und Oligodendrozyten, welche unterschiedliche Wirkungen und Funktionen ausüben. Astrozyten und Mikroglia nehmen dabei aktiv am Abwehrprozess teil, während Oligodendrozyten eine eher unterstützende Funktion zu haben scheinen. Um die Rolle der Gliazellen bei neuroinflammatorischen Prozessen zu verstehen und zu charakterisieren, ist es entscheidend, ein Modellsystem zu etablieren, das die Pathologie der Alzheimer-Krankheit darstellt und eine individuelle Untersuchung dieser Zellen ermöglicht. Es konnte bereits gezeigt werden, dass Mikroglia erfolgreich mit dem Bisphosphonat Clodronat aus organotypisch hippocampalen Schnittkulturen depletiert werden konnten. Es fehlt jedoch noch ein System, um die individuelle Rolle von Astrozyten und Oligodendrozyten *ex vivo* zu untersuchen. In der vorliegenden Arbeit wurden zwei verschiedene Ansätze auf ihre Eignung für Ablationsstudien an Astrozyten und Oligodendrozyten *in vitro* und *ex vivo* getestet. Für die *in vitro* Versuche wurden gewonnene Primärzellen entweder von embryonalen oder postnatalen Mäusen verwendet. Die *ex vivo* Versuche wurden an Schnittkulturen von Mäusen durchgeführt, die im Allgemeinen ein ausgezeichnetes Modellsystem zur Untersuchung von Zell-Zell-Interaktionen und -Kommunikationen darstellen. Die Depletion von Astrozyten durch Antikörper-Toxin-Konjugate zeigte *in vitro* vielversprechende Ergebnisse, diese konnten *ex vivo* aber nicht bestätigt werden. Der Zelloberflächentransporter GLAST-1 erwies sich als ein vielversprechender Kan-

didat, da die Internalisierungssignale am stärksten waren und die Behandlung der Schnitte konzentrationsabhängig ansprach. Die Behandlung der Schnitte mit der L-α-Aminoadipinsäure führte zu einer Reduktion von Astrozyten *in vitro* und liefert Hinweise auf deren Bedeutung für die Aufrechterhaltung der Zytoarchitektur und damit für die Beeinflussung der Lebensfähigkeit neuronaler Zellen. Antikörper-Toxin-Konjugate wurden auch für die Ablation von *Olineu* Zellen *in vitro* verwendet. Unter diesen Konjugaten zeigte die Kombination mit dem Oberflächenprotein-Antikörper Claudin-11 größere Auswirkungen auf die Lebensfähigkeit als eine Kombination mit dem Rezeptor-Antikörper GPR17. Die zugrundeliegenden Prozesse für die Internalisierung sind von großem Interesse, da diese Methode für Studien zur Verabreichung von Medikamenten an verschiedene spezifische Zellen weiterentwickelt werden könnte. Diese Methode könnte zu einem breiteren Spektrum von Möglichkeiten für die gezielte Verabreichung von Medikamenten führen, wie sie in der Krebsbehandlung eingesetzt wird.

6. References

Aguzzi, A.; Barres, B. A.; Bennett, M. L., 2013. Microglia: scapegoat, saboteur, or something else? Science, 339(6116): 156–161.

Akama, K. T.; Albanese, C.; Pestell, R. G.; van Eldik, L. J., 1998. Amyloid beta-peptide stimulates nitric oxide production in astrocytes through an NFkappaB-dependent mechanism. Proceedings of the National Academy of Sciences of the United States of America, 95(10): 5795–5800.

Akiyama, H.; Arai, T.; Kondo, H.; Tanno, E.; Haga, C.; Ikeda, K., 2000a. Cell Mediators of Inflammation in the Alzheimer Disease Brain. Alzheimer Disease and Associated Disorders, 14(Supplement): S47-S53.

Akiyama, H.; Barger, S.; Barnum, S.; Bradt, B.; Bauer, J.; Cole, G. M.; Cooper, N. R.; Eikelenboom, P.; Emmerling, M.; Fiebich, B. L.; Finch, C. E.; Frautschy, S.; Griffin, W. S.; Hampel, H.; Hull, M.; Landreth, G.; Lue, L.; Mrak, R.; Mackenzie, I. R.; McGeer, P. L.; O'Banion, M. K.; Pachter, J.; Pasinetti, G.; Plata-Salaman, C.; Rogers, J.; Rydel, R.; Shen, Y.; Streit, W.; Strohmeyer, R.; Tooyoma, I.; van Muiswinkel, F. L.; Veerhuis, R.; Walker, D.; Webster, S.; Wegrzyniak, B.; Wenk, G.; Wyss-Coray, T., 2000b. Inflammation and Alzheimer's disease. Neurobiology of Aging, 21(3): 383–421.

Alzheimer, A., 1907. Über eine eigenartige Erkrankung der Hirnrinde. Allg Zeitschr Psychiatr, 64: 146–148.

Alzheimer, A.; Stelzmann, R. A.; Schnitzlein, H. N.; Murtagh, F. R., 1995. An English translation of Alzheimer's 1907 paper, "Über eine eigenartige Erkankung der Hirnrinde". Clinical anatomy, 8(6): 429–431.

Ashford, J. W., 2004. APOE genotype effects on Alzheimer's disease onset and epidemiology. Journal of molecular neuroscience, 23(3): 157–165.

Bamberger, M. E.; Landreth, G. E., 2001. Microglial interaction with beta-amyloid: implications for the pathogenesis of Alzheimer's disease. Microscopy research and technique, 54(2): 59–70.

Bancher, C.; Braak, H.; Fischer, P.; Jellinger, K. A., 1993. Neuropathological staging of Alzheimer lesions and intellectual status in Alzheimer's and Parkinson's disease patients. Neuroscience letters, 162(1-2): 179–182.

Bature, F.; Guinn, B.-A.; Pang, D.; Pappas, Y., 2017. Signs and symptoms preceding the diagnosis of Alzheimer's disease: a systematic scoping review of literature from 1937 to 2016. BMJ open, 7(8): e015746.

Beckstrøm, H.; Julsrud, L.; Haugeto, Ø.; Dewar, D.; Graham, D. I.; Lehre, K. P.; Storm-Mathisen, J.; Danbolt, N. C., 1999. Interindividual differences in the levels of the glutamate transporters GLAST and GLT, but no clear correlation with Alzheimer's disease. Journal of Neuroscience Research, 55(2): 218–229.

Berger, T.; Frotscher, M., 1994. Distribution and morphological characteristics of oligodendrocytes in the rat hippocampus in situ and in vitro: an immunocytochemical study with the monoclonal Rip antibody. Journal of neurocytology, 23(1): 61–74.

Birgbauer, E.; Rao, T. S.; Webb, M., 2004. Lysolecithin induces demyelination in vitro in a cerebellar slice culture system. Journal of Neuroscience Research, 78(2): 157–166.

Blasko, I.; Stampfer-Kountchev, M.; Robatscher, P.; Veerhuis, R.; Eikelenboom, P.; Grubeck-Loebenstein, B., 2004. How chronic inflammation can affect the brain and support the development of Alzheimer's disease in old age: the role of microglia and astrocytes. Aging Cell, 3(4): 169–176.

Boissonneault, V.; Filali, M.; Lessard, M.; Relton, J.; Wong, G.; Rivest, S., 2009. Powerful beneficial effects of macrophage colony-stimulating factor on beta-amyloid deposition and cognitive impairment in Alzheimer's disease. Brain: a journal of neurology, 132(Pt 4): 1078–1092.

Bostanci, N.; Thurnheer, T.; Aduse-Opoku, J.; Curtis, M. A.; Zinkernagel, A. S.; Belibasakis, G. N., 2013. Porphyromonas gingivalis regulates TREM-1 in human polymorphonuclear neutrophils via its gingipains. PloS one, 8(10): e75784.

Boulter, C. A.; Wagner, E. F., 1987. A universal retroviral vector for efficient constitutive expression of exogenous genes. Nucleic Acids Research, 15(17): 7194.

Breder, C. D.; Tsujimoto, M.; Terano, Y.; Scott, D. W.; Saper, C. B., 1993. Distribution and characterization of tumor necrosis factor-alpha-like immunoreactivity in the murine central nervous system. The Journal of comparative neurology, 337(4): 543–567.

Bridges, R. J.; Hatalski, C. G.; Shim, S. N.; Cummings, B. J.; Vijayan, V.; Kundi, A.; Cotman, C. W., 1992. Gliotoxic actions of excitatory amino acids. Neuropharmacology, 31(9): 899–907.

Bronstein, J. M.; Chen, K.; Tiwari-Woodruff, S.; Kornblum, H. I., 2000a. Developmental expression of OSP/claudin-11. Journal of Neuroscience Research, 60(3): 284–290.

Bronstein, J. M.; Tiwari-Woodruff, S.; Buznikov, A. G.; Stevens, D. B., 2000b. Involvement of OSP/claudin-11 in oligodendrocyte membrane interactions: Role in biology and disease. Journal of Neuroscience Research, 59(6): 706–711.

Brosseron, F.; Krauthausen, M.; Kummer, M.; Heneka, M. T., 2014. Body fluid cytokine levels in mild cognitive impairment and Alzheimer's disease: a comparative overview. Molecular neurobiology, 50(2): 534–544.

Broussard, G. J.; Mytar, J.; Li, R.-c.; Klapstein, G. J., 2012. The role of inflammatory processes in Alzheimer's disease. Inflammopharmacology, 20(3): 109–126.

Brown, D. R.; Kretzschmar, H. A., 1998. The glio-toxic mechanism of alpha-aminoadipic acid on cultured astrocytes. Journal of neurocytology, 27(2): 109–118.

Bushong, E. A.; Martone, M. E.; Jones, Y. Z.; Ellisman, M. H., 2002. Protoplasmic astrocytes in CA1 stratum radiatum occupy separate anatomical domains. The Journal of neuroscience: the official journal of the Society for Neuroscience, 22(1): 183–192.

Castell, J. V.; Andus, T.; Kunz, D.; Heinrich, P. C., 1989. Interleukin-6. The major regulator of acute-phase protein synthesis in man and rat. Annals of the New York Academy of Sciences, 557: 87-101.

Chang, F. W.; Wang, S. D.; Lu, K. T.; Lee, E.H.Y., 1993. Differential interactive effects of gliotoxin and MPTP in the substantia nigra and the locus coeruleus in BALB/c mice. Brain Research Bulletin, 31(3-4): 253–266.

Chiti, F.; Dobson, C. M., 2006. Protein misfolding, functional amyloid, and human disease. Annual Review of Biochemistry, 75: 333–366.

Cho, S.; Wood, A.; Bowlby, M. R., 2007. Brain slices as models for neurodegenerative disease and screening platforms to identify novel therapeutics. Current neuropharmacology, 5(1): 19–33.

Colton, C. A., 2009. Heterogeneity of microglial activation in the innate immune response in the brain. Journal of neuroimmune pharmacology: the official journal of the Society on NeuroImmune Pharmacology, 4(4): 399–418.

Compston, A.; Coles, A., 2008. Multiple sclerosis. The Lancet, 372(9648): 1502–1517.

Cornejo, V. H.; Hetz, C., 2013. The unfolded protein response in Alzheimer's disease. Seminars in immunopathology, 35(3): 277–292.

Costero, I.; Pomerat, C. M., 1951. Cultivation of neurons from the adult human cerebral and cerebellar cortes. The American journal of anatomy, 89(3): 405–467.

Coveler, A. L.; Ko, A. H.; Catenacci, D. V. T.; Hoff, D. von; Becerra, C.; Whiting, N. C.; Yang, J.; Wolpin, B., 2016. A phase 1 clinical trial of ASG-5ME, a novel drug-antibody conjugate targeting SLC44A4, in patients with advanced pancreatic and gastric cancers. Investigational new drugs, 34(3): 319–328.

Crain, S. M., 1966. Development of "organotypic" bioelectric activities in central nervous tissues during maturation in culture. International review of neurobiology, 9: 1–43.

Cunningham, E. L.; McGuinness, B.; Herron, B.; Passmore, A. P., 2015. Dementia. The Ulster medical journal, 84(2): 79–87.

Czeh, M.; Gressens, P.; Kaindl, A. M., 2011. The yin and yang of microglia. Developmental neuroscience, 33(3-4): 199–209.

El Khoury, J. B.; Moore, K. J.; Means, T. K.; Leung, J.; Terada, K.; Toft, M.; Freeman, M. W.; Luster, A. D., 2003. CD36 mediates the innate host response to beta-amyloid. The Journal of experimental medicine, 197(12): 1657–1666.

Engelhardt, E.; Gomes, M. d. M., 2015. Alzheimer's 100th anniversary of death and his contribution to a better understanding of Senile dementia. Arquivos de neuro-psiquiatria, 73(2): 159–162.

Farfara, D.; Lifshitz, V.; Frenkel, D., 2008. Neuroprotective and neurotoxic properties of glial cells in the pathogenesis of Alzheimer's disease. Journal of Cellular and Molecular Medicine, 12(3): 762–780.

Fassbender, K.; Walter, S.; Kuhl, S.; Landmann, R.; Ishii, K.; Bertsch, T.; Stalder, A. K.; Mühlhauser, F.; Liu, Y.; Ulmer, A. J.; Rivest, S.; Lentschat, A.; Gulbins, E.; Jucker, M.; Staufenbiel, M.; Brechtel, K.; Walter, J.; Multhaup, G.; Penke, B.; Adachi, Y.; Hartmann, T.; Beyreuther, K., 2004. The LPS receptor (CD14) links innate immunity with Alzheimer's disease. FASEB journal: official publication of the Federation of American Societies for Experimental Biology, 18(1): 203–205.

Ferretti, M. T.; Bruno, M. A.; Ducatenzeiler, A.; Klein, W. L.; Cuello, A. C., 2012. Intracellular Abeta-oligomers and early inflammation in a model of Alzheimer's disease. Neurobiology of Aging, 33(7): 1329–1342.

Fetler, L.; Amigorena, S., 2005. Neuroscience. Brain under surveillance: the microglia patrol. Science, 309(5733): 392–393.

Fillit, H.; Ding, W. H.; Buee, L.; Kalman, J.; Altstiel, L.; Lawlor, B.; Wolf-Klein, G., 1991. Elevated circulating tumor necrosis factor levels in Alzheimer's disease. Neuroscience letters, 129(2): 318–320.

Fleisher, A. S.; Pontecorvo, M. J.; Devous, M. D.; Lu, M.; Arora, A. K.; Truocchio, S. P.; Aldea, P.; Flitter, M.; Locascio, T.; Devine, M.; Siderowf, A.; Beach, T. G.; Montine, T. J.; Serrano, G. E.; Curtis, C.; Perrin, A.; Salloway, S.; Daniel, M.; Wellman, C.; Joshi, A. D.; Irwin, D. J.; Lowe, V. J.; Seeley, W. W.; Ikonomovic, M. D.; Masdeu, J. C.; Kennedy, I.; Harris, T.; Navitsky, M.; Southekal, S.; Mintun, M. A., 2020. Positron Emission Tomography Imaging With 18Fflortaucipir and Postmortem Assessment of Alzheimer Disease Neuropathologic Changes. JAMA neurology,

Fornés, A.; Núñez, E.; Alonso-Torres, P.; Aragón, C.; López-Corcuera, B., 2008. Trafficking properties and activity regulation of the neuronal glycine transporter GLYT2 by protein kinase C. The Biochemical journal, 412(3): 495–506.

Frohman, E. M.; Racke, M. K.; Raine, C. S., 2006. Multiple sclerosis--the plaque and its pathogenesis. The New England journal of medicine, 354(9): 942–955.

Fullana, N.; Gasull-Camós, J.; Tarrés-Gatius, M.; Castañé, A.; Bortolozzi, A.; Artigas, F., 2020. Astrocyte control of glutamatergic activity: Downstream effects on serotonergic function and emotional behavior. Neuropharmacology, 166): 107914.

Fumagalli, M.; Daniele, S.; Lecca, D.; Lee, P. R.; Parravicini, C.; Fields, R. D.; Rosa, P.; Antonucci, F.; Verderio, C.; Trincavelli, M. L.; Bramanti, P.; Martini, C.; Abbracchio, M. P., 2011. Phenotypic changes, signaling pathway, and functional correlates of GPR17-expressing neural precursor cells during oligodendrocyte differentiation. Journal of Biological Chemistry, 286(12): 10593–10604.

Gähwiler, B. H., 1981. Organotypic monolayer cultures of nervous tissue. Journal of neuroscience methods, 4(4): 329–342.

Galimberti, I.; Gogolla, N.; Alberi, S.; Santos, A. F.; Muller, D.; Caroni, P., 2006. Long-term rearrangements of hippocampal mossy fiber terminal connectivity in the adult regulated by experience. Neuron, 50(5): 749–763.

Gao, X.; Dong, Y.; Liu, Z.; Niu, B., 2013. Silencing of triggering receptor expressed on myeloid cells-2 enhances the inflammatory responses of alveolar macrophages to lipopolysaccharide. Molecular medicine reports, 7(3): 921–926.

Garthwaite, J.; Regan, C. M., 1980. Toxic effects of α-aminoadipate on cultured cerebellar cells. Brain research, 194(2): 603–607.

Gegelashvili, G.; Danbolt, N. C.; Schousboe, A., 1997. Neuronal soluble factors differentially regulate the expression of the GLT1 and GLAST glutamate transporters in cultured astroglia. Journal of Neurochemistry, 69(6): 2612–2615.

Gey, G. O.; Gey, M. K., 1936. The maintenance of human normal cells and tumor cells in continuous culture. Amer. J. Cancer): 45–76.

Glass, C. K.; Saijo, K.; Winner, B.; Marchetto, M. C.; Gage, F. H., 2010. Mechanisms underlying inflammation in neurodegeneration. Cell, 140(6): 918–934.

Gochenauer, G. E.; Robinson, M. B., 2001. Dibutyryl-cAMP (dbcAMP) up-regulates astrocytic chloride-dependent L-3Hglutamate transport and expression of both system xc(-) subunits. Journal of Neurochemistry, 78(2): 276–286.

Goldstein, E. Z.; Church, J. S.; Hesp, Z. C.; Popovich, P. G.; McTigue, D. M., 2016. A silver lining of neuroinflammation: Beneficial effects on myelination. Experimental Neurology, 283): 550–559.

Gordon, S., 2003. Alternative activation of macrophages. Nature Reviews Immunology, 3(1): 23–35.

Gordon, S.; Taylor, P. R., 2005. Monocyte and macrophage heterogeneity. Nature Reviews Immunology, 5(12): 953–964.

Griffin, W. S.; Sheng, J. G.; Royston, M. C.; Gentleman, S. M.; McKenzie, J. E.; Graham, D. I.; Roberts, G. W.; Mrak, R. E., 1998. Glial-neuronal interactions in Alzheimer's disease: the potential role of a 'cytokine cycle' in disease progression. Brain pathology (Zurich, Switzerland), 8(1): 65–72.

Guerreiro, R. J.; Gustafson, D. R.; Hardy, J., 2012. The genetic architecture of Alzheimer's disease: beyond APP, PSENs and APOE. Neurobiology of Aging, 33(3): 437–456.

Haass, C., 2004. Take five--BACE and the gamma-secretase quartet conduct Alzheimer's amyloid beta-peptide generation. The EMBO journal, 23(3): 483–488.

Halassa, M. M.; Fellin, T.; Takano, H.; Dong, J.-H.; Haydon, P. G., 2007. Synaptic islands defined by the territory of a single astrocyte. The Journal of neuroscience : the official journal of the Society for Neuroscience, 27(24): 6473–6477.

Hanger, D. P.; Anderton, B. H.; Noble, W., 2009. Tau phosphorylation. Trends in Molecular Medicine, 15(3): 112–119.

Hanzel, C. E.; Pichet-Binette, A.; Pimentel, L. S.B.; Iulita, M. F.; Allard, S.; Ducatenzeiler, A.; Do Carmo, S.; Cuello, A. C., 2014. Neuronal driven pre-plaque inflammation in a transgenic rat model of Alzheimer's disease. Neurobiology of Aging, 35(10): 2249–2262.

Hardy, J.; Selkoe, D. J., 2002. The amyloid hypothesis of Alzheimer's disease: progress and problems on the road to therapeutics. Science, 297(5580): 353–356.

Hardy, J. A.; Higgins, G. A., 1992. Alzheimer's disease: the amyloid cascade hypothesis. Science, 256(5054): 184–185.

Hardy, S. J., 2002. The amyloid hypothesis of Alzheimer’s disease: Progress and problems on the road to therapeutics. Science's compass(297): 353–356.

Heneka, M. T.; Carson, M. J.; Khoury, J. E.; Landreth, G. E.; Brosseron, F.; Feinstein, D. L.; Jacobs, A. H.; Wyss-Coray, T.; Vitorica, J.; Ransohoff, R. M.; Herrup, K.; Frautschy, S. A.; Finsen, B.; Brown, G. C.; Verkhratsky, A.; Yamanaka, K.; Koistinaho, J.; Latz, E.; Halle, A.; Petzold, G. C.; Town, T.; Morgan, D.; Shinohara, M. L.; Perry, V. H.; Holmes, C.; Bazan, N. G.; Brooks, D. J.; Hunot, S.; Joseph, B.; Deigendesch, N.; Garaschuk, O.; Boddeke, E.; Dinarello, C. A.; Breitner, J. C.; Cole, G. M.; Golenbock, D. T.; Kummer, M. P., 2015. Neuroinflammation in Alzheimer's disease. The Lancet Neurology, 14(4): 388–405.

Heneka, M. T.; Kummer, M. P.; Latz, E., 2014. Innate immune activation in neurodegenerative disease. Nature Reviews Immunology, 14(7): 463–477.

Heneka, M. T.; Wiesinger, H.; Dumitrescu-Ozimek, L.; Riederer, P.; Feinstein, D. L.; Klockgether, T., 2001. Neuronal and glial coexpression of argininosuccinate synthetase and inducible nitric oxide synthase in Alzheimer disease. Journal of neuropathology and experimental neurology, 60(9): 906–916.

Henn, A.; Lund, S.; Hedtjärn, M.; Schrattenholz, A.; Pörzgen, P.; Leist, M., 2009. The suitability of BV2 cells as alternative model system for primary microglia cultures or for animal experiments examining brain inflammation. ALTEX, 26(2): 83–94.

Heppner, F.; Ransohoff, R.; Becher, B., 2015. Immune attack: the role of inflammation in AD. Review. Nature(16): 358–372.

Higgins, S. C.; Fillmore, H. L.; Ashkan, K.; Butt, A. M.; Pilkington, G. J., 2015. Dual targeting NG2 and GD3A using Mab-Zap immunotoxin results in reduced glioma cell viability in vitro. Anticancer research, 35(1): 77–84.

Hinson, S. R.; Roemer, S. F.; Lucchinetti, C. F.; Fryer, J. P.; Kryzer, T. J.; Chamberlain, J. L.; Howe, C. L.; Pittock, S. J.; Lennon, V. A., 2008. Aquaporin-4-binding autoantibodies in patients with neuromyelitis optica impair glutamate transport by down-regulating EAAT2. The Journal of experimental medicine, 205(11): 2473–2481.

Hinson, S. R.; Romero, M. F.; Popescu, B. F. G.; Lucchinetti, C. F.; Fryer, J. P.; Wolburg, H.; Fallier-Becker, P.; Noell, S.; Lennon, V. A., 2012. Molecular outcomes of neuromyelitis optica (NMO)-IgG binding to aquaporin-4 in astrocytes. Proceedings of the National Academy of Sciences of the United States of America, 109(4): 1245–1250.

Hogue, M. J., 1947. Human fetal brain cells in tissue cultures; their identification and motility. The Journal of experimental zoology, 106(1): 85–107.

Hou, L.; Liu, Y.; Wang, X.; Ma, H.; He, J.; Zhang, Y.; Yu, C.; Guan, W.; Ma, Y., 2011. The effects of amyloid-beta42 oligomer on the proliferation and activation of astrocytes in vitro. In vitro cellular & developmental biology. Animal, 47(8): 573–580.

Hsu, H.; Shu, H. B.; Pan, M. G.; Goeddel, D. V., 1996. TRADD-TRAF2 and TRADD-FADD interactions define two distinct TNF receptor 1 signal transduction pathways. Cell, 84(2): 299–308.

Huck, S.; Grass, F.; Hatten, M. E., 1984. Gliotoxic effects of α-aminoadipic acid on monolayer cultures of dissociated postnatal mouse cerebellum. Neuroscience, 12(3): 783–791.

Husemann, J.; Loike, J. D.; Anankov, R.; Febbraio, M.; Silverstein, S. C., 2002. Scavenger receptors in neurobiology and neuropathology: their role on microglia and other cells of the nervous system. Glia, 40(2): 195–205.

Jack, C. R.; Knopman, D. S.; Jagust, W. J.; Shaw, L. M.; Aisen, P. S.; Weiner, M. W.; Petersen, R. C.; Trojanowski, J. Q., 2010. Hypothetical model of dynamic biomarkers of the Alzheimer's pathological cascade. The Lancet Neurology, 9(1): 119–128.

Jackson, M. J.; Zielke, H. R.; Zielke, C. L., 1996. Induction of astrocyte argininosuccinate synthetase and argininosuccinate lyase by dibutyryl cyclic AMP and dexamethasone. Neurochemical research, 21(10): 1161–1165.

Jäkel, S.; Dimou, L. Glial Cells and Their Function in the Adult Brain: A Journey through the History of Their Ablation. Frontiers in cellular neuroscience, 11: 24.

Jankowsky, J. L.; Fadale, D. J.; Anderson, J.; Xu, G. M.; Gonzales, V.; Jenkins, N. A.; Copeland, N. G.; Lee, M. K.; Younkin, L. H.; Wagner, S. L.; Younkin, S. G.; Borchelt, D. R., 2004. Mutant presenilins specifically elevate the levels of the 42 residue beta-amyloid peptide in vivo: evidence for augmentation of a 42-specific gamma secretase. Human molecular genetics, 13(2): 159–170.

Jay, T. R.; Saucken, V. E. von; Landreth, G. E., 2017. TREM2 in Neurodegenerative Diseases. Molecular neurodegeneration, 12(1): 56.

Jinno, S.; Fleischer, F.; Eckel, S.; Schmidt, V.; Kosaka, T., 2007. Spatial arrangement of microglia in the mouse hippocampus: a stereological study in comparison with astrocytes. Glia, 55(13): 1334–1347.

Johnston, H.; Boutin, H.; Allan, S. M., 2011. Assessing the contribution of inflammation in models of Alzheimer's disease. Biochemical Society transactions, 39(4): 886–890.

Jung, J. S.; Bhat, R. V.; Preston, G. M.; Guggino, W. B.; Baraban, J. M.; Agre, P., 1994. Molecular characterization of an aquaporin cDNA from brain: candidate osmoreceptor and regulator of water balance. Proceedings of the National Academy of Sciences of the United States of America, 91(26): 13052–13056.

Jung, M.; Krämer, E.; Grzenkowski, M.; Tang, K.; Blakemore, W.; Aguzzi, A.; Khazaie, K.; Chlichlia, K.; Blankenfeld, G. von; Kettenmann, H., 1995. Lines of murine oligodendroglial precursor cells immortalized by an activated neu tyrosine kinase show distinct degrees of interaction with axons in vitro and in vivo. The European journal of neuroscience, 7(6): 1245–1265.

Juurlink, B. H., 1997. Response of glial cells to ischemia: roles of reactive oxygen species and glutathione. Neuroscience and biobehavioral reviews, 21(2): 151–166.

Juurlink, B. H.J.; Devon, R. M., 1990. Macromolecular translocation — a possible function of astrocytes. Brain research, 533(1): 73–77.

Karch, C. M.; Goate, A. M., 2015. Alzheimer's disease risk genes and mechanisms of disease pathogenesis. Biological Psychiatry, 77(1): 43–51.

Kashon, M. L.; Ross, G. W.; O'Callaghan, J. P.; Miller, D. B.; Petrovitch, H.; Burchfiel, C. M.; Sharp, D. S.; Markesbery, W. R.; Davis, D. G.; Hardman, J.; Nelson, J.; White, L. R., 2004. Associations of cortical astrogliosis with cognitive performance and dementia status. Journal of Alzheimer's disease : JAD, 6(6): 595-604; discussion 673-81.

Kayed, R.; Lasagna-Reeves, C. A. Molecular mechanisms of amyloid oligomers toxicity. Journal of Alzheimer's disease : JAD, 33 Suppl 1: S67-78.

Kettenmann, H.; Hanisch, U.; Noda, M.; Verkhratsky, A., 2011. Physiology of microglia. Physiological Reviwes, 91(2): 461–553.

Kho, D. T.; Johnson, R. H.; O'Carroll, S. J.; Angel, C. E.; Graham, E. S., 2017. Biosensor Technology Reveals the Disruption of the Endothelial Barrier Function and the Subsequent Death of Blood Brain Barrier Endothelial Cells to Sodium Azide and Its Gaseous Products. Biosensors, 7(4).

Khurgel, M.; Koo, A. C.; Ivy, G. O., 1996. Selective ablation of astrocytes by intracerebral injections of a-aminoadipate. Glia, 16(4): 351–358.

Kirkley, K. S.; Popichak, K. A.; Afzali, M. F.; Legare, M. E.; Tjalkens, R. B., 2017. Microglia amplify inflammatory activation of astrocytes in manganese neurotoxicity. Journal of neuroinflammation, 14(99).

Kohls, M. D.; Lappi, D. A., 2000. Mab-Zap: A Tool for Evaluating Antibody Efficacy for Use in an Immunotoxin. BioTechniques, 28(1): 162–165.

Kondo, K.; Hashimoto, H.; Kitanaka, J.; Sawada, M.; Suzumura, A.; Marunouchi, T.; Baba, A., 1995. Expression of glutamate transporters in cultured glial cells. Neuroscience letters, 188(2): 140–142.

Kumamaru, H.; Saiwai, H.; Kobayakawa, K.; Kubota, K.; van Rooijen, N.; Inoue, K.; Iwamoto, Y.; Okada, S., 2012. Liposomal clodronate selectively eliminates microglia from primary astrocyte cultures. Journal of Neuroinflammation, 9: 116.

Kumar, A.; Singh, A.; Ekavali, 2015. A review on Alzheimer's disease pathophysiology and its management: an update. Pharmacological reports: PR, 67(2): 195–203.

Kumar, A.; Stoica, B. A.; Sabirzhanov, B.; Burns, M. P.; Faden, A. I.; Loane, D. J., 2013. Traumatic brain injury in aged animals increases lesion size and chronically alters microglial/macrophage classical and alternative activation states. Neurobiology of Aging, 34(5): 1397–1411.

Lawson, L. J.; Perry, V. H.; Dri, P.; Gordon, S., 1990. Heterogeneity in the distribution and morphology of microglia in the normal adult mouse brain. Neuroscience, 39(1): 151–170.

Lee, C. Y. D.; Landreth, G. E., 2010. The role of microglia in amyloid clearance from the AD brain. Journal of Neural Transmission, 117(8): 949–960.

Lee, M.; Schwab, C.; McGeer, P. L., 2011. Astrocytes are GABAergic cells that modulate microglial activity. Glia, 59(1): 152–165.

Lei, P.; Ayton, S.; Finkelstein, D. I.; Adlard, P. A.; Masters, C. L.; Bush, A. I., 2010. Tau protein. The International Journal of Biochemistry & Cell Biology, 42(11): 1775–1778.

Li, C.; Zhao, R.; Gao, K.; Wei, Z.; Yin, M. Y.; Lau, L. T.; Chui, D.; Yu, A. C. H., 2011. Astrocytes: implications for neuroinflammatory pathogenesis of Alzheimer's disease. Current Alzheimer research, 8(1): 67–80.

Li, S.; Mallory, M.; Alford, M.; Tanaka, S.; Masliah, E., 1997. Glutamate transporter alterations in Alzheimer disease are possibly associated with abnormal APP expression. Journal of neuropathology and experimental neurology, 56(8): 901–911.

Liberto, C. M.; Albrecht, P. J.; Herx, L. M.; Yong, V. W.; Levison, S. W., 2004. Pro-regenerative properties of cytokine-activated astrocytes. Journal of Neurochemistry, 89(5): 1092–1100.

Liddelow, S. A.; Barres, B. A., 2017. Reactive Astrocytes. Immunity, 46(6): 957–967.

Liddelow, S. A.; Guttenplan, K. A.; Clarke, L. E.; Bennett, F. C.; Bohlen, C. J.; Schirmer, L.; Bennett, M. L.; Münch, A. E.; Chung, W.-S.; Peterson, T. C.; Wilton, D. K.; Frouin, A.; Napier, B. A.; Panicker, N.; Kumar, M.; Buckwalter, M. S.; Rowitch, D. H.; Dawson, V. L.; Dawson, T. M.; Stevens, B.; Barres, B. A., 2017. Neurotoxic reactive astrocytes are induced by activated microglia. Nature, 541(7638): 481–487.

Lima, A.; Sardinha, V. M.; Oliveira, A. F.; Reis, M.; Mota, C.; Silva, M. A.; Marques, F.; Cerqueira, J. J.; Pinto, L.; Sousa, N.; Oliveira, J. F., 2014. Astrocyte pathology in the prefrontal cortex impairs the cognitive function of rats. Molecular psychiatry, 19(7): 834–841.

Liu, B.; Hong, J.-S., 2003. Role of microglia in inflammation-mediated neurodegenerative diseases: mechanisms and strategies for therapeutic intervention. The Journal of pharmacology and experimental therapeutics, 304(1): 1–7.

Liu, Y.; Walter, S.; Stagi, M.; Cherny, D.; Letiembre, M.; Schulz-Schaeffer, W.; Heine, H.; Penke, B.; Neumann, H.; Fassbender, K., 2005. LPS receptor (CD14): a receptor for phagocytosis of Alzheimer's amyloid peptide. Brain, 128(8): 1778–1789.

Loder, M. K.; Melikian, H. E., 2003. The dopamine transporter constitutively internalizes and recycles in a protein kinase C-regulated manner in stably transfected PC12 cell lines. Journal of Biological Chemistry, 278(24): 22168–22174.

Lönn, J.; Ljunggren, S.; Klarström-Engström, K.; Demirel, I.; Bengtsson, T.; Karlsson, H., 2018. Lipoprotein modifications by gingipains of Porphyromonas gingivalis. Journal of periodontal research, 53(3): 403–413.

Lopategui Cabezas, I.; Herrera Batista, A.; Pentón Rol, G., 2014. The role of glial cells in Alzheimer disease: potential therapeutic implications. Neurologia, 29(5): 305–309.

Lue, L.-F.; Kuo, Y.-M.; Beach, T.; Walker, D. G., 2010. Microglia activation and anti-inflammatory regulation in Alzheimer's disease. Molecular neurobiology, 41(2-3): 115–128.

Lynch, M. A., 2014. The impact of neuroimmune changes on development of amyloid pathology; relevance to Alzheimer's disease. Immunology, 141(3): 292–301.

Mahley, R. W., 1988. Apolipoprotein E: cholesterol transport protein with expanding role in cell biology. Science, 240(4852): 622–630.

Mahmoud, S.; Gharagozloo, M.; Simard, C.; Gris, D., 2019. Astrocytes Maintain Glutamate Homeostasis in the CNS by Controlling the Balance between Glutamate Uptake and Release. Cells, 8(2).

Maragakis, N. J.; Rothstein, J. D., 2006. Mechanisms of Disease: astrocytes in neurodegenerative disease. Nature Clinical Practice Neurology, 2(12): 679–689.

Masuch, A.; van der Pijl, R.; Füner, L.; Wolf, Y.; Eggen, B.; Boddeke, E.; Biber, K., 2016. Microglia replenished OHSC: A culture system to study in vivo like adult microglia. Glia, 64(8): 1285–1297.

Mattie, M.; Raitano, A.; Morrison, K.; Morrison, K.; An, Z.; Capo, L.; Verlinsky, A.; Leavitt, M.; Ou, J.; Nadell, R.; Aviña, H.; Guevara, C.; Malik, F.; Moser, R.; Duniho, S.; Coleman, J.; Li, Y.; Pereira, D. S.; Doñate, F.; Joseph, I. B. J.; Challita-Eid, P.; Benjamin, D.; Stover, D. R., 2016. The Discovery and Preclinical Development of ASG-5ME, an Antibody-Drug Conjugate Targeting SLC44A4-Positive Epithelial Tumors Including Pancreatic and Prostate Cancer. Molecular cancer therapeutics, 15(11): 2679–2687.

Matzku, S.; Tilgen, W.; Kalthoff, H.; Schmiegel, W. H.; Bröcker, E. B., 1988. Dynamics of antibody transport and internalization. International journal of cancer. Supplement = Journal international du cancer. Supplement, 2: 11–14.

Mazzitelli, S.; Filipello, F.; Rasile, M.; Lauranzano, E.; Starvaggi-Cucuzza, C.; Tamborini, M.; Pozzi, D.; Barajon, I.; Giorgino, T.; Natalello, A.; Matteoli, M., 2016. Amyloid-β 1-24 C-terminal truncated fragment promotes amyloid-β 1-42 aggregate formation in the healthy brain. Acta neuropathologica communications, 4(1): 110.

McBean, G. J., 1994. Inhibition of the glutamate transporter and glial enzymes in rat striatum by the gliotoxin, alpha aminoadipate. British journal of pharmacology, 113(2): 536–540.

McCarthy, K. D.; Vellis, J. de, 1980. Preparation of separate astroglial and oligodendroglial cell cultures from rat cerebral tissue. The Journal of cell biology, 85(3): 890–902.

McGeer, P. L.; Itagaki, S.; Boyes, B. E.; McGeer, E. G., 1988. Reactive microglia are positive for HLA-DR in the substantia nigra of Parkinson's and Alzheimer's disease brains. Neurology, 38(8): 1285–1291.

McGeer, P. L.; McGeer, E. G., 1995. The inflammatory response system of brain: implications for therapy of Alzheimer and other neurodegenerative diseases. Brain research. Brain research reviews, 21(2): 195–218.

McHugh, D.; Eisenberger, M.; Heath, E. I.; Bruce, J.; Danila, D. C.; Rathkopf, D. E.; Feldman, J.; Slovin, S. F.; Anand, B.; Chu, R.; Lackey, J.; Reyno, L.; Antonarakis, E. S.; Morris, M. J., 2019. A phase I study of the antibody drug conjugate ASG-5ME, an SLC44A4-targeting antibody carrying auristatin E, in metastatic castration-resistant prostate cancer. Investigational new drugs, 37(5): 1052–1060.

Megias, L.; Guerri, C.; Fornas, E.; Azorin, I.; Bendala, E.; Sancho-Tello, M.; Durán, J. M.; Tomás, M.; Gomez-Lechon, M. J.; Renau-Piqueras, J., 2000. Endocytosis and transcytosis in growing astrocytes in primary culture. Possible implications in neural development. The International journal of developmental biology, 44(2): 209–221.

Millington, C.; Sonego, S.; Karunaweera, N.; Rangel, A.; Aldrich-Wright, J. R.; Campbell, I. L.; Gyengesi, E.; Munch, G., 2014. Chronic neuroinflammation in Alzheimer's disease: new perspectives on animal models and promising candidate drugs. BioMed Research International, 2014): 309129.

Min, K.-J.; Yang, M.-s.; Kim, S.-U.; Jou, I.; Joe, E.-h., 2006. Astrocytes induce hemeoxygenase-1 expression in microglia: a feasible mechanism for preventing excessive brain inflammation. The Journal of neuroscience : the official journal of the Society for Neuroscience, 26(6): 1880–1887.

Minogue, A. M., 2017. Role of infiltrating monocytes/macrophages in acute and chronic neuroinflammation: Effects on cognition, learning and affective behaviour. Progress in Neuro-Psychopharmacology and Biological Psychiatry, 79: 15–18.

Mogha, A.; D'Rozario, M.; Monk, K. R., 2016. G Protein-Coupled Receptors in Myelinating Glia. Trends in pharmacological sciences, 37(11): 977–987.

Morita, K.; Sasaki, H.; Fujimoto, K.; Furuse, M.; Tsukita, S., 1999. Claudin-11/OSP-based tight junctions of myelin sheaths in brain and Sertoli cells in testis. The Journal of cell biology, 145(3): 579–588.

Mosmann, T., 1983. Rapid colorimetric assay for cellular growth and survival: application to proliferation and cytotoxicity assays. Journal of immunological methods, 65(1-2): 55–63.

Mosser, D. M., 2003. The many faces of macrophage activation. Journal of Leukocyte Biology, 73(2): 209–212.

Mrak, R. E.; Sheng, J. G.; Griffin, W. S., 1996. Correlation of astrocytic S100 beta expression with dystrophic neurites in amyloid plaques of Alzheimer's disease. Journal of neuropathology and experimental neurology, 55(3): 273–279.

Müller, U.; Winter, P.; Graeber, M. B., 2013. A presenilin 1 mutation in the first case of Alzheimer's disease. The Lancet Neurology, 12(2): 129–130.

Murgas, P.; Godoy, B.; Bernhardi, R. von, 2012. Abeta potentiates inflammatory activation of glial cells induced by scavenger receptor ligands and inflammatory mediators in culture. Neurotoxicity research, 22(1): 69–78.

Nagele, R. G.; D'Andrea, M. R.; Lee, H.; Venkataraman, V.; Wang, H.-Y., 2003. Astrocytes accumulate A beta 42 and give rise to astrocytic amyloid plaques in Alzheimer disease brains. Brain research, 971(2): 197–209.

Nagele, R. G.; Wegiel, J.; Venkataraman, V.; Imaki, H.; Wang, K.-C.; Wegiel, J., 2004. Contribution of glial cells to the development of amyloid plaques in Alzheimer's disease. Neurobiology of Aging, 25(5): 663–674.

Nägerl, U. V.; Eberhorn, N.; Cambridge, S. B.; Bonhoeffer, T., 2004. Bidirectional activity-dependent morphological plasticity in hippocampal neurons. Neuron, 44(5): 759–767.

Nath, N.; Godat, B.; Zimprich, C.; Dwight, S. J.; Corona, C.; McDougall, M.; Urh, M., 2016. Homogeneous plate based antibody internalization assay using pH sensor fluorescent dye. Journal of immunological methods, 431: 11–21.

N'Diaye, E.-N.; Branda, C. S.; Branda, S. S.; Nevarez, L.; Colonna, M.; Lowell, C.; Hamerman, J. A.; Seaman, W. E., 2009. TREM-2 (triggering receptor expressed on myeloid cells 2) is a phagocytic receptor for bacteria. The Journal of cell biology, 184(2): 215–223.

Nielsen, S.; Arnulf Nagelhus, E.; Amiry-Moghaddam, M.; Bourque, C.; Agre, P.; Petter Ottersen, O., 1997. Specialized Membrane Domains for Water Transport in Glial Cells: High-Resolution Immunogold Cytochemistry of Aquaporin-4 in Rat Brain. Journal of Neuroscience, 17(1): 171–180.

Nimmerjahn, A.; Kirchhoff, F.; Helmchen, F., 2005. Resting microglial cells are highly dynamic surveillants of brain parenchyma in vivo. Science, 308(5726): 1314–1318.

Nishimura, R. N.; Santos, D.; Fu, S. T.; Dwyer, B. E., 2000. Induction of cell death by L-alpha-aminoadipic acid exposure in cultured rat astrocytes: relationship to protein synthesis. Neurotoxicology, 21(3): 313–320.

Oksenberg, J. R.; Baranzini, S. E.; Sawcer, S.; Hauser, S. L., 2008. The genetics of multiple sclerosis: SNPs to pathways to pathogenesis. Nature Reviews Genetics, 9(7): 516–526.

Olney, J. W.; Gubareff, T. de; Collins, J. F., 1980. Stereospecificity of the gliotoxic and anti-neurotoxic actions of alpha-aminoadipate. Neuroscience letters, 19(3): 277–282.

Olney, J. W.; Ho, O. L.; Rhee, V., 1971. Cytotoxic effects of acidic and sulphur containing amino acids on the infant mouse central nervous system. Experimental brain research, 14(1): 61–76.

Orre, M.; Kamphuis, W.; Dooves, S.; Kooijman, L.; Chan, E. T.; Kirk, C. J.; Dimayuga Smith, V.; Koot, S.; Mamber, C.; Jansen, A. H.; Ovaa, H.; Hol, E. M., 2013. Reactive glia show increased immunoproteasome activity in Alzheimer's disease. Brain : a journal of neurology, 136(5): 1415–1431.

Papageorgiou, I. E.; Lewen, A.; Galow, L. V.; Cesetti, T.; Scheffel, J.; Regen, T.; Hanisch, U.-K.; Kann, O., 2016. TLR4-activated microglia require IFN-γ to induce severe neuronal dysfunction and death in situ. Proceedings of the National Academy of Sciences of the United States of America, 113(1): 212–217.

Parkin, G. M.; Udawela, M.; Gibbons, A.; Dean, B., 2018. Glutamate transporters, EAAT1 and EAAT2, are potentially important in the pathophysiology and treatment of schizophrenia and affective disorders. World journal of psychiatry, 8(2): 51–63.

Parslow, A. C.; Parakh, S.; Lee, F.-T.; Gan, H. K.; Scott, A. M., 2016. Antibody-Drug Conjugates for Cancer Therapy. Biomedicines, 4(3).

Pascual, O.; Ben Achour, S.; Rostaing, P.; Triller, A.; Bessis, A., 2012. Microglia activation triggers astrocyte-mediated modulation of excitatory neurotransmission. Proceedings of the National Academy of Sciences of the United States of America, 109(4): E197-205.

Perego, C.; Vanoni, C.; Bossi, M.; Massari, S.; Basudev, H.; Longhi, R.; Pietrini, G., 2000. The GLT-1 and GLAST glutamate transporters are expressed on morphologically distinct astrocytes and regulated by neuronal activity in primary hippocampal cocultures. Journal of Neurochemistry, 75(3): 1076–1084.

Pertusa, M.; García-Matas, S.; Rodríguez-Farré, E.; Sanfeliu, C.; Cristòfol, R., 2007. Astrocytes aged in vitro show a decreased neuroprotective capacity. Journal of Neurochemistry, 101(3): 794–805.

Peters, C.; Brown, S., 2015. Antibody-drug conjugates as novel anti-cancer chemotherapeutics. Bioscience reports, 35(4).

Petzold, A.; Jenkins, R.; Watt, H. C.; Green, A. J. E.; Thompson, E. J.; Keir, G.; Fox, N. C.; Rossor, M. N., 2003. Cerebrospinal fluid S100B correlates with brain atrophy in Alzheimer's disease. Neuroscience letters, 336(3): 167–170.

Piazza, A.; Lynch, M. A., 2009. Neuroinflammatory changes increase the impact of stressors on neuronal function. Biochemical Society Transactions, 37(1): 303–307.

Price, J. L.; Morris, J. C., 1999. Tangles and plaques in nondemented aging and "preclinical" Alzheimer's disease. Annals of neurology, 45(3): 358–368.

Rahbek-Clemmensen, T.; Bay, T.; Eriksen, J.; Gether, U.; Jørgensen, T. N., 2014. The serotonin transporter undergoes constitutive internalization and is primarily sorted to late endosomes and lysosomal degradation. Journal of Biological Chemistry, 289(33): 23004–23019.

Raible, D. W.; McMorris, F. A., 1993. Oligodendrocyte differentiation and progenitor cell proliferation are independently regulated by cyclic AMP. Journal of Neuroscience Research, 34(3): 287–294.

Ransohoff, R. M.; Perry, V. H., 2009. Microglial Physiology: Unique Stimuli, Specialized Responses. Annual review of immunology, 27: 119–145.

Richter, M.; Vidovic, N.; Biber, K.; Dolga, A.; Culmsee, C.; Dodel, R., 2020. The neuroprotective role of microglial cells against amyloid beta-mediated toxicity in organotypic hippocampal slice cultures. Brain pathology, 30(3): 589–602.

Ridolfi, E.; Barone, C.; Scarpini, E.; Galimberti, D., 2013. The Role of the Innate Immune System in Alzheimer’s Disease and Frontotemporal Lobar Degeneration: An Eye on Microglia. Clinical and Developmental Immunology, 2013: 1–11.

Rogaeva, E., 2002. The Solved and Unsolved Mysteries of the Genetics of Early-Onset Alzheimer 's Disease. NeuroMolecular Medicine, 2(1): 1–10.

Rogers, J.; Strohmeyer, R.; Kovelowski, C. J.; Li, R., 2002. Microglia and inflammatory mechanisms in the clearance of amyloid beta peptide. Glia, 40(2): 260–269.

Rose, C. R.; Ziemens, D.; Untiet, V.; Fahlke, C., 2018. Molecular and cellular physiology of sodium-dependent glutamate transporters. Brain Research Bulletin, 136: 3–16.

Rossner, S.; Lange-Dohna, C.; Zeitschel, U.; Perez-Polo, J. R., 2005. Alzheimer's disease beta-secretase BACE1 is not a neuron-specific enzyme. Journal of Neurochemistry, 92(2): 226–234.

Roth, A. D.; Ramírez, G.; Alarcón, R.; Bernhardi, R. von, 2005. Oligodendrocytes damage in Alzheimer's disease: beta amyloid toxicity and inflammation. Biological research, 38(4): 381–387.

Rothstein, J. D.; Martin, L.; Levey, A. I.; Dykes-Hoberg, M.; Jin, L.; Wu, D.; Nash, N.; Kuncl, R. W., 1994. Localization of neuronal and glial glutamate transporters. Neuron, 13(3): 713–725.

Rubio-Perez, J. M.; Morillas-Ruiz, J. M., 2012. A Review: Inflammatory Process in Alzheimer's Disease, Role of Cytokines. The Scientific World Journal, 2012(1): 1–15.

Saffran, B. N.; Crutcher, K. A., 1987. Putative gliotoxin, α-aminoadipic acid, fails to kill hippocampal astrocytes in vivo. Neuroscience letters, 81(1-2): 215–220.

Schmitt, A.; Asan, E.; Püschel, B.; Kugler, P., 1997. Cellular and Regional Distribution of the Glutamate Transporter GLAST in the CNS of Rats: Nonradioactive In Situ Hybridization and Comparative Immunocytochemistry. The Journal of neuroscience : the official journal of the Society for Neuroscience, 17(1): 1–10.

Schousboe, A.; Svenneby, G.; Hertz, L., 1977. Uptake and metabolism of glutamate in astrocytes cultured from dissociated mouse brain hemispheres. Journal of Neurochemistry, 29(6): 999–1005.

Schultze, J. L., 2015. Transcriptional programming of human macrophages: on the way to systems immunology. Journal of Molecular Medicine, 93(6): 589–597.

Segovia, G.; Porras, A.; Del Arco, A.; Mora, F., 2001. Glutamatergic neurotransmission in aging: a critical perspective. Mechanisms of ageing and development, 122(1): 1–29.

Selkoe, D. J., 2004. Cell biology of protein misfolding: the examples of Alzheimer's and Parkinson's diseases. Nature cell biology, 6(11): 1054–1061.

Shadfar, S.; Hwang, C. J.; Lim, M.-S.; Choi, D.-Y.; Hong, J. T., 2015. Involvement of inflammation in Alzheimer's disease pathogenesis and therapeutic potential of anti-inflammatory agents. Archives of pharmacal research, 38(12): 2106–2119.

Sheng, J. G.; Mrak, R. E.; Rovnaghi, C. R.; Kozlowska, E.; van Eldik, L. J.; Griffin, W. S., 1996. Human brain S100 beta and S100 beta mRNA expression increases with age: pathogenic implications for Alzheimer's disease. Neurobiology of Aging, 17(3): 359–363.

Shoshan, Y.; Nishiyama, A.; Chang, A.; Mörk, S.; Barnett, G. H.; Cowell, J. K.; Trapp, B. D.; Staugaitis, S. M., 1999. Expression of oligodendrocyte progenitor cell antigens by gliomas: implications for the histogenesis of brain tumors. Proceedings of the National Academy of Sciences of the United States of America, 96(18): 10361–10366.

Siddiqui, T. A.; Lively, S.; Schlichter, L. C., 2016. Complex molecular and functional outcomes of single versus sequential cytokine stimulation of rat microglia. Journal of Neuroinflammation, 13(1): 24.

Siest, G.; Pillot, T.; Regis-Bailly, A.; Leininger-Muller, B.; Steinmetz, J.; Galteau, M. M.; Visvikis, S., 1995. Apolipoprotein E: an important gene and protein to follow in laboratory medicine. Clinical chemistry, 41(8 Pt 1): 1068–1086.

Simoni, A. de; Yu, L. M. Y., 2006. Preparation of organotypic hippocampal slice cultures: interface method. Nature protocols, 1(3): 1439–1445.

Simpson, J. E.; Ince, P. G.; Lace, G.; Forster, G.; Shaw, P. J.; Matthews, F.; Savva, G.; Brayne, C.; Wharton, S. B., 2010. Astrocyte phenotype in relation to Alzheimer-type pathology in the ageing brain. Neurobiology of Aging, 31(4): 578–590.

Söhl, G.; Hombach, S.; Degen, J.; Odermatt, B., 2013. The oligodendroglial precursor cell line Oli-neu represents a cell culture system to examine functional expression of the mouse gap junction gene connexin29 (Cx29). Frontiers in Pharmacology, 4: 83.

Steiner, J.; Bernstein, H.-G.; Bielau, H.; Berndt, A.; Brisch, R.; Mawrin, C.; Keilhoff, G.; Bogerts, B., 2007. Evidence for a wide extra-astrocytic distribution of S100B in human brain. BMC Neuroscience, 8(1): 739.

Stewart, C. R.; Stuart, L. M.; Wilkinson, K.; van Gils, J. M.; Deng, J.; Halle, A.; Rayner, K. J.; Boyer, L.; Zhong, R.; Frazier, W. A.; Lacy-Hulbert, A.; El Khoury, J.; Golenbock, D. T.; Moore, K. J., 2010. CD36 ligands promote sterile inflammation through assembly of a Toll-like receptor 4 and 6 heterodimer. Nature immunology, 11(2): 155–161.

Stoppini, L.; Buchs, P. A.; Muller, D., 1991. A simple method for organotypic cultures of nervous tissue. Journal of neuroscience methods, 37(2): 173–182.

Storck, T.; Schulte, S.; Hofmann, K.; Stoffel, W., 1992. Structure, expression, and functional analysis of a Na(+)-dependent glutamate/aspartate transporter from rat brain. Proceedings of the National Academy of Sciences of the United States of America, 89(22): 10955–10959.

Strooper, B. de; Karran, E., 2016. The Cellular Phase of Alzheimer's Disease. Cell, 164(4): 603–615.

Studzian, M.; Bartosz, G.; Pulaski, L., 2015. Endocytosis of ABCG2 drug transporter caused by binding of 5D3 antibody: trafficking mechanisms and intracellular fate. Biochimica et biophysica acta, 1853(8): 1759–1771.

Suh, Y.-H.; Checler, F., 2002. Amyloid precursor protein, presenilins, and alpha-synuclein: molecular pathogenesis and pharmacological applications in Alzheimer's disease. Pharmacological reviews, 54(3): 469–525.

Sun, C.; Fukushi, Y.; Wang, Y.; Yamamoto, S., 2018. Astrocytes Protect Neurons in the Hippocampal CA3 Against Ischemia by Suppressing the Intracellular Ca2+ Overload. Frontiers in cellular neuroscience, 12: 280.

Sun, W.; McConnell, E.; Pare, J.-F.; Xu, Q.; Chen, M.; Peng, W.; Lovatt, D.; Han, X.; Smith, Y.; Nedergaard, M., 2013. Glutamate-dependent neuroglial calcium signaling differs between young and adult brain. Science, 339(6116): 197–200.

Suzuki, Y.; Claflin, J.; Wang, X.; Lengi, A.; Kikuchi, T., 2005. Microglia and macrophages as innate producers of interferon-gamma in the brain following infection with Toxoplasma gondii. International Journal for Parasitology, 35(1): 83–90.

Tabata, H., 2015. Diverse subtypes of astrocytes and their development during corticogenesis. Frontiers in neuroscience, 9: 114.

Takada, M.; Hattori, T., 1986. Fine structural changes in the rat brain after local injections of gliotoxin, alpha-aminoadipic acid. Histology and histopathology, 1(3): 271–275.

Takaki, J.; Fujimori, K.; Miura, M.; Suzuki, T.; Sekino, Y.; Sato, K., 2012. L-glutamate released from activated microglia downregulates astrocytic L-glutamate transporter expression in neuroinflammation: the 'collusion' hypothesis for increased extracellular L-glutamate concentration in neuroinflammation. Journal of neuroinflammation, 9: 275.

Takami, K.; Terai, K.; Matsuo, A.; Walker, D. G.; McGeer, P. L., 1997. Expression of presenilin-1 and -2 mRNAs in rat and Alzheimer's disease brains. Brain research, 748(1-2): 122–130.

Tang, Y.; Li, T.; Li, J.; Yang, J.; Liu, H.; Zhang, X. J.; Le, W., 2014. Jmjd3 is essential for the epigenetic modulation of microglia phenotypes in the immune pathogenesis of Parkinson's disease. Cell death and differentiation, 21(3): 369–380.

Tarawneh, R.; Holtzman, D. M., 2012. The clinical problem of symptomatic Alzheimer disease and mild cognitive impairment. Cold Spring Harbor Perspectives in Medicine, 2(5): a006148.

Tellechea, P.; Pujol, N.; Esteve-Belloch, P.; Echeveste, B.; García-Eulate, M. R.; Arbizu, J.; Riverol, M., 2018. Enfermedad de Alzheimer de inicio precoz y de inicio tardío: ¿son la misma entidad? Neurologia, 33(4): 244–253.

Testen, A.; Ali, M.; Sexton, H. G.; Hodges, S.; Dubester, K.; Reissner, K. J.; Swartzwelder, H. S.; Risher, M.-L., 2019. Region-Specific Differences in Morphometric Features and Synaptic Colocalization of Astrocytes During Development. Neuroscience, 400: 98–109.

Todd, S.; Barr, S.; Passmore, A. P., 2013. Cause of death in Alzheimer's disease: a cohort study. QJM : monthly journal of the Association of Physicians, 106(8): 747–753.

Tomaskova, H.; Kuhnova, J.; Cimler, R.; Dolezal, O.; Kuca, K., 2016. Prediction of population with Alzheimer's disease in the European Union using a system dynamics model. Neuropsychiatric disease and treatment, 12: 1589–1598.

Traiffort, E.; Zakaria, M.; Laouarem, Y.; Ferent, J., 2016. Hedgehog: A Key Signaling in the Development of the Oligodendrocyte Lineage. Journal of developmental biology, 4(3).

Tsai, M. J.; Chang, Y.-F.; Schwarcz, R.; Brookes, N., 1996. Characterization ofl-α-aminoadipic acid transport in cultured rat astrocytes. Brain research, 741(1-2): 166–173.

Venegas, C.; Kumar, S.; Franklin, B. S.; Dierkes, T.; Brinkschulte, R.; Tejera, D.; Vieira-Saecker, A.; Schwartz, S.; Santarelli, F.; Kummer, M. P.; Griep, A.; Gelpi, E.; Beilharz, M.; Riedel, D.; Golenbock, D. T.; Geyer, M.; Walter, J.; Latz, E.; Heneka, M. T., 2017. Microglia-derived ASC specks cross-seed amyloid-β in Alzheimer’s disease. Nature, 552(7685): 355–361.

Viana, R. J. S.; Nunes, A. F.; Rodrigues, C. M. P., 2012. Endoplasmic reticulum enrollment in Alzheimer's disease. Molecular neurobiology, 46(2): 522–534.

Viganò, F.; Schneider, S.; Cimino, M.; Bonfanti, E.; Gelosa, P.; Sironi, L.; Abbracchio, M. P.; Dimou, L., 2016. GPR17 expressing NG2-Glia: Oligodendrocyte progenitors serving as a reserve pool after injury. Glia, 64(2): 287–299.

Vinet, J.; van Weering, H. R. J.; Heinrich, A.; Kälin, R. E.; Wegner, A.; Brouwer, N.; Heppner, F. L.; van Rooijen, N.; Boddeke, H. W. G. M.; Biber, K., 2012. Neuroprotective function for ramified microglia in hippocampal excitotoxicity. Journal of neuroinflammation, 9: 27.

Vodovotz, Y.; Lucia, M. S.; Flanders, K. C.; Chesler, L.; Xie, Q. W.; Smith, T. W.; Weidner, J.; Mumford, R.; Webber, R.; Nathan, C.; Roberts, A. B.; Lippa, C. F.; Sporn, M. B., 1996. Inducible nitric oxide synthase in tangle-bearing neurons of patients with Alzheimer's disease. The Journal of experimental medicine, 184(4): 1425–1433.

Walsh, D. M.; Selkoe, D. J., 2004a. Deciphering the molecular basis of memory failure in Alzheimer's disease. Neuron, 44(1): 181–193.

Walsh, D. M.; Selkoe, D. J., 2004b. Oligomers on the brain: the emerging role of soluble protein aggregates in neurodegeneration. Protein and peptide letters, 11(3): 213–228.

Walter, J.; Kaether, C.; Steiner, H.; Haass, C., 2001. The cell biology of Alzheimer's disease: uncovering the secrets of secretases. Current opinion in neurobiology, 11(5): 585–590.

White, J. A.; Manelli, A. M.; Holmberg, K. H.; van Eldik, L. J.; Ladu, M. J., 2005. Differential effects of oligomeric and fibrillar amyloid-beta 1-42 on astrocyte-mediated inflammation. Neurobiology of Disease, 18(3): 459–465.

Wisniewski, H. M.; Wegiel, J., 1991. Spatial relationships between astrocytes and classical plaque components. Neurobiology of Aging, 12(5): 593–600.

Wu, Z.; Nakanishi, H., 2015. Lessons from Microglia Aging for the Link between Inflammatory Bone Disorders and Alzheimer's Disease. Journal of Immunology Research, 2015(4): 1–9.

Wyss-Coray, T.; Rogers, J., 2012. Inflammation in Alzheimer disease-a brief review of the basic science and clinical literature. Cold Spring Harbor Perspectives in Medicine, 2(1): a006346.

Xia, N.; Zhang, P.; Fang, F.; Wang, Z.; Rothstein, M.; Angulo, B.; Chiang, R.; Taylor, J.; Reijo Pera, R. A., 2016. Transcriptional comparison of human induced and primary midbrain dopaminergic neurons. Scientific reports, 6: 20270.

Xie, Q. W.; Cho, H. J.; Calaycay, J.; Mumford, R. A.; Swiderek, K. M.; Lee, T. D.; Ding, A.; Troso, T.; Nathan, C., 1992. Cloning and characterization of inducible nitric oxide synthase from mouse macrophages. Science (New York, N.Y.), 256(5054): 225–228.

Xue, J.; Schmidt, S. V.; Sander, J.; Draffehn, A.; Krebs, W.; Quester, I.; Nardo, D. de; Gohel, T. D.; Emde, M.; Schmidleithner, L.; Ganesan, H.; Nino-Castro, A.; Mallmann, M. R.; Labzin, L.; Theis, H.; Kraut, M.; Beyer, M.; Latz, E.; Freeman, T. C.; Ulas, T.; Schultze, J. L., 2014. Transcriptome-based network analysis reveals a spectrum model of human macrophage activation. Immunity, 40(2): 274–288.

Yan, S. D.; Chen, X.; Fu, J.; Chen, M.; Zhu, H.; Roher, A.; Slattery, T.; Zhao, L.; Nagashima, M.; Morser, J.; Migheli, A.; Nawroth, P.; Stern, D.; Schmidt, A. M., 1996. RAGE and amyloid-beta peptide neurotoxicity in Alzheimer's disease. Nature, 382(6593): 685–691.

Yang, X.; Lou, Y.; Liu, G.; Wang, X.; Qian, Y.; Ding, J.; Chen, S.; Xiao, Q., 2017. Microglia P2Y6 receptor is related to Parkinson's disease through neuroinflammatory process. Journal of neuroinflammation, 14(1): 38.

Zhang, L.-N.; Wang, Q.; Xian, X.-H.; Qi, J.; Liu, L.-Z.; Li, W.-B., 2019. Astrocytes enhance the tolerance of rat cortical neurons to glutamate excitotoxicity. Molecular medicine reports, 19(3): 1521–1528.

Zhang, X.; Li, Y.; Xu, H.; Zhang, Y.-W., 2014a. The gamma-secretase complex: from structure to function. Frontiers in cellular neuroscience, 8: 427.

Zhang, Y.; Chen, K.; Sloan, S. A.; Bennett, M. L.; Scholze, A. R.; O'Keeffe, S.; Phatnani, H. P.; Guarnieri, P.; Caneda, C.; Ruderisch, N.; Deng, S.; Liddelow, S. A.; Zhang, C.; Daneman, R.; Maniatis, T.; Barres, B. A.; Wu, J. Q., 2014b. An RNA-sequencing transcriptome and splicing database of glia, neurons, and vascular cells of the cerebral cortex. Journal of Neuroscience, 34(36): 11929–11947.

Zhu, X.; Bergles, D. E.; Nishiyama, A., 2008. NG2 cells generate both oligodendrocytes and gray matter astrocytes. Development (Cambridge, England), 135(1): 145–157.

Zubenko, G. S.; Zubenko, W. N.; McPherson, S.; Spoor, E.; Marin, D. B.; Farlow, M. R.; Smith, G. E.; Geda, Y. E.; Cummings, J. L.; Petersen, R. C.; Sunderland, T., 2003. A collaborative study of the emergence and clinical features of the major depressive syndrome of Alzheimer's disease. The American journal of psychiatry, 160(5): 857–866.

7. Appendix

7.1 Supplemental data

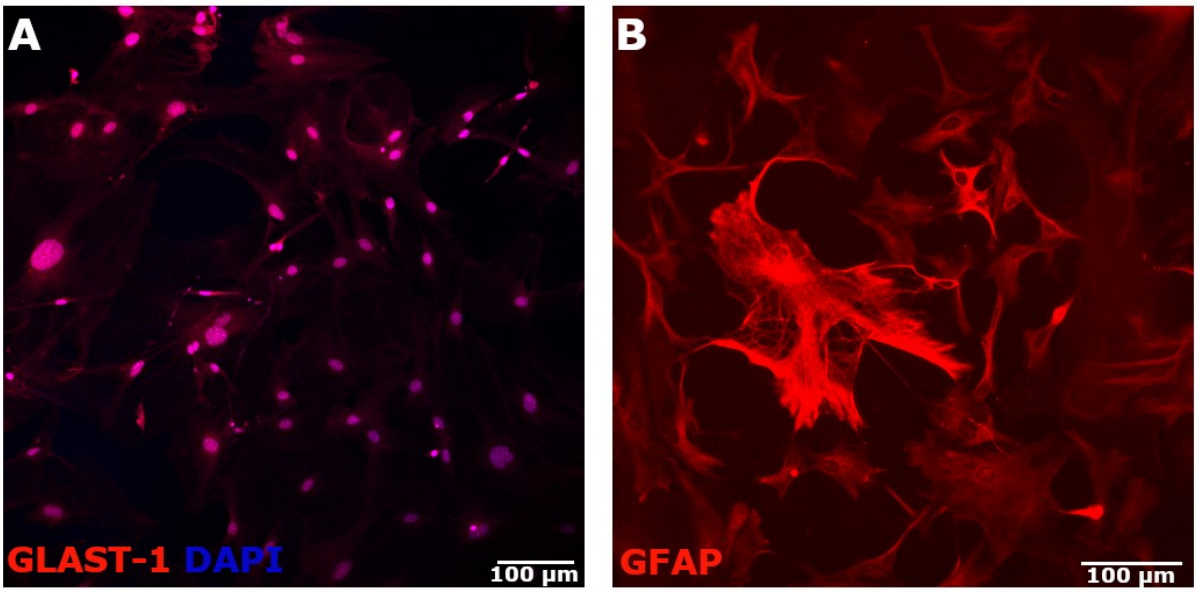

Fig. 6.1 Verification of antibody-binding on primary astrocytes. *Primary astrocytes were cultured on chamber slides fixated and stained with anti-GLAST-1 (A) and anti-GFAP (B) (1:500; secondary antibody 1:1000) antibody (red) and DAPI (blue). Images were taken with a CLSM at a magnification of 20x/ 0.70 and a zoom of 0.75.*

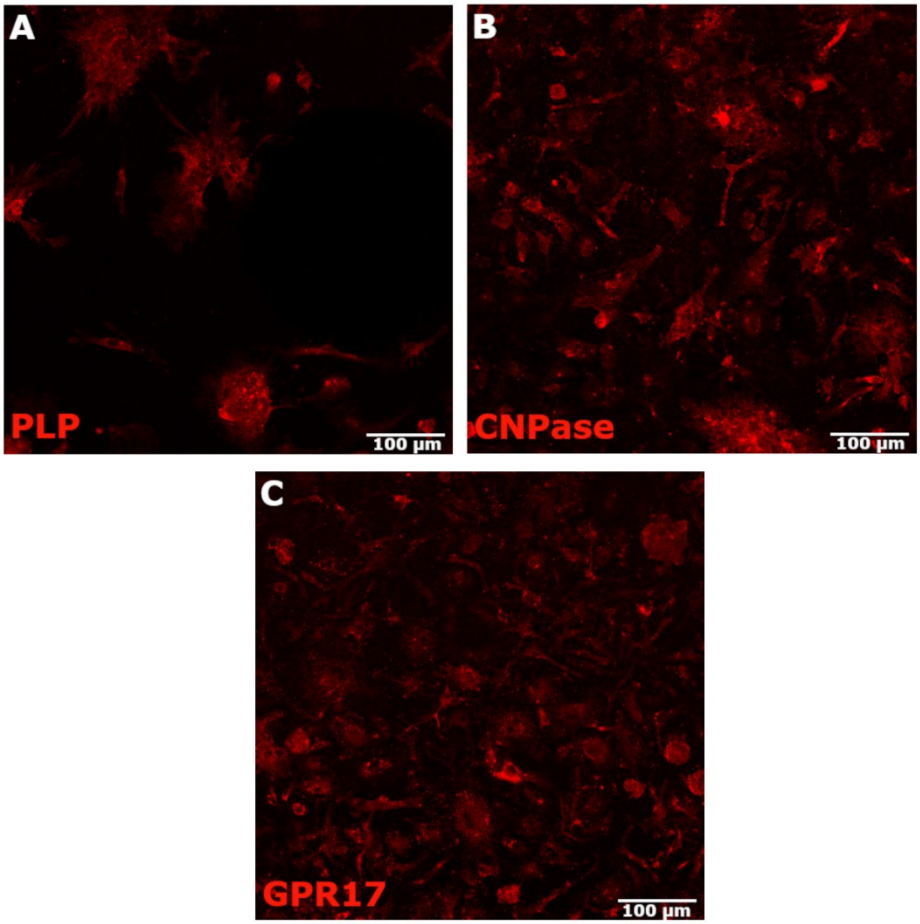

Fig. 6.2 Staining of primary oligodendrocytes reveals maturation-level. *Primary oligodendrocytes were cultured on chamber slides, fixated and stained with anti-PLP (A), anti-CNPase (B) and anti-GPR17 (C). Images were taken with an CLSM and an 20x/ 0.70 objective with a zoom of 0.75. Antibodies were diluted 1:500 each.*

7.2 Publications

Vidovic N, Heneka MT, Dodel R. Role of glial cells in neuroinflammation of neurodegenerative disorders. Review. submitted

Albus, A, Kronimus Y, Neumann S, **Vidovic N**, Frenzel A, Kuhn P, Seifert M, Ziehm T, van der Wurp H, Dodel R. Effects of a multimerized recombinant autoantibody against Amyloid-β. Neurosc. 2021 May; 463:355-369. doi: 10.1016/j.neuroscience.2021.03.006

Richter M, **Vidovic N**, Biber K, Dolga AM, Culmsee C, Dodel R. The neuroprotective role of microglial cells in a model of beta Amyloid-mediated cytotoxicity in organotypic hippocampal slice cultures. Brain Pathol. 2020 May;30(3):589-602. doi: 10.1111/bpa.12807

Richter M, **Vidovic N**, Honrath B, Mahavadi P, Dodel R, Dolga AM, Culmsee C. Activation of SK2 channels preserves ER Ca^{2+} homeostasis and protectes against ER stress-induced cell death. Cell Death Differ. 2016;23(5):814-27. doi: 10.1038/cdd.2015.146

7.3 Directory of academic teachers

Maastricht University:

A.W. Ambergen	G.H. Goossens	S.E. Köhler
A. Bast	G.R.M.M. Haenen	G. Plasqui
J.J. Briedé	G.J. Hageman	U. von Rango - Hilmes
W.R.M. Dassen	D.G.J. Jennen	F.J. Van Schooten
L.M.T. Eijssen	H. Kenis	J.H.O. Van Tilburg
R.W.L. Godschalk	T.M.C.M. de Kok	G.M.W.R. de Wert

Philipps-University Marburg:

A. Batschauer	C. Exner	J. Przyborski
S. Bauer	J. Heider	J. Schachtner
S. Becker	U. Homberg	M. Thanbichler
A. Brandis-Heep	A. Maisner	P. Yu

7.4 Acknowledgements

Lieber Herr Dodel, Ihnen gebührt mein größter Dank, da Sie mir die Möglichkeit gegeben haben meine Doktorarbeit unter Ihrer Aufsicht anzufertigen und unter erschwerten Bedingungen abzuschließen. Sie haben mir stets mit Kompetenz und Fachwissen den Rücken gestärkt und mich ermutigt weiterzumachen. Ich weiß sehr zu schätzen, was Sie neben Ihrer Tätigkeit als Mediziner, Familienvater und Arbeitsgruppenleiter für mich und meine Kollegen im Labor erreicht und möglich gemacht haben.

Liebe Mama, lieber Papa, Euch bin ich zutiefst dankbar für die Unterstützung moralischer, seelischer und finanzieller Art, die mir den Weg geebnet und mich zu der gemacht hat, die ich heute bin. Der Weg war nicht leicht, aber ihr habt nicht aufgehört an mich zu glauben und deswegen ist dies auch euer Erfolg. Ich kann mir keine besseren Eltern wünschen!

Lieber Bruder, Dir danke ich für Deine geerdete Art und Weise, die Dinge gelassener zu sehen.

Familie: Wo das Leben seinen Anfang nimmt und die Liebe niemals endet.

Lieber Lukas, Dir danke ich für Deine Geduld, Deinen guten Zuspruch, Deine Liebe und Wärme, die mich in manch dunklen Tagen wieder auf den Pfad der Vernunft gebracht hat. Mein Leben wäre ohne dich nicht ganz und du bist zurecht meine bessere Hälfte.

[Er hat] mich gerettet […] in jeder Weise, wie man von einem Menschen gerettet werden kann. (Rose – Titanic)

Liebe Alexx, lieber Yannick, ich danke euch sehr für eure Unterstützung, sowohl im Beruflichen als auch im Privaten. Wir sind in den letzten Jahren eng zusammengewachsen und haben so manche Krise gemeinsam überwunden. Ihr werdet mir ganz besonders fehlen. Wenn aus Kollegen Freunde werden: Das ist für mich nicht nur ein Spruch, sondern Realität geworden.

Je schöner und voller der Erinnerung, desto schwerer ist die Trennung. Aber die Dankbarkeit verwandelt die Erinnerung in eine stille Freude. (Dietrich Bonhoeffer)

Liebe Susanne, liebe Rosi, liebe Tine und lieber Michael, Euch danke ich für Eure Herzlichkeit, mit der ihr mich in Marburg empfangen und über die Jahre begleitet habt. Die Laune konnte morgens noch so trüb sein, Ihr habt mich ganz schnell wieder strahlen lassen.